The Application of a Machine Vision System to Relate Froth Surface Characteristics to the Metallurgical Performance of a PGM Flotation Process

Craig Gaven Sweet

A dissertation submitted to the Faculty of Engineering and the Built Environment, the University of Cape Town, in fulfilment of the requirements for the degree of Master of Science in Engineering.

April 2000

Declaration

I declare that this thesis, submitted for the degree of Master of Science in Engineering at the University of Cape Town is my own work. It has not been submitted prior to this for any degree or examination, at this or any other university.

Signed by candidate

Craig Gaven Sweet

Acknowledgements

My thanks are due to many whom have been instrumental in this thesis, and the research on which it is based.

Firstly, to my supervisor, Dr Dee Bradshaw for not only her supervision and patience, but also for the great personal effort put into in all aspects of the project.

Furthermore, thanks are due to Associate Prof. Peter Harris and Prof. Gerhard de Jager for the much appreciated help and insight that both gave generously throughout the project.

To Messrs Sandy Lambert and Martin Wright, not only for their support, facilitation and administration of the project, but also for their willingness to share very valuable engineering experience and knowledge.

To the Anglo American Platinum Corporation Ltd. (AMPLATS), for sponsorship of all aspects of the project and for the incredible opportunity that secondment to the University of Cape Town indeed was.

To the Department of Trade and Industry's "Technology and Human Resources for Industries Project" (THRIP) for the partial financial backing of my secondment to the University of Cape Town.

To the staff of Rustenburg Platinum Mines – Amandelbult Section, in particular Messrs Sarel Pelser and Hubert Mostert, for their assistance with the "on-plant" test campaign. Thanks are also due to the other members of the metallurgical technical team for collecting the sample for the batch flotation test work.

To Mr Leo Knopjes and the DML staff for assisting in the preparation of the ore sample used for the batch flotation test programme.

To Messrs Peter Hey, Bruce Walters and Paul Rixom for their input into the mineralogical and geological descriptions of the Amandelbult Merensky ore body, and for assisting in the choice of ore sample during the early parts of the project.

To the members of the "Froth Imagining Team": Ben Wright, Jerome Francis and Esther Ventura-Medina, for their friendship and all that they made possible.

To Mrs Jenni Sweet for (for want of a better way of expressing it) everything.

Abstract

This dissertation describes the use of a machine vision system to explore the relationships between the structure of the flotation froth surface, flotation performance and selected operational parameters in a flotation operation aimed at the beneficiation of Platinum Group Minerals. The machine vision system employed made use of the Fast Watershed Transform to resolve the froth surface into a distribution of bubble sizes. This distribution was then used to describe changes occurring in the structure of the flotation froth surface.

An initial batch flotation programme concentrated on the influences that changing the frother and depressant dosage levels had on a flotation system treating a sample of Merensky ore, which originated from Rustenburg Platinum Mine's Amandelbult Section. It was found that both depressant and frother dosage had marked influences on the metallurgical performance of the flotation system. Furthermore, it was found that changes in these operational variables resulted in changes in the structure of the flotation froth surface, which were quantified by the machine vision system. These results highlighted the potential of the machine vision system to identify when either the frother or the depressant dosages had moved towards levels that would negatively influence flotation performance.

A plant-based experimental campaign was then conducted on the Amandelbult Merensky Primary Rougher Flotation Section, in which the frother and depressant levels were manipulated. In terms of metallurgical performance of the flotation system, it was found that a strong relationship existed between the grade of concentrate being recovered and the rate of mass yield from the flotation unit. Furthermore, it was found that increasing the frother dosage led to an increased rate of mass yield and a decrease in concentrate grade, while increasing the depressant led to a decreased rate of mass yield at an increase in concentrate grade. As both of these variables influence metallurgical performance, a strategy that enables the automatic identification of which reagent dosage had deviated from the desired level would clearly be of great value.

A strategy based on the observation of bubble size distributions at the top and bottom of the flotation bank, and which is capable of identifying whether either the frother or the depressant dosages are changing, is suggested in this work.

Contents

List of Figures

List of Tables

1 Introduction

For many years the process of froth flotation has been employed as one of the primary means of separating a variety of minerals, and in particular sulphide minerals, from their host rock. In the past, operations employing flotation have harnessed (among other techniques) the ability of human operators to make rapid assessments of process performance by simple visual observation, as a means of maintaining process efficiency.

Recently, the advent of cost-effective computers with ever increasing computational capabilities, as well as the availability of optical equipment, has lead to the development of machine vision systems capable of rapidly extracting information from the visual medium. Advantages such as high degrees of reproducibility, consistency and speed, render machine vision systems attractive for applications such as performance monitoring and control of the flotation process.

This dissertation describes an investigation employing machine vision techniques in determining the relationship between the appearance of the flotation froth surface, the variables that may bring about a change in this appearance and the resulting implications on the metallurgical performance of a platinum group mineral (PGM) flotation system. A better understanding of the mechanisms that affect the metallurgical performance and the relationships that these have on the froth appearance, as measured by a machine vision system, will lead to better operation, management and control of flotation plants.

The following diagram aims to place the research presented in this thesis into the broader context of research aimed at improving both the performance of flotation systems and the understanding of the complex interactions present in flotation systems:

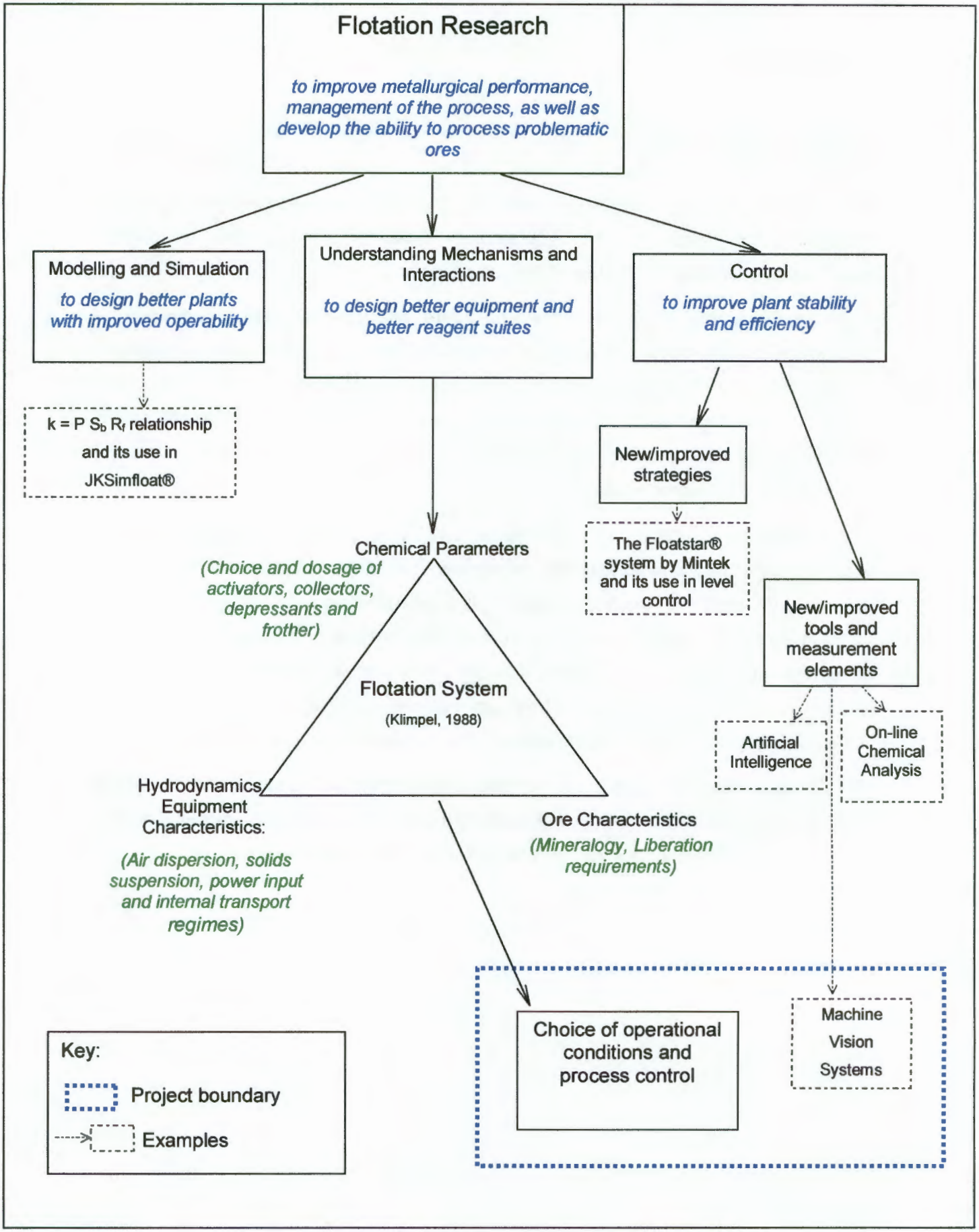

Figure 1.1: The Context of this Research within Flotation Research

1.1 Description of flotation

Flotation is arguably one of the most important processes currently employed in the beneficiation of sulphide minerals. It exploits the propensity of minerals' surfaces to be wetted by a liquid; in most cases this liquid is water. In flotation, air bubbles are passed through a slurry (finely ground mixture of minerals suspended in water, also often called *pulp*). A great many collisions will occur between the air bubbles and the solid particles in the slurry. For any mineral particles present in the slurry that have a greater affinity for air than for water (i.e. they are *hydrophobic*), these collisions may result in their attachment to the air bubbles. Thereafter the bubble-particle aggregates will be buoyed towards the upper surface of the slurry. Hydrophilic particles, those that have a greater affinity for water than for air, will remain in the slurry. By this method a separation between hydrophobic and hydrophilic particles is effected.

A second zone, known as the *froth phase* is typically established above the slurry. Here, strongly attached highly hydrophobic particles are suspended in a three-phase foam. Weakly hydrophobic particles and hydrophilic particles that have incorrectly reported to the froth phase, are given an opportunity to *drop back* into the slurry. Thus further up-grading of the stream rich in hydrophobic minerals occurs in the froth phase.

The hydrophobic-mineral-rich froth phase is then either scraped off the top of the flotation vessel, or migrates by itself over a weir and is known as the *concentrate*. The hydrophobic-mineral-lean slurry follows the bulk liquid and is either discarded or is given further treatment to recover additional valuable minerals. This stream is often called the *tail*.

In the majority of cases, the valuable minerals are those that are hydrophobic. However, there are a number of industrial applications where the valuable minerals are hydrophilic, and the non-valuable minerals are inherently (or are made to be) hydrophobic. Such applications of flotation are termed *reverse flotation*. This dissertation will focus on the treatment of Platinum Group Mineral (PGM) bearing ore, in which the valuable minerals are among those that are hydrophobic.

1.2 Flotation requirements

For successful separation to occur by flotation, a number factors need to be achieved. These include factors such as the amenability of the slurry to be treated by flotation, desirable conditions in the vessel in which flotation is to take place and froth characteristics suitable for mineral transport and upgrading. These will be discussed in turn in the following paragraphs.

1.2.1 Slurry Requirements

As stated above, the starting point for flotation is a *slurry* consisting of finely ground minerals suspended in a solution which is predominantly water. This slurry should possess a number of properties that would make it suitable for flotation. These include the correct interactions between the various solids and the solution, the optimum particle size distribution of the solids and the correct slurry rheology. The nature of solid surfaces, their interactions with the flotation solution and chemical means of modifying these will be discussed when the various flotation reagents and their roles are described below (Section 2.1.5). Brief descriptions of a number of further requirements of flotation slurries follow.

1.2.1.1 Optimum particle size distribution

The desired degree of fineness of the minerals is dictated mainly by two requirements: firstly, the need for adequate liberation; and secondly, the optimum size at which particles of the various minerals interact with air bubbles.

Typical ore bodies contain the valuable minerals as finely disseminated granules in amongst masses of barren host rock – known as gangue. To achieve the desired separation, valuable minerals need to be exposed or cleaved from the barren host rock, thereby allowing the required interactions (Leja, 1982).

Furthermore, particles should ideally consist of discrete minerals, for the greatest separation efficiency. Particles of this nature are known as *fully liberated,* and stand the greatest chance of reporting to the correct stream (be this either the *concentrate* or the *tail* stream). If a particle consists of a combination of minerals, it is typically termed a *middling* particle. Should such a particle consist primarily of gangue material, but include a small amount of valuable mineral, it stands a good chance of reporting to the tail stream. The inefficiency in such a case is that part of the total valuable mineral present is

lost to the discard. Should a particle be a composite consisting largely of valuable mineral, but include some gangue mineral, it may indeed report to the concentrate. In this instance the inefficiency is that the barren portion of the particle contributes to the overall dilution of the valuable mineral in the concentrate.

In general, therefore, the finer the particle size distribution in the slurry, the greater the degree of liberation.

A further particle size requirement, often conflicting with the first, is that there exists an optimum particle size range for flotation. Hydrophobic particles smaller than this size range do not respond well to flotation. This has been observed by a number of authors (among others: Trahar, 1981, Warren 1984 and Senior *et al.,* 1994). Some authors feel that the reason for this is that small particles do not have enough energy and therefore have low bubble collision rates (Sutherland and Wark, 1955). Others postulate that chemical factors also play a role in the responses of small particles (Senior *et al.*, 1994). The important point, however, is that there exists a lower bound to the range of particles that are amenable to flotation.

In addition to this, as particles become finer, there is a greater chance that they will report to the concentrate by non-selective mechanical entrainment (described by many authors, among whom are Subrahmanyam and Forssberg, 1988 and Smith and Warren, 1989). In this case particles are dragged along in the wake of rising bubbles and are drawn into the flotation froth along with a fraction of the process water. Under conditions where minerals are known to be hydrophilic, they are observed to report to the concentrate more in the finer size fractions than the coarser size fractions (Senior *et al.*, 1994).

Apart from liberation considerations (discussed above), an upper bound also exists to the particle size range that is amenable to flotation. Authors such as Subrahmanyam and Forssberg (1988) attribute this to the increase in density of the bubble-particle aggregate, owing to the increased mass of the larger particle. This in turn means that the density of the aggregate approaches that of the surrounding slurry and therefore there will be a decrease in the buoyancy.

The following figure taken from Senior *et al.* (1994) shows very clearly the lower and upper boundaries of floatability for pentlandite ($(Fe,Ni)_9S_8$, which is the hydrophobic species in this case). In addition to the above, it is clear that quartz (SiO_2, the hydrophilic species) enjoys increased recovery in the finer size fractions, presumably through entrainment.

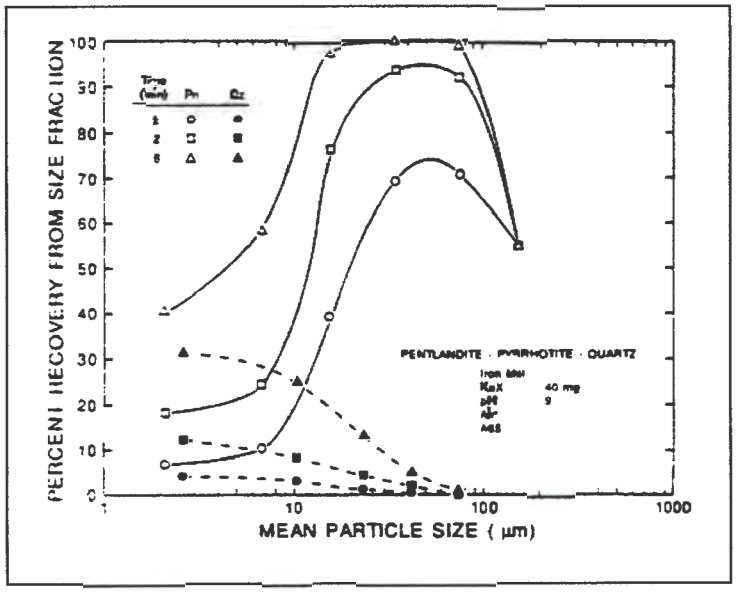

Figure 1.2: Size-by-size recovery of Pentlandite and Quartz (Senior *et al.*, 1994), showing optimum flotation size range for Pentlandite, as well as the recovery of fine hydrophilic gangue particles (quartz).

1.2.1.2 Other important slurry related considerations:

Gaudin (1957) points out that there are a number of advantages of operating at high solids concentrations. Among others there are issues of water savings, equipment size and effective reagent concentrations. Furthermore, he notes that at high solids concentrations, a greater chance exists of inclusion of barren minerals in the concentrate through non-selective mechanisms.

A further important aspect of the properties of the slurry is the rheology. Ore bodies that have a very high clay-type-mineral content are typically treated as slurries with low solids concentrations (Gaudin, 1957). This is partly because they result in slurries that have high viscosities (Leja, 1982), which impair the rise of mineralised bubbles.

1.2.2 Froth Requirements

Harris (1982) touches on the desired attributes that flotation froths should have. He states that good flotation froths should:

- have a stability great enough to allow further separation between valuable minerals that have reported to the froth phase by true flotation and material that has been entrained into the froth phase by other means, and;
- break down readily once removed from the flotation machine, to allow pumping and further treatment.

Furthermore, it stands to reason that a good flotation froth should be stable enough to carry large valuable particles until they are transported over the concentrate weir. In addition to this it should not be so stable as to resist flow in the direction of the concentrate weir.

1.2.3 Machine Requirements

Over the many years that flotation has been employed in the beneficiation of minerals a vast number of flotation machines have been designed and used. A brief look at an historical text such as Taggart's *Handbook of Ore Dressing* (1927) confirms this. A fair variety of machines (including flotation columns, pneumatic cells and mechanically agitated cells) enjoy industrial application today.

Glembotskii *et al.* (1961) listed the following requirements of flotation machines:

- They should "aerate the pulp as completely as possible", in other words be effective both in terms of bubble generation and gas dispersion;
- They should keep the solids in suspension;
- They should be able to be operated easily and in a continuous fashion.

By far the most popular flotation machines employed all over the world today are of the mechanically agitated variety, such as the one depicted below:

Figure 1.3: Typical Mechanically Agitated Flotation Cell

1.2.4 Flotation Reagents: Their purposes and effects

Flotation reagents are chemical agents added to the flotation process to perform a myriad of important functions. Amongst others reagents are added to control the hydrophobicity of solids surfaces, assist in gas dispersion and the establishment of a froth phase. The following paragraphs will give a brief description of the various classes of reagents, as well as examples of these as used in the flotation in the Platinum Industry.

1.2.4.1 Depressants

In order for an effective and selective separation to be achieved by means of flotation, there needs to be a sharp difference in the hydrophobicities of valuable and valueless or gangue minerals. In bulk sulphide flotation (as practised in the platinum industry), gangue minerals which are naturally hydrophobic (e.g. talc), must be rendered hydrophilic in order for this requirement to be achieved. Reagents whose purpose it is to alter the surface properties of minerals, to limit their recovery by flotation, are known as *depressants*.

In the platinum industry one of the primary minerals that is targeted for depression is talc $Mg_3(Si_2O_5)_2(OH)_2$. Two reagent types that enjoy industrial application for this purpose are modified guar gums (e.g. the commercial reagent *IMP4*) and carboxymethylated cellulose (known as CMCs, an example of which is *Depramin 267*).

Talc particles that report to the froth greatly increase the stability of the froth phase. This in turn results in increased entrainment of material (which could be either weakly or non-floating in nature) and hence results in lower grade concentrates. The influence of talc on the flotation performance is therefore disproportionate to its concentration in the ore.

On the other hand total depression of talc would lead to unstable froths, which would result in reduced recovery of valuable minerals. In addition to this, selectivity may be lost at very high depressant dosages, as depressant may adsorb onto the wanted minerals, rendering them less hydrophobic. It is therefore clear that the effective use of depressants is critical to flotation performance.

From the above it is clear that depressants influence the solid phase.

1.2.4.2 Frothers

Frothers are of great importance in flotation in that they play a role in a number of key sub-processes, which make the physical requirements of flotation possible.

- Frothers aid in the generation of the flotation froth phase, hence their name. This is arguably their most important function as froth is an inseparable part of flotation (Lekki and Laskowski, 1975).
- They also assist in gas dispersion, presumably by minimising coalescence of the air bubbles in the pulp zone (mentioned by a number of authors among whom are Harris, 1982 and Sweet *et al.*, 1997). This results in an increased number of smaller bubbles available to effect flotation, compared to cases when no frother is present (given the same volume of air).

Frothers are typically heteropolar molecules, consisting of a hydrocarbon, non-polar end as well as a polar end that will interact with water. Harris (1982) points out that the polar end is most often one of the following groups: hydroxyl (-OH), carbonyl (-CO), ester (-COOR) and carboxyl (-COOH). Laskowski (1998) also discusses frothers built primarily on ether linkages (-O-), many of whom enjoy widespread industrial application (an example of which is the commercial frother *Dowfroth 200*).

The heteropolar nature of frother molecules allows them orientate themselves at the air-water interface of an air bubble in water. The most logical orientation is with the non-polar group facing the air and the polar group facing the water. The presence of these species at the air-water interface allows them to alter the nature of this interface. There are many plausible explanations for the mechanisms by which this occurs, among which are the following:

- Frother molecules may change the elasticity of the interface, affecting its ability to repair itself after a local disturbance (Harris, 1982).
- Frothers may change the viscosity of the liquid that constitutes bubble shells. The importance of bubble shell properties in froth phase mineral transport is emphasised by Sadr-Kazemi and Cilliers (1997). In terms of generally accepted theory, Harris (1982) states that increasing the viscosity of this fluid effects the natural thinning of the liquid film between two bubbles, slowing coalescence and bursting. Retarding coalescence would result in finer bubbles in both the pulp and froth phases, while a reduction in bursting would lead to a more stable froth.
- Laskowski (1998) points out that, should the frother molecules be branched, they could retard coalescence by a steric mechanism, thereby resulting in smaller bubbles in the slurry phase aiding gas dispersion.

It is clear from the above that, regardless of which mechanism is taking place, frothers influence primarily the solution phase and its interaction with the air phase.

1.2.4.3 Collectors, Activators and Regulators

Collectors are the very important class of reagents added to the flotation slurry with the specific purpose of selectively imparting a hydrophobic nature to the surface of the valuable mineral. This is achieved by imparting a "hydrocarbon-like" (Gaudin, 1957) nature to an otherwise ionic mineral surface.

The choice of collector is specific to the mineral type or species that is targeted for flotation (Sutherland and Wark, 1955). An example of this is the use of *xanthates* and *dithiophosphates,* which are the most often used collectors in sulphide flotation (Wills, 1992). These collectors are also used in platinum flotation, as a number platinum group minerals are either sulphides themselves or are intimately associated with base metal sulphides. Glembotskii *et al.* (1961) classified *xanthates* and *dithiophosphates* into the group of collectors described as "ionising anionic collectors based on bivalent sulphur". The molecules can be described as being *heteropolar*, in that they consist of a non-polar group and an ionising polar group. The non-polar group is strongly water repellent, while the ionic group interacts with water and the mineral surface. The following diagram represents the general structure of these two reagent types:

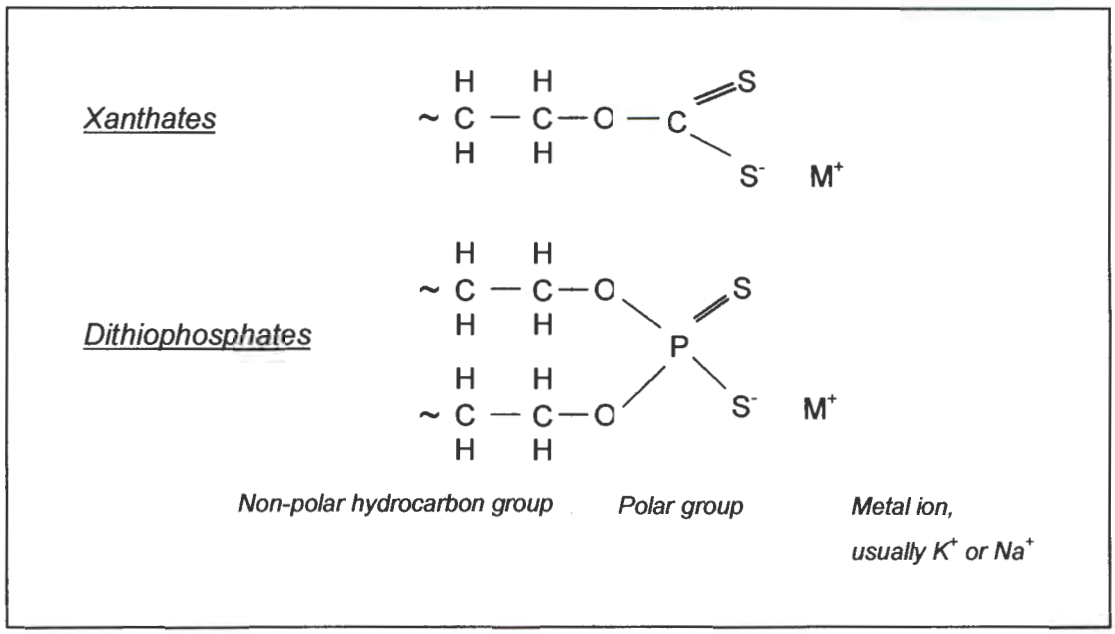

Figure 1.6: The structure of the collector species: *xanthates and dithiophosphates*, as used in platinum and other sulphide flotation operations.

The final class of flotation reagents is the large group described as being *activators* and *regulators*. The reagents generally control the environment in which flotation is to take place. This may be done by rendering the desired mineral surfaces more amenable to

collector adsorption (eg copper sulphate as an activator for zinc flotation), correcting the pH or to maintain the *redox potential* (an abbreviation of: 'reduction-oxidation potential')

1.3 Process Control of Flotation Plants

> "It is better where possible to prevent disturbances from occurring than to compensate for them using a control system after they have occurred, but in practice disturbances are inevitable and frequent."
>
> Lynch *et al.*, (1981)

Many authors on the subject of flotation control (among others, Lynch *et al.*, 1981; Bascar and Herbst, 1982; Lynch and McKee, 1984 and McKee, 1992) make the point that many problems stand in the way of effective flotation control, not the least of which is the complexity of the flotation system. In addition to this, when compared to other areas in mineral processing, flotation suffers from a far larger number of disturbance variables. The greatest of these are probably changes in ore type.

While it remains a complicated problem, much attention has been focused on the subject of flotation control over the last three decades. The inevitable trend towards the treatment of lower grade and more complex ores (a result of the depletion of high grade and easy to treat ores) has meant that flotation plants are required to operate closer to optimum with respect to both throughput and separation efficiency. This is probably the primary reason that the need for good process control of flotation operations has developed.

1.3.1 Flotation Control Objectives

Broadly speaking, the objectives of control are either to stabilise operation or to optimise process performance. There is little doubt as to which of these needs to be achieved first, as shown in the following statement by McKee (1992):

> "Only after stable circuit operation has been achieved should the next goal of process optimisation be attempted."

1.3.2 Stabilisation Control

Systems that have found lasting industrial application in flotation plants are those largely aimed solely at stabilisation, and are often based on simple feedback control loops. An example of these is cell level control, which itself plays an important role in determining the rate of concentrate recovery from the cell in question.

In the most common form of level control, the valve at the end flotation bank (typically a dart or pinch valve) is opened or closed so as to maintain a target pulp level in the cell in which the level is actually measured. A possible draw back of simple feed back level controllers is that they have been observed to propagate surge-related disturbances throughout the flotation process. Recently, advanced strategies for stabilising cell levels across an entire flotation plant have been developed. A good example of this is the *Floatstar*.® system developed by Mintek in South Africa (Schubert *et al.*, 1999), which aims to eliminate the propagation of cell level fluctuations.

1.3.3 Optimisation Control

Lynch *et al.* (1981) define the objective of optimisation control as being to ensure that the process is operated at the optimum point (itself defined by a great many considerations) on the optimum grade-recovery relationship.

A number of simple strategies which aim to improve the level of efficiency with which the flotation operation operates have found industrial use. One such strategy is the simple feed forward based scaling of the flotation reagent dosage rates to the measured feed rate (an easy parameter to measure). It is based on the principle that an increase in material fed to the plant would require a greater amount of reagent to affect the same metallurgical performance. While this strategy will ensure that the reagent dosage will be moved in the correct direction (Lynch *et al.*, 1981), this is not a true *optimisation* strategy in that it is based on an intuitive inference. The strategy does not measure the performance of the system, or any improvements to this performance brought about by control actions. Furthermore, while it is a better approximation to the system's reagent needs than a constant reagent flow rate would be, it is unable to react to changes in reagent requirement, should for instance the ore type change (Lynch *et al.*, 1981).

Frequent efficiency estimations are needed, both for the identification of sub-optimal performance and in the assessment of the success of control actions, for control aimed at optimisation to be achievable. Prior to the advent of on-line grade measurement devices (almost three decades ago (McKee, 1992)), infrequent assays and subjective observations were all that was available as means of estimating the efficiency of the flotation process. For this reason true optimisation control of flotation plants was not possible prior to this time. McKee (1992), however, makes the point that even after the advent of this advanced instrumentation, very few advanced optimisation control strategies enjoyed lasting success. Among the possible reasons put forward by McKee are the difficulties associated with defining true, explicit and achievable control objectives for the already highly complex process of flotation.

A final point that must be made regarding the two objectives of control, is that it is possible for the same system to have both stabilisation and optimisation as its objectives. An example of this is a system discussed by Lynch and co-authors (1981) which has a number of levels of control. The first level is *regulatory* control, which aims to control a particular process variable to a specific set-point. The second levels makes measurements of the process efficiency, determines the difference between current efficiency and targeted efficiency, and then choose a new process variable set point for the first level controller to target. This second level of control is therefore in a *supervisory* capacity. The third level of control is *optimising* control, and makes use of a thorough understanding of the process (possibly some sort of model) to search for the optimum operation point for the process. Furthermore, it is possible for the lower levels of this controller to continue to operate when the higher levels are not operational.

1.3.4 Practical Aspects of Flotation Control

Many of the strategies applicable to coal and base metal sulphide flotation systems (as discussed by Lynch *et al.,* 1981 and McKee, 1992) are not directly applicable to flotation as practiced in the platinum industry, for reasons of grade measurement. At the very low concentrations typically encountered in these flotation circuits, automatic online grade measurement is limited to the concentrates and at best may include the feed to the flotation processes. Given the value of the minerals of interest in these systems, the performance of a plant is typically gauged to be the inverse to the amount of values lost to the tailings. The quality of the product (i.e. the concentrate grade) is often secondary in the performance assessment. In cases where the feed concentrations of the value minerals can be measured online, the errors associated with flow, density and concentration at the other points of the system make inference of the tailings grades, with any confidence, near impossible.

Nonetheless, from the studies by the above authors, a number of observations were made that are applicable to the control of all flotation circuits. The following paragraphs aim to highlight some of the pertinent points made by these authors.

1.3.4.1 Prerequisites for the control of flotation plants

Lynch and co-workers (1981) listed three requirements that need to be fulfilled prior to the control being attempted on a flotation plant. These are:

- Grinding circuit product must be kept constant with the minimum discharge of coarse particles into the flotation circuit;

- Pumps on the streams entering the flotation circuit, as well as circulating material within the flotation circuit, must deliver steady flows and if a load change is necessary the control of these pumps should change the flow rate in a way that does not have adverse influences on the operation of the flotation plant; and finally,
- There should already be good control over the aeration rates and the reagent dosage rates.

1.3.4.2 Potential control strategies and their implications

a) Collector dosage as a control variable

As discussed earlier, the role of the collector is to impart (or improve) a hydrophobic nature to the surface of the desired mineral, in order for it to adhere to a rising air bubble. If there is an insufficiency of collector, desired minerals may be lost to the tailings. Using the collector dosage as a control variable is, however, complicated because it is difficult to determine the optimum dosage of collector or indeed the collector requirements of changing ore types. While it is obvious that an insufficiency is undesirable, an excess of collector might lead to either a decrease in the hydrophobic nature of the desired minerals' surface, or in the imparting of a hydrophobic nature to the gangue minerals which would impair the selectivity of the separation.

For the above reasons, the use of collector as a control variable is often limited to the simple scaling of the collector dosage with respect to the flotation feed rate as described by Lynch *et al.* (1981).

b) Depressant and activator dosage as control variables

The complications discussed above with respect to the use collector as a control variable apply largely to the manipulation of activator and depressant dosages for the same purpose. Optimum dosages of these reagents are difficult to determine with typical measuring elements and penalties exist for deviations on either side of the optimum dosages.

c) Frother dosage as a control variable

The role of the frother is (among other things) to provide a stable froth phase at the top of the flotation cell. Too little frother will result in an unstable froth that is not able to transport the flotation particles to the concentrate launder. As the frother dosage rate is increased, stability is imparted to the froth and the rate of transport to the concentrate launder is increased, which is typically accompanied by a drop in concentrate grade. It is

therefore possible that the frother dosage could be used to control the rate with which concentrate is recovered from a flotation machine.

The complications associated with manipulating frother dosage as a control variable lie in the fact that changes in frother dosage have marked influences on downstream flotation operations. Lynch and co-authors (1981) give an example where the frother dosage was manipulated on rougher-cleaner circuit aimed at the flotation of chalcopyrite (Mount Isa Mines, Australia). While increasing the frother addition rate to the rougher led to a rapid increase in copper recovery, it had a marked negative effect on the cleaner concentrate grade. Furthermore, while the increase of frother to the rougher was very brief (less than 7 minutes), it took the cleaner a lot longer to return to its initial value (about an hour). The use of frother as a control variable to increase the rate of recovery is therefore not recommended as it will influence not only the unit of direct interest, but also all down-stream operations. Furthermore, it could create compounding complications where recirculating loads exist.

d) Froth height and aeration rates as control variables

Decreasing the froth height (the vertical distance between the concentrate weir and the pulp-froth interface) or alternatively, increasing the aeration rate typically result in increases in the rate of valuable mineral recovery (higher mass pulls, however, at the expense of concentrate grades).

The advantage of using the froth height or the aeration rate to effect a change in the mass recovery of the flotation unit (as opposed to changing the frother addition rate as suggested in the previous section) is that they would have no residual influence on the rest of the flotation circuit. Froth height and aeration rate are therefore very good candidate variables for flotation control. Lynch and co-authors (1981) and McKee (1992) do however discuss a number of practical implications of using aeration rate and froth height as control variables.

Among the practical considerations mentioned by Lynch *et al.* (1981) is that there appears to be a minimum practical aeration rate, below which "froth saturation" sets in, resulting in limited flotation performance. Furthermore, in cases where small froth heights are employed, there may not be enough room over which control action can be effective (McKee, 1992).

1.3.5 The Future of Process Control for Flotation

There is little doubt that there exists an ever-growing requirement for the development of effective control strategies for flotation plants. The low success rates of advanced

flotation control strategies mentioned by McKee (1992) points towards a very real requirement for innovation and development in the field.

One area of potential improvement is the speed of the systems aimed at detecting changes in process performance. Lynch and co-workers (1981) noted that feed back control strategies which are based on on-line measurements of concentrate and tails grades are often slow to respond to changes in flotation performance. This is due to the time delays associated with flotation bank residence times, on-line analysis system lag time and the like. One of the suggestions made by these authors is that analysis should be concentrated on the products from the first few cells, as changes in flotation characteristics will become apparent shortly after the material enters the flotation bank.

While the advantages of improved detection times and the resulting potential for faster controller responses may be obvious, it would not make the process control of flotation operations more attainable. The reasons for the limited success rates among flotation control strategies lies in the complex nature of the flotation process. For this reason, it appears that completely novel approaches need to be developed and employed.

It would appear that there exists a need for an automatic method of determining the flotation "wellness". With the technology that is currently available, control strategies concentrate on ..."circuit *operation* in contrast to the *condition* which relies on manual interpretation of and reaction to process changes." (Arbiter *et al.*, 1985). By this it is meant that with the tools available (such as on-line grade measurement devices), it is possible to determine *what* is happening with respect to flotation efficiency, but the interpretation as to *why* it is happening is largely left up to human operators.

To summarise, there exists a need for a fast method of determining flotation efficiency and the reasons for a particular deviation from the desired flotation efficiency. If it were ever found, such a strategy would go along way to increasing the applicability of automatic process control of flotation plants. The remainder of this thesis will explore the possibility of the application of a machine vision system to give rapid determinations of the reasons for changes in flotation performance.

1.4 The Influence of Flotation Froth Contents on Froth Structure

Any study into the role of froth structure in determining flotation performance would be incomplete without a brief digression into the influences that the contents of flotation froths have on the structures of these froths.

Froth structure is to a large degree determined by film stability. Film rupture may either result in bubble coalescence (both within the bubble column and at the froth surface) which would lead to fewer but larger bubbles, or bubbles bursting (on the froth surface). The role of the reagent class *frothers* has been discussed above in section 1.2.4.2 and it is therefore the influence of the solid particles in flotation froths that will be discussed here.

The presence of solid particles in flotation froths is intimately associated with the objectives of flotation as a mineral beneficiation process. Authors such as Dippenaar (1982a and 1982b) and Johansson and Pugh (1991) have studied the influence of particle hydrophobicity on film stability and both parties found that based on hydrophobicity, particles could influence film stability in three ways:

- weakly and non-hydrophobic particles would not influence film stability;
- particles of intermediate hydrophobicity would slow film drainage stabilising the film and hence also the flotation froth; and,
- particles with high hydrophobicities that would quench the froth by accelerating film drainage.

Dippenaar (1982a) found that particle shape and surface texture played an important role in determining whether particles would cause either stabilisation or destabilisation. He found that cubic particles with smooth sides (such as galena) would cause destabilisation. Plate-like particles and particles with rough surfaces would tend to cause film stabilisation.

In terms of particle size, Dippenaar (1982b) found that for particles that are capable of destabilisation, larger particles would result in far more rapid destabilisation than comparable smaller particles.

The point of the above discussion is to highlight the fact that changing the hydrophobic nature of the particles in the froth, or indeed the type of particles reporting to the froth, could alter froth structure. Parameters that alter the characteristics of the solid particles (e.g. the grind, ore type, collector and depressant dosages) would therefore also indirectly influence the flotation froth structure.

1.5 Applications of Machine Vision Systems in Flotation

In recent years, there has been a considerable amount of activity in the field of machine vision as applied to the process of froth flotation (examples are Symonds and de Jager, 1992; Moolman *et al.*, 1994; Nguyen and Thornton, 1995; Hargrave *et al.*, 1996; Sadr-

Kazemi and Cilliers, 1997; and Guarini *et al.*, 1997). Primarily, the focus of this work has been in two related fields, the first being as a potential method of control and the second in the modelling of the flotation process.

The following table aims to summarise some of the pertinent points from the many publications on machine vision in the field of flotation. Thorough descriptions of the methodologies used by the various groups to extract the measurements discussed below can be found in Wright (1999).

University of Mining and Metallurgy, Cracow, Poland			
Measurements	Information extracted/inferred	Flotation system	References
Optical density and inferred bubble size (by optical and digital Fourier Transforms)	Estimation of froth metal content	(unclear)	Kordek and Lenczowski, 1988 Kordek and Kulig, 1997
University of Stellenbosch (and later Hatch Africa and Crusader Systems)			
Measurements	Information extracted/inferred	Flotation system	References
"Copper peak" (a colour ratio derived from froth image greyscale histogram.) Bubble size and shape information (from fast Fourier transforms)	Estimation of froth copper content Froth characterisation	Copper PMC SouthAfrica	Moolman *et al.*,1994
Froth stability, mobility and bubble size - all extracted from textural measures of the froth surface, using the Spatial Grey Level Dependence Matrix (SGLDM) and Neighbouring Grey Level Dependence Matrix (NGLDM)	Relationships found between these measures and reagent dosage levels (Collector and activator dosages)	Copper and Pyritic ore from Buffelsfontein Gold Mine South Africa	Moolman *et al.*,1995a
Froth stability, bubble size and relative grey level, measured as above	Smaller bubble sizes and greater stability, found to be beneficial for cases in which "high intensity conditioning" was applied	PGM (Merensky) ore from Impala Platinum Ltd, South Africa	Aldrich *et al.*, 1997
(This group has also explored the use of advanced computational techniques such as Neural Networks to extract information from the textural parameters that describe froth surfaces and for the classification of froths)			Moolman *et al.*,1995b Moolman *et al.*,1995c Moolman *et al.*,1996a Moolman *et al.*,1996b Van Deventer *et al.*, 1997

Julius Kruttschnitt Mineral Research Centre			
Measurements	Information extracted/inferred	Flotation system	References
A *Texture Spectrum*, provides a textural "finger print" of the froth appearance. Furthermore, an average bubble size can be inferred from *the Texture Spectrum.*	Froth images are grouped into "good" and "bad" predefined bins according to this characterisation A soft sensor approach also allowed the prediction of ash and solids loading estimations of the flotation froths	Coal	Nguyen and Thornton, 1995
Froth Surface velocity and direction of flow measured by *Pixel Tracing*	This allows a simple control strategy, in which the air flow rate to the cell is manipulated, to be implemented.	Coal (but later applied to Copper, Minera Escondida, Chile)	Nguyen and Holtham, 1997 Nguyen, 1999
University of Nottingham			
Measurements	Information extracted/inferred	Flotation system	References
Colour (grey level measurements)	Estimates of ash contents and flow rates of flotation froths given.	Coal	Hargrave *et al.*, 1996
Colour and bubble size distribution (by the watershed transform) and Fractal Dimensions.	Colour (relative redness) gave an indication of the grade of the flotation froth. Froth structure inferred from the fractal dimension, which is a way of describing the bubble size distribution	Tin flotation, Wheal Jane, UK	Hargrave and Hall, 1997 Hargrave *et al.*, 1997
University of Manchester			
Measurements	Information extracted/inferred	Flotation system	References
Bubble Size and Shape distributions (by a number of methods)	Froths characterised and flotation rates accurately predicted using the model initially developed by Flynn and Woodburn (1987)	Coal	Woodburn *et al.*, 1994 Sadr-Kazemi and Cilliers, 1997 Banford et al., 1998
	Later, the rates of recovery of mineral and coal where related to dosages of reagents	Coal	Asplin et al., 1998

Catholic University of Chile			
Measurements	Information extracted/inferred	Flotation system	References
Colour information Average bubble diameter and ellipticity Froth velocity and stability	The information extracted from froth image appearance is diagnosed by an expert system, known as *ACEFLOT*. Control is effected via a rule-base which links the appearance of sub-optimal froths to possible causes of the appearance.	Copper	Guarini *et al.*, 1995 Cipriano *et al.*, 1997 Cipriano *et al.*, 1998

Table 1.1: Research involving the application of Machine Vision in the field of flotation.

It is clear from the above that machine vision has been the focus of much research over the past decade. However at the time that this project was initiated two areas existed where it was felt that more knowledge was needed before machine vision could be employed as a control tool:

- the first being the need for a technique that could provide more information about *froth structure* within a *real time* reference frame (in other words an advanced bubble size measurement too that could be used as an on-line control tool);
- the second being the need for more information about the suitability of machine vision to extract information which could be used fto control PGM flotation processes.

Regarding the first point, many of the systems aimed at industrial flotation control made/make use of textural measures of the froth surface (eg. Moolman *et al.* 1994 and Nguyen and Thornton, 1995). From these measures parameters such as average bubble size were/are then inferred. It was felt that more advanced measurement techniques such as the *Watershed Transform* used at the University of Nottingham and UMIST, which return complete bubble size distributions would be better suited to explore the influences that changes in operational parameters had on flotation froth structure. The problem was that these techniques are typically computationally expensive and are therefore often applied "off-line", by analysing video images post an experiment. Recently, however, improvements in the computational capabilities of personal computers and the use of improved algorithms (e.g. the *Fast Watershed Transform* (Wright, 1999)) have allowed such tools to become available in both research and industrial applications.

Regarding the second point, only a small fraction of the work reported has focused on the PGM flotation process. The exceptions to this statement being of the valuable work reported by Aldrich *et al.*, 1997 and a number of works by Moolman *et al.* (1995b, 1995c and 1996a). The work by these authors is however based on a textural approach, and it is felt that the advent of more advanced measures of froth structure (such as the complete surface bubble size distributions) would allow improved studies into this field. In particular it would allow further exploration into the relationships that exist between the structure of the flotation froth surface, the metallurgical performance of the flotation system and the operational variables that could be manipulated to effect process control on a PGM flotation system.

2 Objectives of this Research

In the previous section, it was shown that there exists a need in the field of flotation control for innovative methods which allow the early detection of sub-optimal performance. In the majority of flotation plants, and in particular in the platinum industry which forms the focus of this project, control is by operator adjustment of operational parameters based primarily on a subjective visual inspection of the flotation froth surface. Machine vision systems provide a means of extracting information about the froth appearance and behaviour in much the same way as a human operator would. This information could then potentially be used in the automatic control of flotation operations.

The following are the objectives of the research presented in this thesis:

- To ascertain the suitability of machine vision systems to extract information pertaining to the appearance of the froth surface on a selected PGM flotation system.
- To develop a three way understanding of the relationship between the appearance of the flotation froth surface, changes in various operating parameters and the resulting changes in metallurgical performance of the flotation system.
- To assess the potential for the use of machine vision systems in the control of platinum flotation operations.
- To develop a strategy to correct or improve flotation performance using the relationships between operating parameters, froth appearance and metallurgical performance.

3 Experimental Details

In this section the details of the systems and experiments carried out in the duration of this project will be presented.

A description of the image analysis system employed will be followed by a description of the initial batch flotation experiments carried out on a laboratory bench scale. Finally the procedures and techniques employed during the plant based experimental programme will be presented.

3.1 The Image Analysis System

As the focus of this dissertation is the application of a machine vision system, as opposed to its development, the description of the system given below will be kept brief. For more detail on the system's development and the algorithms it employs, the interested reader is referred to the dissertation entitled *The Development of a Vision-Based Flotation Froth Analysis System* by B Wright (1999).

3.1.1 Introduction to the Image Analysis System

This dissertation concentrates on the use of bubble size and motion information. A brief description of the algorithms used to extract this information from a video source will be given below.

3.1.2 Extracting Bubble Size Information

The assumption on which this project is based is that the structure and appearance of the flotation froth surface is descriptive of the underlying sub-processes occurring both in the pulp and froth phases. For the purpose of this project, the *fast watershed transform* was employed to extract this information from the visual image (Wright, 1999). This algorithm makes use of a segmentation technique, which resolves the froth image into its constituent bubbles. Once this is done, information about the discrete bubbles can be extracted for further use. This technique is in contrast with textural approaches used by a number of other groups (by way of example: Moolman *et al.*, 1994 and Nguyen and Thornton, 1995), which relate parameters like bubble size to a textural descriptor.

3.1.2.1 Image preparation

The image as captured needs to be rendered suitable for segmentation. First a set of procedures described by Wright (1999) as "image pre-processing" are applied, in which various sources of "noise" are eliminated from the image. If this were not done, the noise would result in the segmented image having little resemblance to the original image.

The first step in pre-processing is known as *subsampling*. In this process alternate lines of the image (either the odd or the even lines) are discarded to reduce the distortion due to *interlacing*, which is inherent in the *PAL Television Standard* used for the images in this project (Wright, 1999). This results in an image that has half the vertical dimension of the original image. To correct this, a second step known as *interpolation* is applied to restore the image to its original size.

The uniformity of the image is then improved by a method known as *histogram equalisation*. This process spreads the *grey scale* values in such a way that all grey scale levels are represented by roughly an equal number of pixels within the image. This aids in preventing larger bubbles from being "over-segmented". This is followed by an advanced "noise" removal method known as *Anisotropic Diffusion.* While an explanation of this method is beyond the scope of this dissertation, it suffices to say that the advantage that this method has over *low pass filtering* (another method of noise elimination) is that it does not blur the bubble boundaries (Francis, 1999).

After another application of *histogram equalisation*, a process known as *greyscale dilation* is applied to merge any multiple highlights that may be found on the surfaces of the larger bubbles. If this is not carried out, the multiple highlights on the surfaces of these bubbles would lead the image system to believe that one large bubble is indeed a number of smaller bubbles. The result would be an over-segmentation of the larger bubbles which itself would result in the number of large bubbles being underestimated.

The final step of pre-processing is *image inversion.* This, in effect, results in an image that is a negative of the image that has gone through the other steps of pre-processing. The reason for conducting this process is to deliver an image of a froth surface that is suitable for the application of the watershed transform, whose purpose it is to detect the bubble boundaries. Wright (1999) uses the simile of a topographic surface to explain the concept. After *inversion* the tops of the bubbles will now appear to be catchment basins (regional minima), while the bubble boundaries will be *watersheds.*

3.1.2.2 The watershed transform

Only once the image has been prepared for the segmentation is the *watershed transform* applied. While a number of strategies exist for the application of the watershed transform, the one followed in the segmentation carried out in this project is known as the *immersion method*.

To describe the *immersion method*, it is useful to return to the topographical analogy used for the inverted froth surface. The hypothetical froth surface is punctured at the lowest point of each catchment basin (previously the highest point on the bubble's surface). The entire topographical surface is then slowly lowered into a lake, which results in each catchment basin slowly filling with water. This continues until the point is reached when the water from two neighbouring basins meet. At this point a "dam wall" is built and the immersion is continued. Once the immersion is completed, each catchment basin will be surrounded by a dam wall, which defines the watershed between itself and neighbouring basins. The following diagram gives a pictorial description of the above explanation:

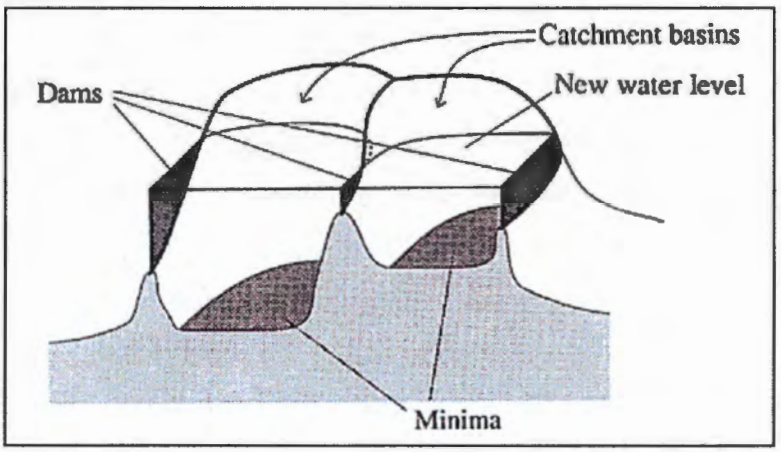

Figure 3.1: The *watershed transform* segmentation algorithm (Wright, 1999).

If this grid of watersheds is then overlaid over the original image, the success of the transform is easy to assess. The following two diagrams show the original image on the left, and the same image after segmentation on the right.

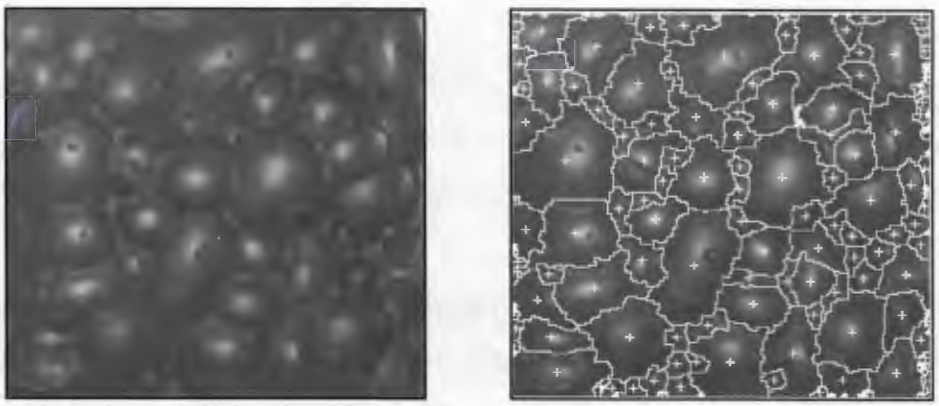

Figures 3.2 and 3.3: Original image and the resulting segmentation using the *watershed transform.*

3.1.3 Extracting Froth Motion Information

A further parameter that was measured from the video image was the froth surface velocity. The method used for this measurement was proposed and applied to flotation froth surface velocity measurement by Nguyen and Holtham (1997), and is known as *pixel tracing.*

The advantage of this as a motion estimation technique is that it is simple and computationally inexpensive. At the start of the algorithm, a small square area is characterised in the center of the froth image by means of its intensity (call this intensity V(0) for the purposed of this description). Following this, a second image (taken at a time step of Δt after the original image) is searched, starting at the region's initial position, for a region that best corresponds to the initially characterised region of the original image. This search is done in fixed increments, and in the eight directions of the compass (N, NE, E, SE, S, SW, W, NW). Once this region has been found, it is possible to compute the number of pixels with which this region has migrated and, as the time step (Δt) is known, it is possible to compute the velocity. In addition to the velocity, the direction of movement is also now known. The following diagram aims to explain the concept:

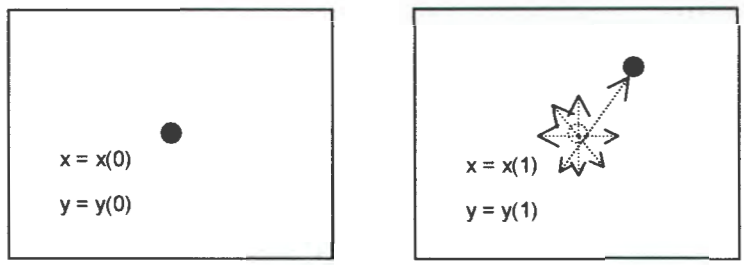

Figure 3.4: Explanation of the *Pixel Tracing* algorithm for motion estimation (redrawn from Nguyen and Holtham, 1997).

In the application of this technique, the assumption is made that the object being observed does not distort during measurement. While this is not always the case with flotation froth motion, Nguyen and Holtham found that the technique worked sufficiently well in practice for meaningful measurements to be made.

3.2 Batch Flotation Programme

3.2.1 Aim of the Batch Flotation Programme

The aim of the batch flotation programme was two fold. Firstly, to provide a variety of froth surface images to allow the development of the machine vision system, as well as a method of interpreting the data collected by such a system.

The second aim of the programme was to assess the influences of frother and depressant dosage levels on the metallurgical performance of the flotation system as well as the visual appearance of the flotation froth surface. These factors were selected as plant operators commonly make changes to the frother and depressant dosage levels, based on their assessment of the appearance of the surface froth and in particular the bubble size distribution of this surface froth.

A further batch flotation programme was conducted which aimed to scout the extent to which the variation of other process factors gave rise to detectable changes in surface froth appearance and metallurgical performance. These tests fall outside the scope of this thesis, however the details of this extension of the batch flotation programme can be found in APPENDIX BIII.

The following sections will describe the methods, materials and procedures used in the programme.

3.2.2 Sample Preparation

The ore sample was collected with the help of the site personnel from the Run-of-Mine feed belt to the Merensky concentrator at Rustenburg Platinum Mines' Amandelbult Section. For the laboratory batch flotation programme, ore from *No. 44 Raise Bore* was used, which is representative of the central area of the Amandelbult mining operation. This was chosen because at the time of the programme, this region of the mine accounted for the largest proportion of the Run-of-Mine ore being treated in the concentrator. (A description of the mine's geology is given in APPENDIX A).

The Run-of-Mine ore sample was then transported to the *Divisional Metallurgical Laboratory*[1] were it was dried, crushed and blended. It was then sub-sampled to achieve a sample of 200 kg, which was transported by rail to the Department of Chemical Engineering at UCT.

On the arrival of the ore at UCT, a total of 50 kg of ore was sub-sampled into 1kg aliquots. This meant that a single aliquot could then be prepared per 3ℓ batch flotation test.

A milling curve was established to determine the milling time required. The aim of the experimental programme was to emulate the conditions of the Primary Rougher Flotation stage of this process, and hence it was attempted to achieve a similar grind to that of the Primary Rougher flotation feed. The target grind was taken to be 40% passing 75 μm, which is approximately that stated as the target for the Amandelbult Merensky Concentrator Primary Milling stage[2].

3.2.3 Test Conditions

The standard conditions used during the batch flotation experiments are given below. The only time that these were deviated from was when the test condition required one of the variables to be set at an alternative level, in which case all other variables were maintained at the standard level.

Cell:	3/ open-topped Leeds Cell
Impeller Speed:	1200 rpm
Aeration Rate:	6 //min
Froth Height (Froth/Pulp Interface):	3 cm

[1] Divisional Metallurgical Laboratory (DML) at Rustenburg Section of Rustenburg Platinum Mines Ltd.
[2] Details as communicated by the Amandelbult Concentrator technical personnel, 17 April 1998.

Method of Froth Removal: Scraping at 15 second intervals

pH: Natural (approximately 8)

Ore : 1 kg Amandelbult Merensky ore per test

(Milled to 40% - 75 μm in a stainless steel rod mill)

Pulp percentage solids: 30%

Concentrate Gathering Times: 1, 2, 4, 6 and 10 mins after commencing test

Reagents:

The collectors used, Sodium Iso-Butyl Xanthate (SIBX) and *Senkol 5* (a Dithiophosphate or DTP) are from the thiol class of collectors and were both supplied by Senmin Ltd. The depressant used for the test programme was a modified guar gum called *IMP4*, and was supplied by Trohall Ltd. The frother used was *DOW200* which is a poly-glycol type frother supplied in South Africa by Betachem Ltd.

The following dosages of the above reagents were used for the base case experiments:

Type and Name	**Standard Dosage***	**Addition Point**
Collector: SIBX: Senkol 5 blend Ratio: 2:3	30 g/t	To mill prior to milling
Depressant: IMP4	28 g/t	Conditioning interval 1 (2min)
Frother: DOW 200	40g/t (dosage not specified by operation)	Conditioning interval 2 (1min)

Table 3.1: Standard reagent levels used throughout the batch flotation programme (unless the condition being assessed required otherwise).

* specified by Amandelbult operation personnel

3.2.4 Experiments Conducted

As stated above, the two variables changed in the first part of the batch flotation programme were the frother and depressant dosages. Briefly the six conditions tested in this part of the programme were as follows:

Condition Name	Frother Dosage (Dowfroth 200, g/t)	Depressant Dosage (IMP4, g/t)
1. Standard	40	28
2. No Depressant	40	0
3. High Frother High Depressant	60	50
4. High Frother Low Depressant	60	10
5. Low Frother High Depressant	20	50
6. Low Frother Low Depressant	20	10

Table 3.2: Experimental conditions for first part of the batch flotation programme.

The second part of the programme assessed the influences of variables other than those tested in the first part of the programme. The following table shows the tests conducted and the level of each variable assessed:

Condition Name	Variable changed (and level assessed)
7. Froth Depth (lower pulp level in cell)	Cell pulp level decreased (distance between pulp and lip increased from 3cm to 4cm.)
8. High Air Flow Rate	Air flow increased (from 6 l/min to 8 l/min)
9. High Collector dosage	Combined SK5 and SIBX dosage increased (from 30 g/t to 45 g/t)
10. Std CMC	Changed depressant type (from IMP4 - guar type, to Dep267 – CMC type, at 28 g/t)
11. High CMC	Changed depressant type and increased dosage (from IMP4 - guar type, to Dep267 – CMC type, at 50 g/t)

Table 3.3: Experimental conditions for the second part of the batch flotation programme.

These tests are not discussed further in this document, as they fall outside the scope of this thesis. The detailed results of these tests are however included in APPENDIX BIII along with a brief discussion of the pertinent points, as an aid to future work.

3.2.5 Test Apparatus

The ore slurry was prepared for flotation by grinding in a *Sala* stainless steel rod mill, and the flotation tests were carried out in a 3ℓ bottom-driven Leeds Cell. This cell was used as it presented a froth surface free of obstructions, allowing images of the entire surface of the froth to be captured. The following figure shows the flotation cell used for the batch flotation programme.

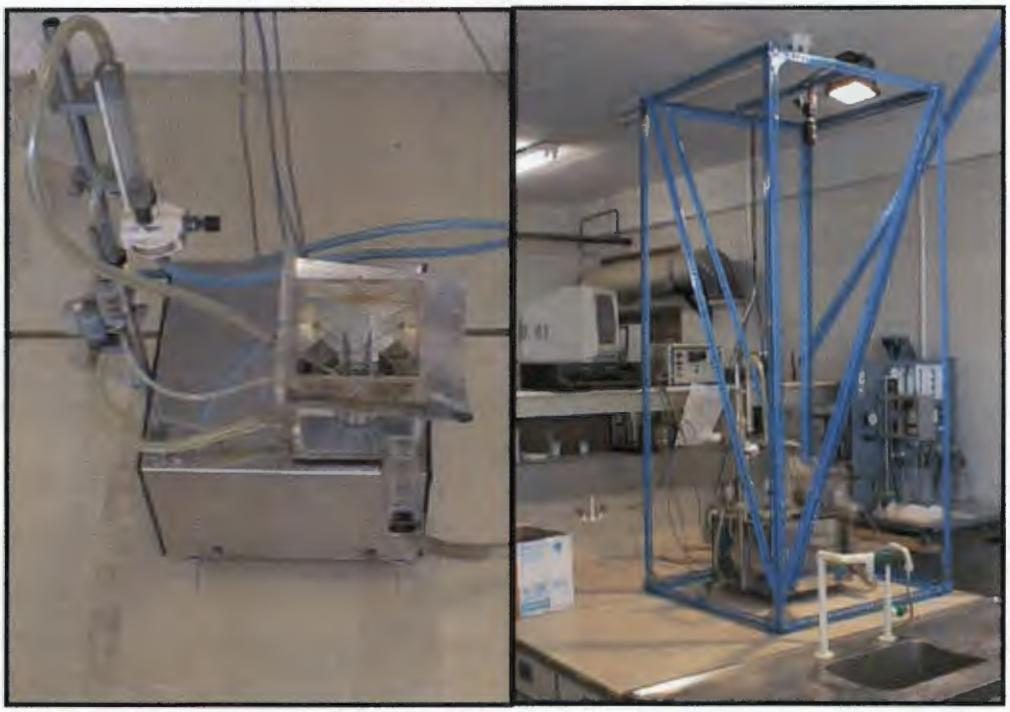

Figure 3.5 (a) and (b): The bottom driven Leeds flotation cell used in the batch flotation programme. (a) shows a close-up of the flotation cell, while (b) shows the mounting frame in position on which the camera and spotlight were mounted.

Images of the flotation tests were captured using a *Cosmicar* CCD camera, the signal of which was recorded directly to SVHS video tape, using a *Panasonic SVHS VCR*. Lighting was provided by a single 500W halogen spotlight, mounted directly above the flotation cell at a distance of 1.5m, as can be seen in the above figure.

3.2.6 Test Procedure

The experimental procedure employed was as follows:

1. 1 kg of dry ore was placed into the stainless steel mill (containing 20 stainless steel rods). 500 mℓ of tap water was then added. 12 g/t SIBX was then added (0.6 mℓ of a 2% solution), followed by 18 g/t *Senkol 5*, a dithiophosphate (18 µl undiluted). The mill was then sealed and milling commenced. The milling time for the required grind of 40% passing 75 µm was determined to be 6 minutes and 20 seconds. The milled

slurry was then washed from the mill and the grinding media, into a plastic bucket, using wash water bottles

2. The pulp was then transferred from the bucket into the flotation cell, again using wash water to facilitate transfer. The flotation cell mechanism was started and the level control activated in order to bring the pulp level up to that required for the flotation experiment. This was set so as to give a distance between the pulp/froth interface and the weir of 3 cm, unless the test condition required otherwise.
3. A feed sample was taken by using a wide-mouthed syringe to draw approximately 50 mℓ of slurry out of the cell.
4. The first conditioning step (2 minutes) was commenced with the addition of the depressant (IMP4) at the level indicated in table 3.1 unless the test condition specified otherwise.
5. The second conditioning step (1 minute) was commenced with the addition of the frother (Dowfroth200) at the level indicated in table 3.1 unless specified otherwise.
6. Flotation was then initiated by turning on the air flow to the cell at a rate of 6 ℓ/min. After a 15 second period to allow the froth to build up, concentrates were recovered by scraping the froth that was proud of the weir into the sample pan, at 15 second intervals. The concentrate sample pans were changed so as to give concentrates representative of the following intervals: 1, 2, 4, 6 and 10 minutes after the initiation of flotation. Water was used to remove the solids from the weir lips and the scraping paddle. Separate wash water bottles were used for each concentrate gathered. These were weighed before as well as after the test to allow the water recovery to be calculated.
7. At the end of the tenth minute, flotation was terminated by closing the air supply to the cell.
8. A tail sample was then taken using a wide-mouthed syringe to draw approximately 50 mℓ of slurry out of the cell.
9. The concentrates were then weighed in their wet state, and then filtered on pre-weighed filter paper. The samples, including those of the feed and tails, were then placed into an oven set at 80°C, to dry overnight.
10. The following day, the samples were allowed to cool to room temperature before they were weighed on the filter paper. The solids were then removed from the filter papers, gently rolled to separate the grains, and then placed into the sample vials.

11. All samples were analysed at UCT for copper and nickel (by means of Atomic Adsorption, after complete digestion in hydroflouric, perchloric and nitric acids) and sulphur (by means of a *Leco* analyser).

The standard condition tests were conducted in quadruplicate to give an indicator of the reproducibility of the methods and procedures. All other tests were conducted in a random order, in duplicate for the purpose of metallurgical results. All the test conditions were then repeated once more for the purpose of video footage capture, to allow the offline analysis of the images.

3.2.7 Image Analysis

As stated above, the entire test programme was repeated in order to collect video footage for the purpose of image analysis. This was conducted at night, so as to minimise the possible influence of ambient light changes. Images were "grabbed" from the SVHS recordings at fifteen-second intervals, just prior to scraping. This was done so that the froth surface phenomena had time to develop before the surface was disturbed by the act of scraping.

The images were then analysed "off-line", using the techniques described in section 3.1.

A number of limitations, inherent to a small batch flotation system, were however experienced. These included the following:

- The 3l flotation cell produced a very limited froth surface area. This resulted in a small number of surface bubbles being available from which appearance information could be gleaned.
- In order to achieve experimental reproducibility, the layer of froth proud of the lip was scraped at regular intervals to produce concentrates. This mechanism of forced removal meant that the froth was not free to attain an equilibrium state, both in terms of surface appearance and movement. It therefore remained to be seen whether the maturation and self-induced migration of a froth surface held additional information.
- The information gathered from the batch system is, by its nature, only indicative of discrete changes in the initial conditions. A continuous system, as is found in industrial applications, would show a dynamic response to a change made at any point preceding the observation point. Being able to *track* the response to a change in an operating variable, would obviously be of great value in the development of a system whose ultimate application would be on such a dynamic process.

The initial batch flotation programme aimed at scouting the manipulable operating parameters; to assess which variables had recognisable signatures on the surface of flotation froths. While this programme was successful in achieving its aim, it was apparent that the relevance of these findings should be assessed in an industrial environment. This lead to the decision to conduct experiments, focusing on the parameters identified in the laboratory, on an industrial flotation plant. This would also permit the analysis of a far greater area of the flotation froth surface than the 3l batch flotation cell allowed.

3.3 Plant Experimental Programme

3.3.1 Aim of the Plant Programme

The aim of the plant-based programme was to extend the findings obtained on the 3l batch flotation cell, while at the same time assessing the ability of the machine vision system to detect changes in variables (similar to those made in the batch flotation programme) on an industrial flotation application.

The section that follows will describe the flotation plant that hosted the experimental programme, describe the typical mineral deportment around the flotation bank on which the experiments were conducted, and the architecture of the machine vision system employed to gather the froth appearance information. The procedures employed in the various tests carried out during the plant-based campaign, as well the reasons for conducting the experiments will also be described.

3.3.2 Description of Process flow

The following diagram is a schematic of the part of the Amandelbult Merensky Concentrator on which the experiments were carried out.

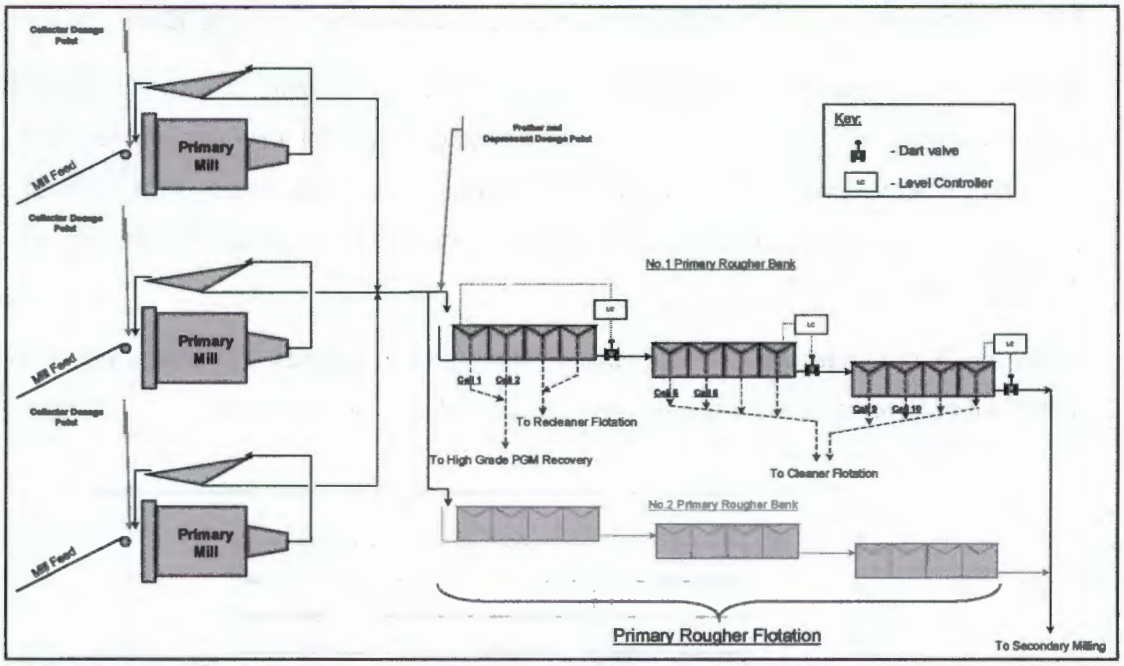

Figure 3.6: Schematic of part of the Amandelbult Merensky Concentrator on which the experiments that comprised the plant-based programme where carried out. The diagram shows the primary mills and the primary roughers, prior to secondary milling.

The experimental programme in the plant-based campaign was conducted on No. 1 Primary Rougher flotation bank of the Merensky concentrator. The slurry that is treated in the primary rougher flotation section originates from the primary milling circuit, which comprises three semi-autogenous mills operating in closed circuit with vibrating screens. The screen oversize is returned to the mills and the screen undersize is the flotation feed. Collectors are added at each mill's inlet. The flotation feed is then divided into two streams, and each of these streams is treated by one of the primary rougher flotation banks. Depressant and frother are dosed at the head of each flotation bank. The primary rougher banks each consist of three four-cell sub-banks of 14 m^3 *Wemco* flotation cells. Each sub-bank has its own level measurement and control device.

The concentrates collected from the first two cells, in each primary rougher bank, are of an exceptionally high grade and are processed in a specialised circuit aimed at recovering a very high grade PGM concentrate, which represents one of the concentrator's final products. Cells 3 and 4 produce a fairly high grade concentrate, which is routed to the *recleaners* for further upgrading by flotation. The concentrates from cell 5 to 12 are combined for further treatment in the *cleaners*, the concentrate from which is itself exposed to flotation again in the *recleaners.*

The tailings product from the primary rougher flotation circuit is milled further in the secondary milling circuit before receiving further flotation in the scavenger flotation circuit.

3.3.3 Typical Deportment of Minerals around the Rougher Flotation Bank

Key to the understanding of the nature of the flotation process that forms the subject of this part of the overall study, is an understanding of the mineral deportment around the process. The following mineralogical information has been taken from internal reports and is presented with the kind permission of the Anglo American Platinum Corporation (Pty) Ltd. (AMPLATS).

In terms of sulphide deportment, the following graph gives the mass percent of the dominant sulphides in the various streams around the rougher bank.

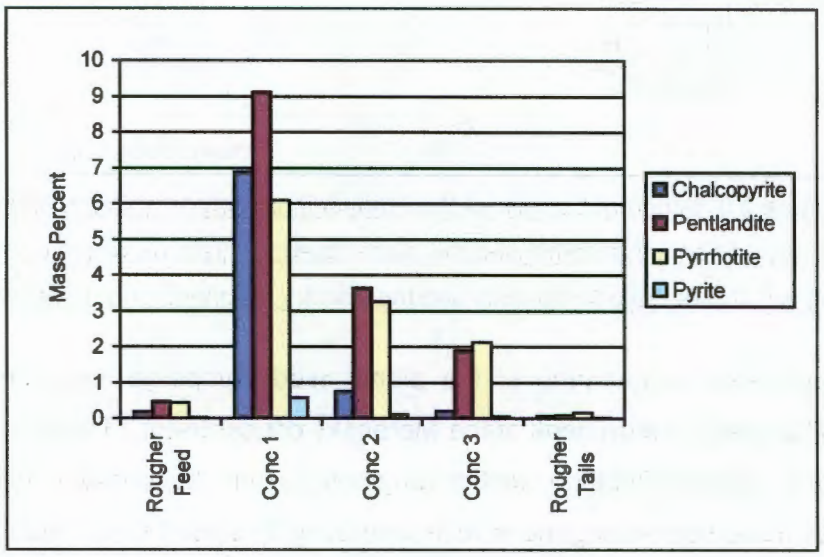

Figure 3.7: Sulphide distribution in the streams around the Amandelbult Primary Rougher bank (reproduced using data from Rixom, 1993.)

It is clear that all sulphides show the greatest abundance in the first rougher concentrate, which is taken from the first two rougher cells

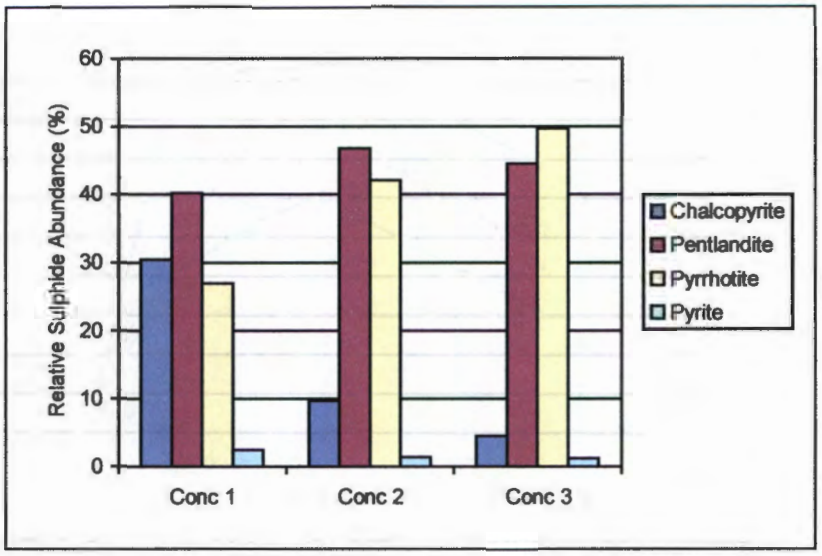

Figure 3.8: Relative sulphide abundance in the concentrates of Amandelbult Primary Rougher bank (reproduced using data from Rixom, 1993.)

Comparing the various sulphides with each other shows that chalcopyrite enjoys its greatest recovery early on in the process, while pyrrhotite is far slower to respond and forms the majority of the sulphides recovered at the end of the flotation process. Pentlandite is recovered fairly consistantly throughout the flotation bank, showing a slight peak in recovery in concentrate 2, when compared to the other sulphides.

With respect to sulphide recovery within the various size fractions the following graph shows the recovery of each species with respect to the total amount of each sulphide present within each size class, in the first rougher concentrate.

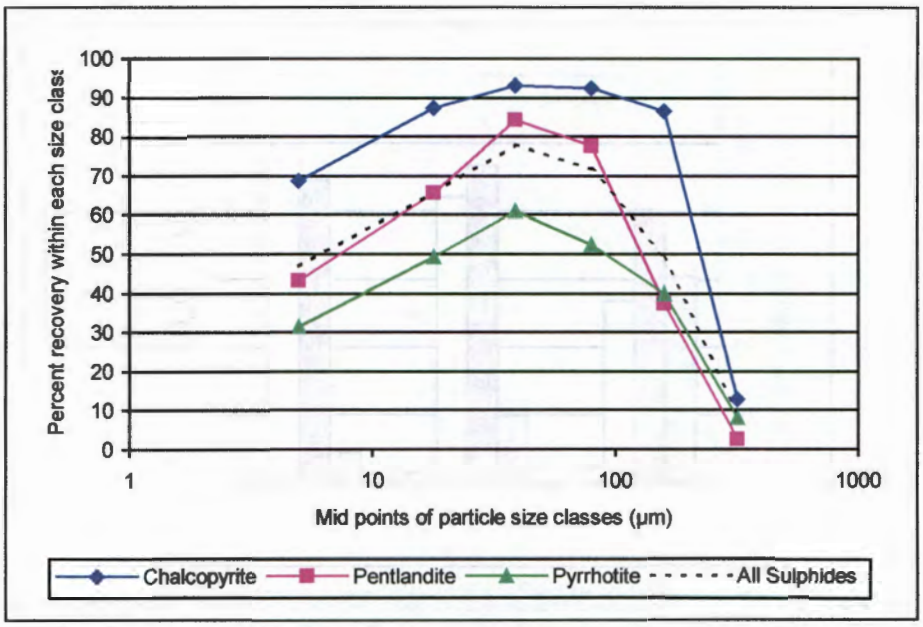

Figure 3.9: Sulphide recovery within each size class in the first concentrate of the Amandelbult Primary Rougher bank (reproduced using data from Rixom, 1993.)

From the above graph it can be seen that the best sulphide recoveries are in the size ranges between 53 µm and 106 µm. However, 60% of the liberated sulphides in the rougher feed (which in turn account for 76% of the total sulphides in this stream) are larger than this. Furthermore, it is clear that chalcopyrite enjoys by far the highest recovery in all size fractions. The chalcopyrite size-by-size recovery is followed by pentlandite and pyrrhotite, respectively.

The inclusion of the "all sulphides" series in the figure 3.9 allows interesting inter mineral comparisons to be made. In particular, while it is clear the on average the sulphides have an "optimum size recovery window" between 25 µm and 106 µm, chalcopyrite still enjoys good recoveries in a further size fraction above this window, notably that between 106 µm and 212 µm.

The following graph shows the gangue mineralogy of the various streams around the rougher bank.

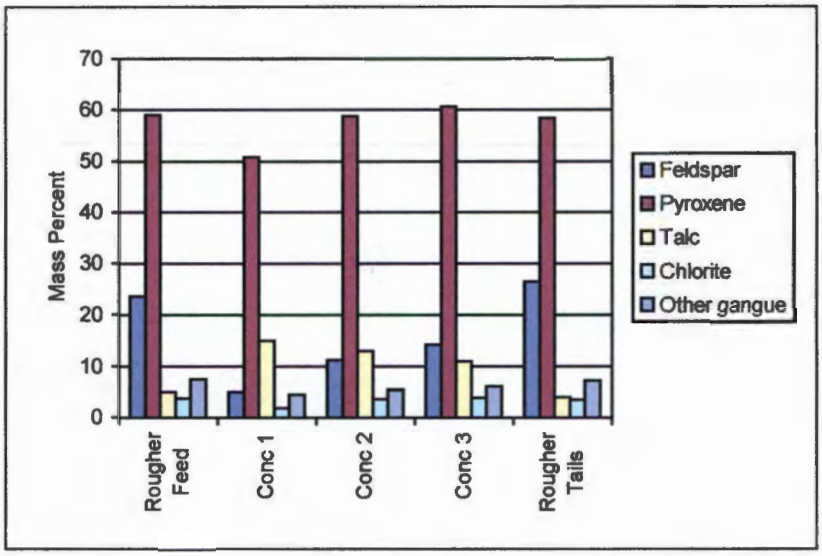

Figure 3.10: Gangue Mineralogy and Deportment around the Amandelbult Primary Rougher bank (reproduced using data from Rixom, 1993.)

Of the total free gangue present in the concentrates, Rixom (1993) states that the majority of the particles are composite particles of pyroxene and talc. Furthermore, free monomineralic gangue particles of pyroxene, talc and chlorite are said to show signs of positive recovery. This trend can be seen in figure 3.10, above. Rixom goes on to state that these minerals show positive recoveries in the size fractions below 53 µm.

3.3.4 Image analysis system architecture and observation points

As the plant programme was to build on the work conducted during the batch flotation programme, a number of the findings of the batch programme were carried forward to the planning of the plant programme. One such finding was that a single point-in-time observation of a batch flotation test was very limited in the information that could be inferred about the relative level of the process variable that was being assessed. A far better indication of which process variable was at a sub-optimal level could be achieved if surface appearance characteristics could be compared between tests throughout the duration of the test. With respect to a continuous type operation, this implies that the process should be observed at a number of different positions down the length of the flotation bank (i.e. at positions that represent a range of total flotation residence times).

During initial planning discussions, Amandelbult's technical staff recommended that the first cell of each sub-bank be avoided as observation points. The reason for this being that the incoming stream (into the first cell) caused disturbances that were clearly visible

on the flotation froth surface. For this reason, the second cell of each sub-bank was identified for observation using the machine vision system. The cameras were thus installed over cells 2, 6 and 10; which were then representative of the beginning, the middle and the end of the flotation process respectively. The following diagram shows the positions of the observation points on the flotation bank:

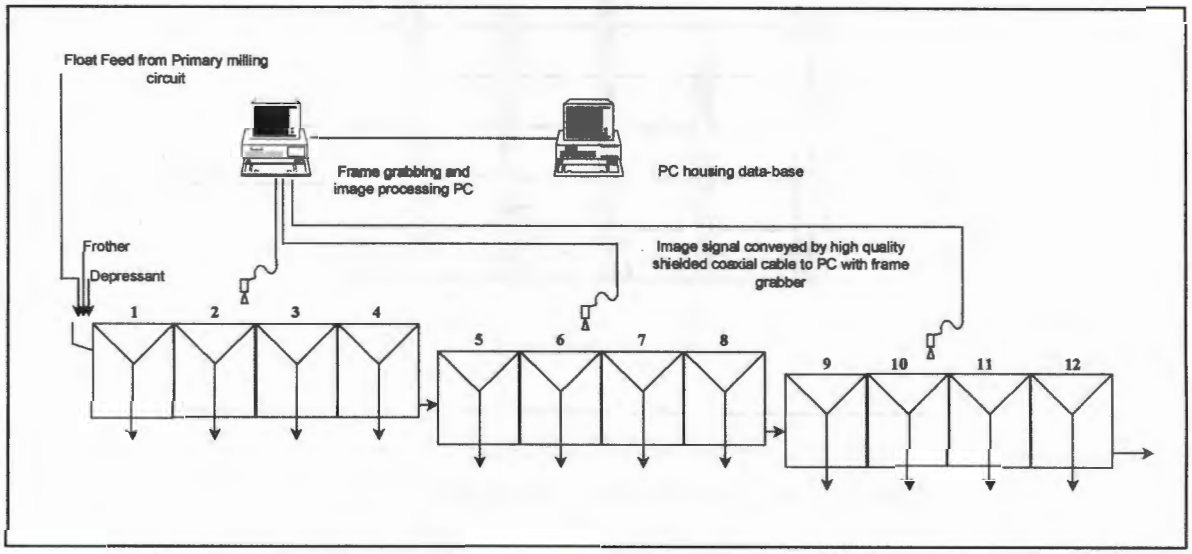

Figure 3.11: Diagram showing the positions that were identified for machine vision observation, down the length of the flotation bank.

The camera assemblies comprised: the camera itself (a *Watec 202-B* CCD, which generates a television quality PAL signal), a power supply for the camera (12V DC) and the lens (*Vicon 12-60mm zoom lens with auto iris function to compensate for light intensity)*. The zoom and the focus of the lenses were remotely controllable allowing adjustments to be carried out after installation of the assemblies.

In order to protect the camera assemblies, they were housed in dust and water proof camera housings. The following figure shows the camera housing as well as the various pieces of equipment that comprised the camera assemblies:

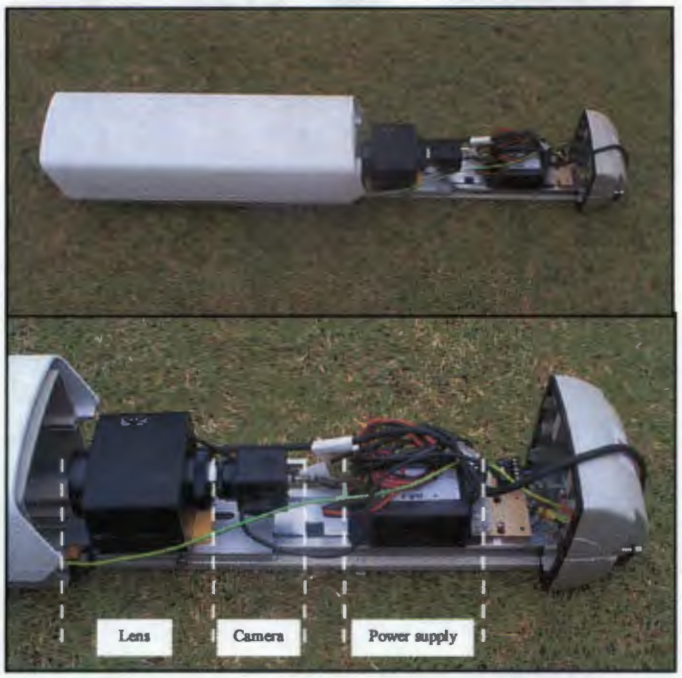

Figure 3.12: Camera assembly as used in the plant-based campaign, showing the lens, camera and power supply.

Lighting was provided by a single 500W halogen spotlight mounted in close proximity to the end of the camera housing, so as to minimise the formation of shadows in the area of focus. The entire installation was mounted approximately 2.5 metres above the flotation froth as to minimise the impact that having the system installed would have on the day to day operation, cleaning and maintenance of the flotation bank. The installation above one of the cells can be seen in the following figure:

Figure 3.13: Camera assembly and spotlight mounted above one of the rougher cells on the Amandelbult Primary Rougher bank.

The video signals were conveyed from each of the camera assemblies to the "frame gabbing and processing computer" by means of high grade shielded co-axial cable (*RG – 59 B/U*). The computer used was an *Intel Pentium II* based 400 megahertz computer, fitted with a *Matrox Meteor II* frame grabbing card which can support up to four video signal inputs. This computer performed the tasks of sampling (frame grabbing) the video signals as well as processing the images to extract the appearance information (using the algorithms described in section 3.1). A second computer (of the same specification) was used to store appearance information, as well as some of the images gathered during the programme (as can be seen in figure 3.11, above).

3.3.5 Procedures

3.3.5.1 Error and Plant Fluctuation Analysis (ANOVA)

Aim

Process fluctuations, as are typically experienced on an industrial flotation plant, confound the use of traditional reproducibility tests to quantify the errors encountered in the experimental programme. For this reason, a separate sampling exercise was conducted to assess the errors attributable to the following causes:

- Fluctuations in the flotation process during the course of the experiment;

- Errors attributable to the actual sampling of the process streams, as well as the biases imposed during the initial stages of sample preparation (such as filtering, drying and coarse screening of the sample before sub-sampling for analysis);
- Errors incurred in the practice of "sub-sampling", which is undertaken to provide samples of reasonable mass for analysis, as well as providing back-up samples;
- Errors due to reproducibility of the analysis technique, which includes errors attributable to the inherent nature of material analysed.

In order to be able to compare the compounding errors from a number of sources, a "nested analysis of variance" experiment was carried out on one of the process streams sampled during the plant campaign. The intention was to provide adequate data to perform a hierarchic analysis of variance. Descriptions of such tests can be found in most general texts on statistics. The notes by Taylor (1990) and Napier-Munn (1996) were used in the planning of the test as well as the analysis of the data.

The stream chosen for the exercise was the concentrate stream from the second cell of the Primary Rougher Bank, which is of a relatively high 4E PGE grade. Lotter (1995) describes a number of complicating phenomena in the analysis of such high grade material, especially when the typical analyses for 4E PGE (notably fire assay methods) are employed. It was therefore felt that conducting the experiment on this stream would furnish the most detailed information with regard to the errors that could be encountered during the campaign.

Procedure employed

The following method was employed in generating the information needed for the exercise:

- Four sets of samples were taken over a period of 45 minutes. *This would provide an indication of the errors associated with short-term process fluctuations that could take place during the course of a sampling exercise.*
- Each set of samples consisted of two duplicate samples, which were taken by alternatively emptying the sample cutter into each of the two sample buckets, until an adequate volume of sample had been collected. *Comparison of the results between these duplicates would provide an indication of the errors typically incurred during sampling, as well as those associated with initial sample preparation. By "initial sample preparation", it is meant the operations of filtering, drying and coarse screening of the sample.*

- Each duplicate sample was then sub-sampled into four samples of approximately equal mass, using a *12-way spinning riffler*. These were then submitted for analysis (for 4E PGE, copper and nickel) in a random order, to eliminate the possibility of systematic errors during analysis. *The combined errors associated with sub-sampling and chemical analysis, would therefore also be highlighted.*

3.3.5.2 Mass Balance Surveys

Aim

The final procedure (to be described below) gives a description of the step tests conducted to provide information about the response of the flotation system to known changes in operating variables. The procedures employed during those tests concentrated exclusively on the performance of the flotation cells being observed by the machine vision system. In order to place the performance of the observed cells into context with respect to the performance of the entire flotation bank, three surveys were conducted to provide a mass and metallurgical balance around the flotation bank.

Procedure

The procedure employed was quite typical of surveys around a single flotation bank, and involved the following steps:

Analysis samples:

1. The flotation feed, concentrates (including those from each cell as well as the combined concentrates) and tail were sampled at half hour time increments, spanning one and a half hours (4 increments).
2. All increments from a particular process stream were combined into a single sample bucket. The sample was then weighed (wet), filtered, dried and then weighed again to provide an indication of the solids content of each sample.
3. Each sample was then screened through a 2-mm aperture screen to break the lumps that had formed as a result of the drying process. The sample was then sub-sampled using a *12-way Spinning Riffler* to provide two samples, one of which was submitted to the Analytical Services Department at AMPLATS Research Centre (Germiston) for analysis for 4E PGE, copper (total), nickel (total), iron (total) and sulphur (total). The remaining sample was retained as a *back-up* sample.

Stream flow rate determination:

1. The flow rate of the flotation feed stream was estimated using the volumetric flow rate and density information as logged by the site's SCADA (Supervisory Control And Data Acquisition) system.
2. The flow rates of the concentrate streams from each cell were measured using the "bucket and stopwatch" method.

All data (both flow and grade figures) were later subjected to a smoothing procedure, which manipulated the values to provide consistency over the entire bank. The smoothing procedure made use of *Microsoft Excel's "solver"* function to find the best solution set to a set of matrices that described the process's flows and grades, to which estimated confidences had been assigned.

3.3.5.3 Step Test Experiments

Aim

The main focus of the plant based programme was to provide information that might point to the relevance (or otherwise) of using a machine vision system to provide real-time information about the performance of an industrial flotation system. Possibly more importantly the tests were to provide an indication of the system's response to changes in operating variables (notably those typically used in the control of the flotation plant).

Procedure

The procedure employed aimed to gather information from each of the observed flotation cells for a particular process condition. Once it was felt that the process had attained steady state (purely by visual assessment), the following steps were carried out:

1. The concentrate from each observed cell was sampled to provide sample for chemical analysis.
2. The analysis sample was weighed (wet), filtered, dried and then weighed again to provide an indication of the solids content of each sample.
3. Each sample was then screened through a 2-mm aperture screen to break the lumps that had formed as a result of the drying process. The sample was then sub-sampled using a *12-way Spinning Riffler* to provide two samples, one of which was submitted to the Analytical Services Department at AMPLATS Research Centre (Germiston) for analysis for 4E PGE, copper (total), nickel (total), iron (total) and sulphur (total). The remaining sample was retained as a *back-up* sample.

4. The flow rate of the concentrate streams from each observed cell was measured using the "bucket and stopwatch" method.

Steps 1 and 4 were carried out at the time of the step test, while steps 2 and 3 were carried out after the test.

Once that above had been carried out, the process variable under investigation was changed to its new value and the process allowed a period of approximately three residence times (between 45 min and 1 hour) to attain steady state. Points 1 and 4 were then repeated, and followed by points 2 and 3 at a later time.

3.3.6 Analytical Techniques

The Analytical Services Department of AMPLATS Research Centre carried out the chemical analyses of the samples generated during the plant- based programme. The 4E PGE (Platinum, Palladium, Rhodium and Gold) analyses were carried out using the following fire assay method (Lotter, 1995):

- The precious metals are collected into a lead button, which the result of fusion of a measured mass of the sample at approximately 1100°C after fluxing with sodium carbonate, borax and assay litharge (lead oxide) and the addition of a reducing agent (maize meal).
- The lead button is then heated to 1100°C under oxidising conditions, on a cupel made of calcined magnesite. The cupel adsorbs the lead oxide formed in the process and the precious metals (now largely only Pt, Pd, Rh and Au as the other elements volatilise off) remain as a small "prill". The prill is then weighed and the 4E PGE grade is calculated.

Copper, nickel, iron and sulphur analyses were conducted using an X-ray based method.

4 Batch Flotation Programme: Results and Discussion

The following section presents and discusses the results gathered during the batch flotation programme. The batch flotation programme concentrated primarily on the influences that changing the depressant and frother dosages had on the batch flotation system. A second phase of the programme explored the influences of a larger group of operating variables, such as air flow rate, froth height collector dosage and depressant type. All results from the programme are detailed in APPENDIX B.

The results from the first part of the batch flotation programme will be presented and discussed here, as the depressant and frother dosage and their influences on the flotation system form the focus of this thesis. The results from the second part of the batch flotation programme are presented in APPENDIX BIII, but will not be discussed further as they fall outside the scope of this thesis.

4.1 Trends observed on the surface of the flotation froth by the machine vision system.

The purpose of digital image analysis, in the context of this project, was to quantify visually apparent phenomena, should they occur. However, before digital analysis was carried out, a qualitative analysis was conducted by comparing images collected during similar tests, in order to assess whether real changes in appearance were indeed induced.

The results from the digital analysis will be presented in a way that highlights the trends visible to the naked eye. For this reason qualitative assessment will be discussed first, and will be followed by the digital analysis results.

4.1.1 Qualitative Assessment.

The table, below, contains typical images as gathered during the batch flotation programme. The two tests presented are the "standard" and the "no depressant" tests. These two tests were chosen as they are directly comparable (identical conditions, apart from the change in depressant dosage).

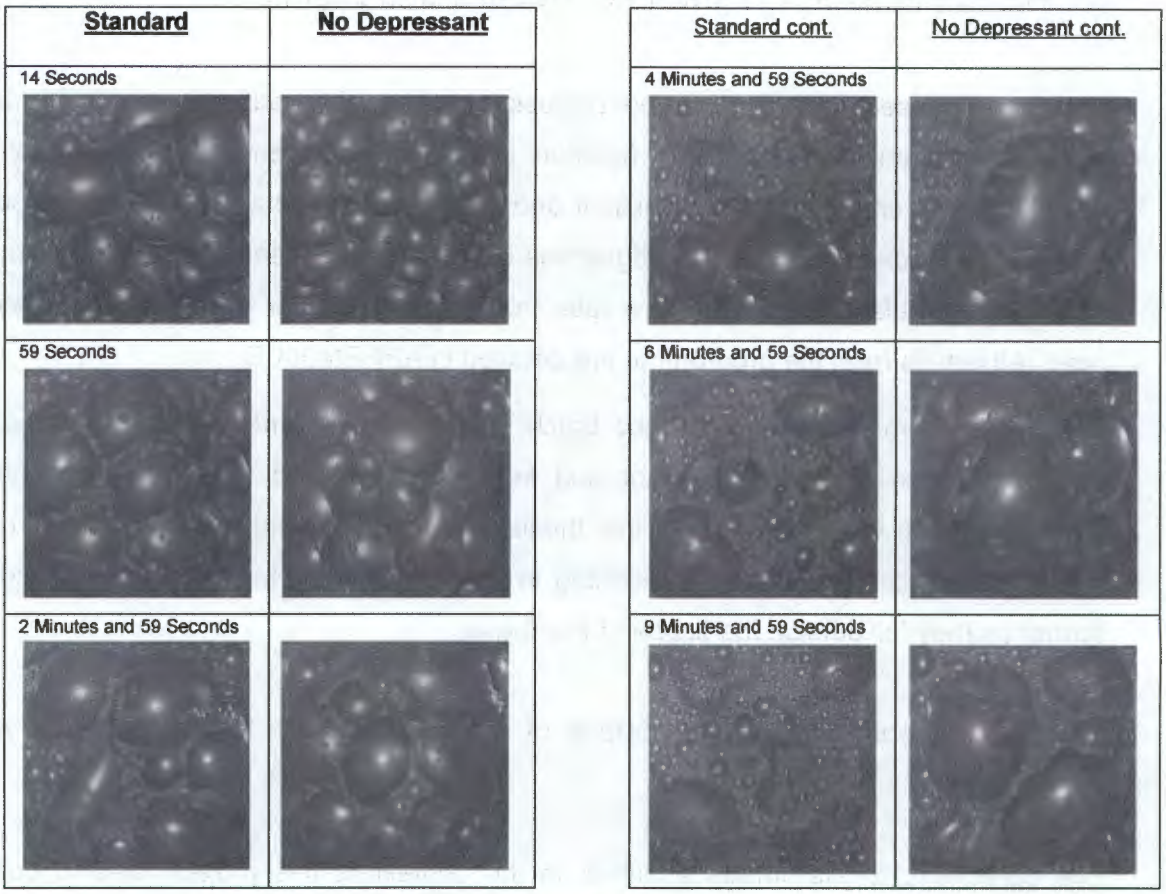

Table 4.1: Images from tests: 'Standard' and 'No Depressant'

Clearly, there are noticeable differences between the appearance of the froth surfaces of the two tests compared above. The following are among the many that could be identified:

- The frames at 14 seconds show that the 'no depressant' test froth surface is covered with fairly uniform large polyhedral bubbles, while the 'standard' test shows large as well as small bubbles. The trend is carried on to the frame captured at 59 seconds, where the 'standard' test shows small bubbles in the regions between the larger bubbles, as well as a lot of detail (smaller bubbles) on the surface of the larger bubbles.
- At 2 minutes and 59 seconds, the 'standard' test starts to show a bimodal distribution of bubble diameters. In the 'no depressant' test small bubbles start to appear in between the larger bubbles.
- As the tests run to completion the most apparent difference between the two tests is the presence of large transparent bubbles in the 'no depressant' test. The surface of

the 'standard' test is however covered with finely textured small bubbles, with very few larger bubbles.

4.1.2 Quantification of Surface Appearance.

The following image, taken from the 'standard' test condition (at 2 minutes and 59 seconds), is an example that describes the methods employed within the machine vision system to quantify trends detectable with the naked eye:

Figure 4.1: Typical froth image.

The above image shows a distribution of bubble sizes that span a considerable range. It is apparent that there is a bimodal distribution of bubble sizes present and clearly, an average bubble size here would not adequately describe the froth surface appearance. The challenge was therefore to preserve the nature of the distributions of bubble sizes in the images, while being able to highlight trends. The strategy followed involved dividing the distribution of bubble sizes into three arbitrarily chosen bubble size classes - small, medium and large bubbles, according to the sizes in table 4.2 below. The data was then represented by the fraction of the total image area that each of these size classes occupied[1].

Qualitative Size Classes	Bubble Area Intervals $(Pixels)^2$	Bubble Area Intervals cm^2
Small	0 – 250	< ca 0.6
Medium	251 – 625	ca 0.6 < and < ca. 1.0
Large	626 – 5000	ca.8.0 to the largest detected

Table 4.2 Qualitative Bubble Size Classes

[1] This strategy was suggested by Prof. G de Jager of the UCT Dept of Electrical Engineering and UCT Minerals Processing Research Unit, June 1998.

Figure 4.2 below, shows the plots of the relative surface area coverage, attributable to the three bubble size classes, for the 'standard' and 'no depressant' tests. These are the same tests as were compared qualitatively, above.

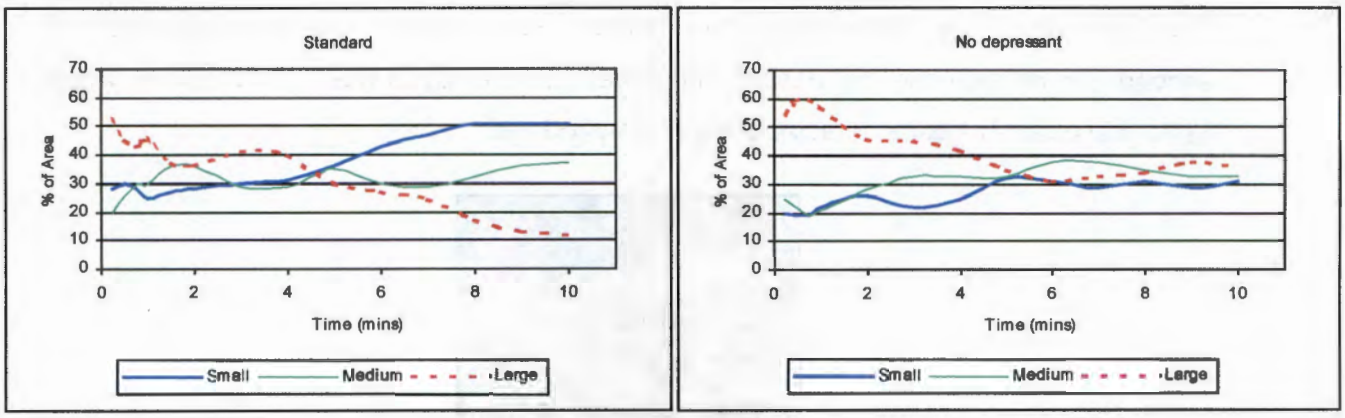

Figure 4.2: Comparison between the image analysis results for the "standard" and the "no depressant" tests.

When considered in conjunction with the images in table 4.1, the trends that are visually apparent can also be seen in the plots of the image analysis results. In particular, when considering the 'standard' test, in the above figure the dominance of the large bubbles quickly giving way to increased area coverage by the smaller bubbles. The end of the test shows that the larger bubbles cover a small fraction of the area, while the small bubbles cover the greater part of the total area.

The "no depressant" test in figure 4.2, shows the large bubbles dominating at the start of the test, with the small and medium bubbles gaining in their contribution to the coverage as the test progresses. The end of the test sees all three bubble classes occupying approximately equal proportions of the surface area. The last point is surprising when comparing this result to the images in table 4.1. The reason for this can be explained by considering the following images along, with the resulting analysis of the images:

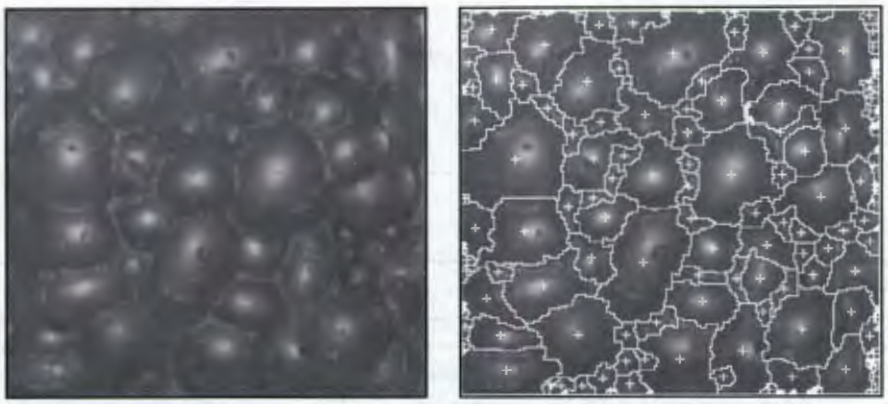

Figures 4.3 and 4.4: Good segmentation - original image and segmented image respectively, 'no depressant' 14 seconds.

Figure 4.3 can be considered a good froth, from an image processing point of view, in that the bubbles are well defined and are fairly uniform in size. The resulting segmentation achieved is good as shown in figure 4.4, with the digital image analysis algorithms detecting the detail fairly well.

This however is not the case for the following set of images:

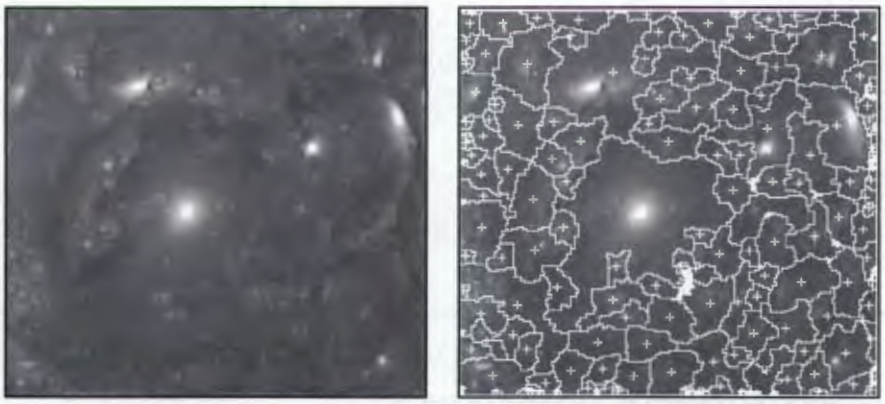

Figures 4.5 and 4.6: Poor segmentation - original image and segmented image, respectively, 'no depressant' 6 minutes 59 seconds

Figure 4.5 shows a number of large transparent bubbles. This transparency causes the next layer of smaller bubbles to be visible. In addition to this, there are small bubbles visible on the surface of the larger bubbles. The combination of the above results in the larger bubbles being 'oversegmented'. In the subsequent analysis of the image, the contribution of the larger bubbles to the total surface area coverage will therefore be underestimated. Nevertheless, the clear differences that can be seen in figure 4.2, which can be related to the trends seen in table 4.1, suggests that the analysis presented by the machine vision system is capable of detecting and quantifying *changes* in surface appearance.

The trends, seen at the standard frother dosage (where the appearance of the surface of the froth is dependent on the depressant dosage), can again be seen in the following plots at 'high' frother dosages:

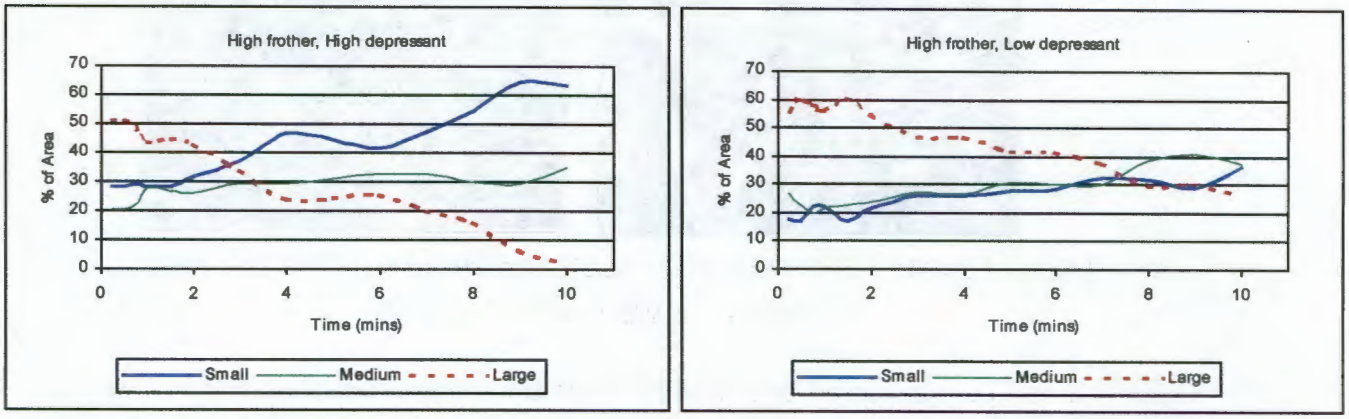

Figure 4.7: Comparison of image analysis results between high and low depressant dosages at high initial frother dosages.

On comparison of the tests at either standard or high depressant dosages in figures 4.2 and 4.7, it becomes apparent that the differences between the area coverage attributable to the large and small bubbles emerge towards the end of the tests. A similar comparison of the tests at either zero or low depressant dosages (again in figures 4.2 and 4.7) shows that the area coverage differences are evident at the beginning of the tests.

The following graphs compare the tests at low initial frother levels:

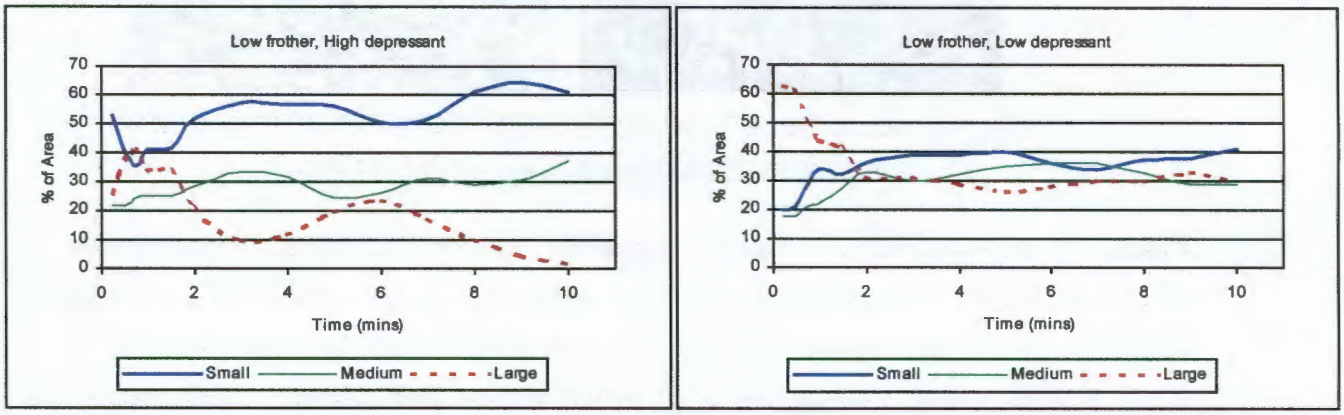

Figure 4.8: Comparison of image analysis results between high and low depressant dosages at low initial frother dosages.

The trends discussed above with respect to relative depressant dosage, for the figures 4.2 and 4.7, can be seen in the figure 4.8. This confirms the dependence of the area coverage attributable to the various bubble sizes, on the initial depressant level at a particular frother dosage.

Bearing in mind that depressants are added primarily to prevent the talcaceous type minerals from floating, it stands to reason that the dependence of the froth structure on depressant dosage lies in the influence that the depressant has on the talc minerals. There are a number of mechanisms with which the presence or absence of talc in a flotation froth might lead to marked differences in structure. Fine talc particles tend to have a plate-like structure (Hey, 1999), which according to Dippenaar (1982a) might retard the drainage from a water film. By retarding the drainage, film thinning is slowed (thinning would result in film rupture given adequate time). The presence of talc would therefore lend a degree of stability to the froth. This in turn would allow the larger bubbles on the froth surface to withstand rupture.

A second possible mechanism for the stabilisation of froth films by talc lies in the concept that surface charge on the talc particle is thought to be unevenly spread (Harris, 1998). The result is a particle that has a heteropolar nature (much like a frother molecule) which could interact with both the water and the air phases. It follows then that talc's presence at the air-water interface would then also slow drainage of the water out of the froth phase, thus retarding film thinning to a point where rupture would occur.

The dependence of the froth surface appearance on the initial frother dosage is not as obvious as that seen for the depressant. The following two figures compare the influence of the frother dosage:

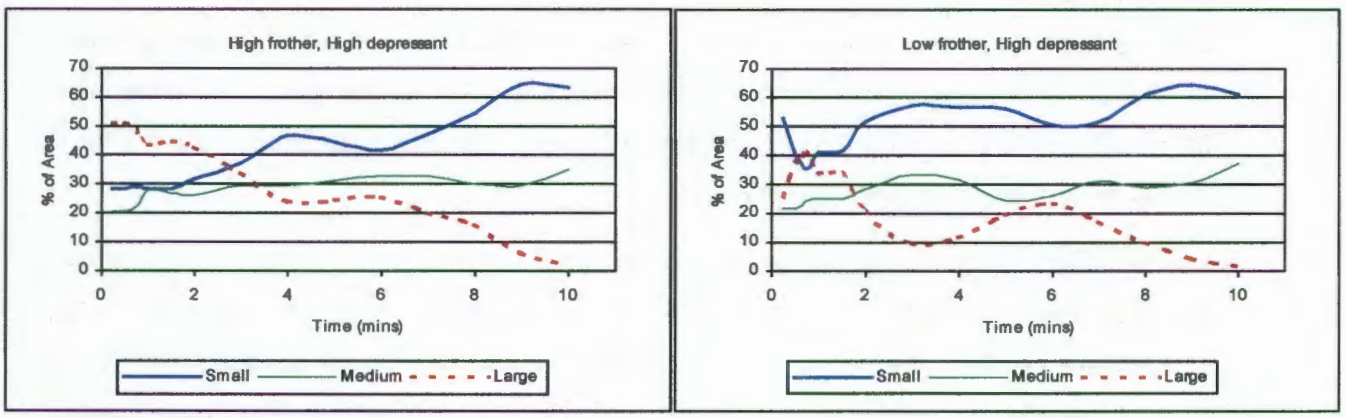

Figure 4.9: Comparison of image analysis results between high and low frother dosages at high initial depressant dosages.

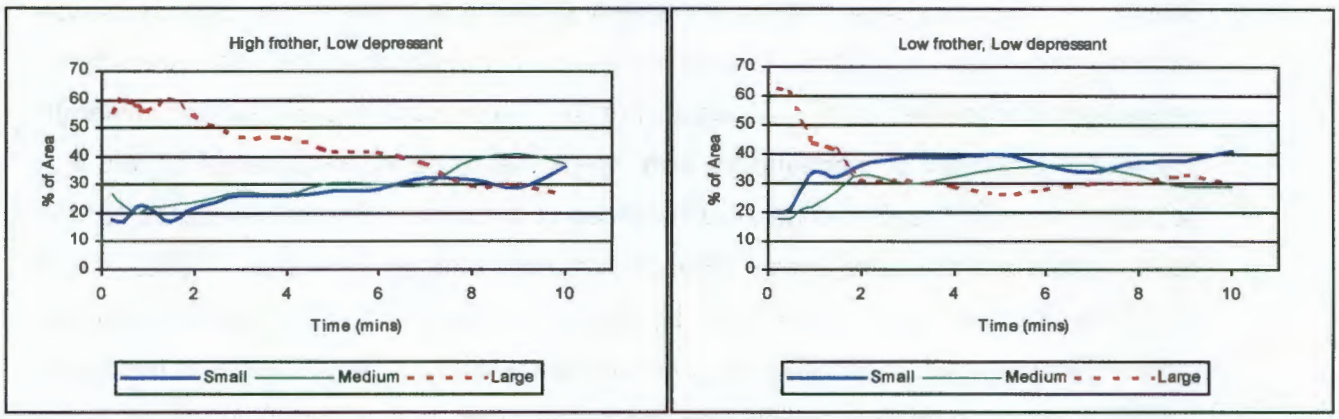

Figure 4.10: Comparison of image analysis results between high and low frother dosages at low initial depressant dosages.

Comparison of Figures 4.9 and 4.10, which compare tests with different frother dosage at comparable depressant dosages, shows that it is indeed depressant dosage that determines the final froth structure. In contrast to this, changing the frother dosage appears to influence the rate with which the froth surface changes, from its initial to its final structure. The right hand sides of both figures 4.9 and 4.10, show that low frother dosages cause the froth appearance to change rapidly and that the final froth structure is reached within two to three minutes of the test commencing.

The reason for the observed rapid change in froth appearance may be that low frother dosages cause the films within the froth to lack stability. This lack of frother induced stability allows the nature of the particles within the froth to have a far greater influence on the sub-processes which define the froth structure. As the depressant is responsible for altering the nature of the solid particles' surfaces, the final froth structure appears to be dependent on the depressant dosage.

As the rapid changes in froth structure are not observed when the normal and high frother dosages are compared, it is postulated that a "critical frother dosage" exists, which lies somewhere between the normal frother dosage and the low frother dosage. Below this "critical dosage", a "frother starved" regime exists; while above it a "normal regime" is found, in which little additional change is noticed as the frother dosage is increased.

Of value is the fact that by tracking the *rate of change* of the froth surface structure, a machine vision system would be able identify conditions such as "frother starved" operation.

4.1.3 Summary of Key Findings with respect to the Froth Surface Appearance.

The following the trends observed were in the surface characteristics of the flotation froth:

- The appearance of the flotation froth was seen to be highly dependent on the initial depressant level.
- It was noted that the differences in surface coverage by three bubble size classes, were observed at the end of the tests with 'standard' and 'high' depressant dosages. In contrast, the 'low' and zero depressant tests showed the greatest differences at the beginning of the tests.
- With respect to the frother dosage, two regimes were observed and could be detected by the machine vision system: The first is a "normal" condition in which the bubble size distribution changes gradually throughout the test, from the start condition to the end condition. This regime was observed for tests in which the frother dosage was either at the standard condition or higher. The second regime observed is the "frother starved" or "sub-optimal" regime, in which a rapid change in froth appearance is seen in the early stages of the test, which indicates a marked instability inherent due to the absence of the stabilising influences of the frother. This phenomenon was observed in the tests conducted at a low frother dosage.

4.2 Metallurgical Response

Detailed tables containing the metallurgical results gathered during the batch flotation programme can be found in Appendix BII. The following tables summarise the metallurgical results with respect to changes in frother and depressant dosage:

Test Name	Solids	Water	Copper		Nickel		Sulphur	
	Recovery (%)	Recovery (g)	Recovery (%)	Grade (%)	Recovery (%)	Grade (%)	Recovery (%)	Grade (%)
Standard	3.96	65.01	76.72	1.12	35.55	2.37	53.93	4.31
No Depressant	4.28	73.75	76.75	0.99	33.33	2.04	47.48	3.85
High Frother High Depressant	4.52	114.45	76.14	0.81	38.21	2.11	58.78	4.17
High Frother Low Depressant	4.48	103.54	78.46	1.01	33.66	2.29	46.26	3.91
Low Frother High Depressant	1.26	10.25	51.30	1.95	12.87	2.79	25.24	6.21
Low Frother Low Depressant	2.02	22.90	49.21	1.21	16.26	1.93	33.91	5.55

Table 4.3: Final grade and recovery data for the initial batch flotation programme.

In the section that follows, data showing the reproducibility of the techniques used is given and is followed by the presentation of the salient aspects of the results from Appendix BII.

4.2.1 Reproducibility of the Batch Flotation Procedures

The following graph shows the mass recoveries of four replicate tests carried out at the standard condition, in order to assess the reproducibility of the batch flotation procedures as employed during the batch flotation campaign:

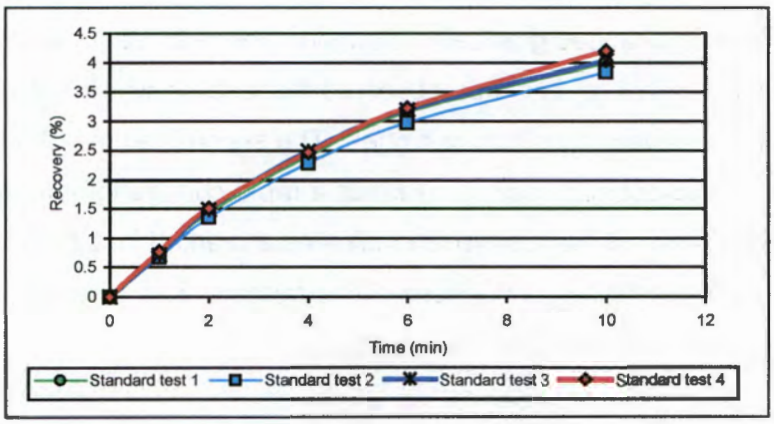

Figure 4.11: Dry solids recoveries from four tests carried out at the standard conditions, showing the reproducibility of the batch flotation techniques.

The above graph shows that the reproducibility of the experimental techniques is sufficient to allow comparison of the different conditions.

4.2.2 Copper

The flotation response of copper can be seen in Figures 4.11 and 4.12 below:

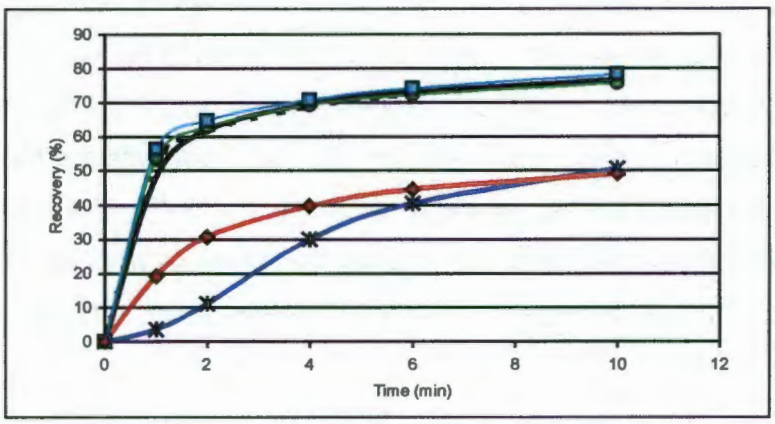

Figure 4.11: Copper recovery versus time curves for the tests in which frother and depressant dosages were changed (legend in Fig 4.12).

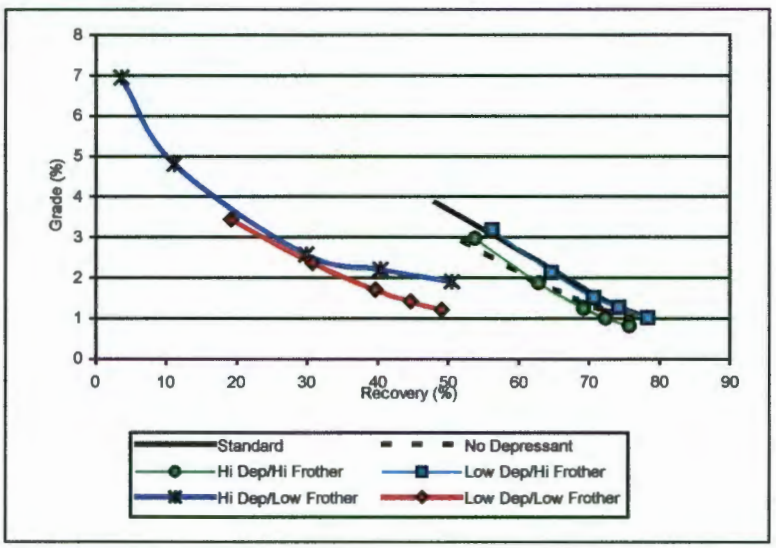

Figure 4.12: Copper grade versus recovery curves for the tests in which frother and depressant dosages were changed.

The copper recovery versus time graph (Fig 4.11) shows a grouping of the tests into two regimes: tests with the 'standard' and 'high' frother levels; and those with low frother level. A similar grouping is evident in the grade versus recovery relationships (Fig 4.12). This observation points towards operation in two distinct regimes: an 'normal regime' (at standard and high frother dosages) and a "sub-optimal regime" or "frother starved regime" (at low frother dosages).

The "frother starved" regime, at the low initial frother concentrations, shows evidence of *froth transport limiting* mechanisms. By this it is meant that at low frother dosages (i.e. the "frother starved regime") the froth is not stable enough to carry the valuable minerals

until they can be recovered over the weir. This is further attested to when considering the test in which the depressant dosage is increased at low frother concentration, which clearly shows a time lag before recovery starts to improve. What is seen here are the effects of only minimal froth stabilisation by the frother, which then allows the froth to be destabilised by other influences. One such influence could be the destabilisation of the froth by highly hydrophobic solids by the mechanisms described by Dippenaar (1982a). The high depressant dosage has prevented the talc from entering the froth, which (as discussed earlier) could lend a degree of stability to the froth. The time lag can then be explained by the argument that it is only after the highly hydrophobic solids (the added cause of froth instability) have been removed from the system that the recoveries start to improve (Harris, 1998).

A further point worth noting is that given adequate transport mechanisms (in other words if the flotation system is operating in the "normal regime" with respect to frother dosage), the copper bearing minerals tend to report to the concentrate in a very consistent manner.

4.2.3 Nickel

The results for nickel's flotation response for the tests concerning depressant and frother dosages show a similar groupings to those seen for copper, as can be seen in Figures 4.13 and 4.14, below:

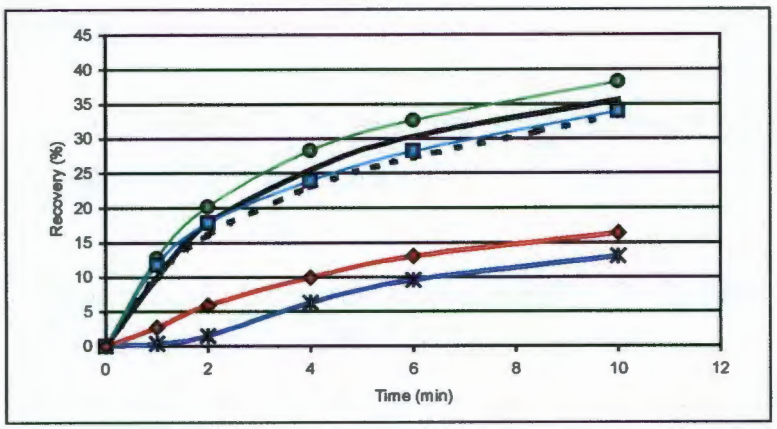

Figure 4.13: Nickel recovery versus time curves for the tests in which frother and depressant dosages were changed (legend in Fig 4.14).

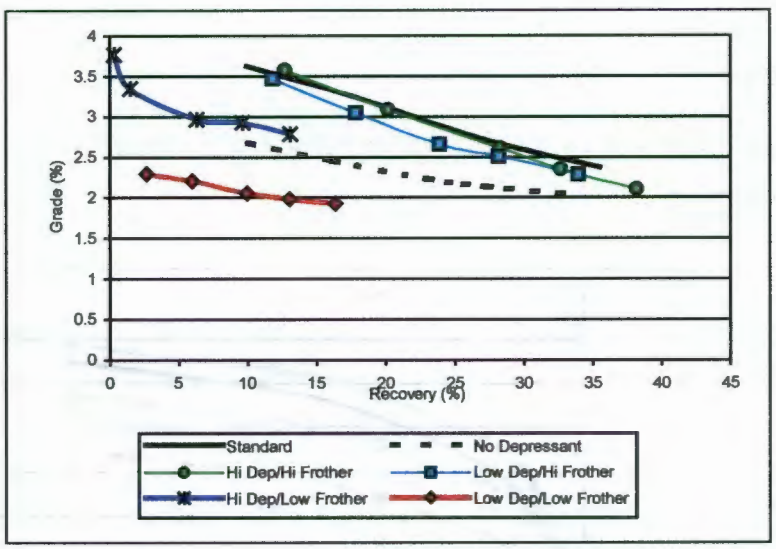

Figure 4.14: Nickel grade versus recovery curves for the tests in which frother and depressant dosages were changed.

It is immediately apparent that the nickel recoveries realised are far lower than those achieved for the copper bearing species. The reason for this is that unlike copper, nickel is found in the Merensky reef both in the sulphide form (most commonly as pentlandite, $(Ni,Fe)_8S_8$, which responds well to flotation), as well as a minor constituent of a number of gangue minerals such as olivine and serpentine (Hey, 1998), which are hydrophilic and are not recovered by flotation. Viljoen (1986) stated that the Merensky reef at Amandelbult (the source of the ore used in this programme) contained significant

amounts of olivine (see APPENDIX A for a brief geological description of the Amandelbult Merensky reef). The chemical analysis carried out measured the *total nickel* in the various flotation products. The flotation recoveries of nickel therefore appear to be low, primarily as only a fraction of the total nickel is in the readily floatable sulphide form.

As can be seen in recovery versus time curves (fig 4.13), there again seems to be a grouping into an "optimal regime" and a "frother starved regime", where the latter are the tests at low frother concentration. In addition to this figure 4.14 shows that the nickel bearing species benefit from the presence of depressant. At the standard and high frother dosages, the nickel bearing species seem to clearly benefit from higher depressant dosages.

The apparent benefit of the depressant could be due to a number of reasons. The first of the two most plausible arguments, is that the nickel sulphides are competing with floatable gangue species (such as talc) for bubble surface area. This implies that when the floatable gangue species are depressed, by difference the nickel sulphides will be preferentially recovered. The second argument is that the depressant is causing a cleaning of the nickel bearing sulphide surfaces (Harris, 1998).

4.2.4 Sulphur

The following graphs show the flotation response of the sulphur bearing species to the conditions tested:

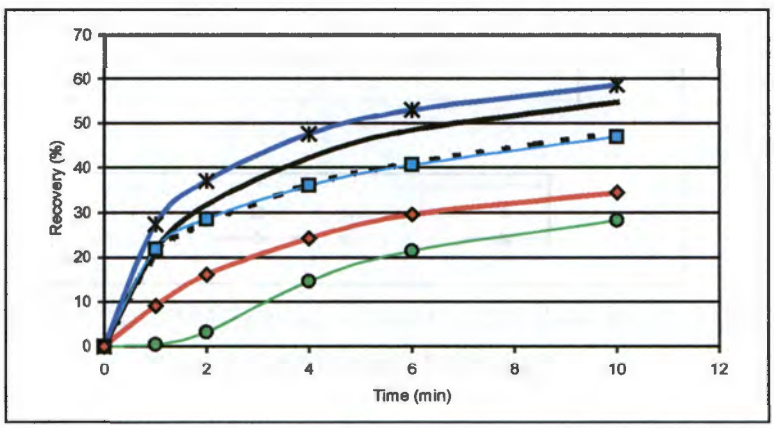

Figure 4.15: Sulphur recovery versus time curves for the tests in which frother and depressant dosages were changed (legend in Fig 4.16).

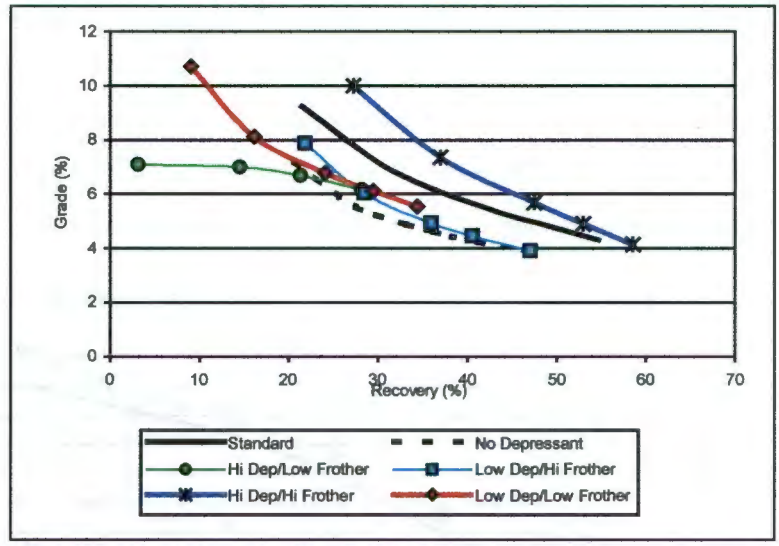

Figure 4.16: Sulphur grade versus recovery curves for the tests in which frother and depressant dosages were changed.

Figures 4.16 shows clearly that the sulphur bearing species respond well to the condition of high frother and depressant dosage, in that this condition shows a superior grade-recovery relationship. Apart from this many of the comments made about the benefits of higher depressant dosages with respect to the performance of the nickel bearing sulphide species can be made for the sulphur bearing species.

4.2.5 Water and Solids

The following graphs described the recovery of water and solids for the different conditions tested in the laboratory batch flotation programme:

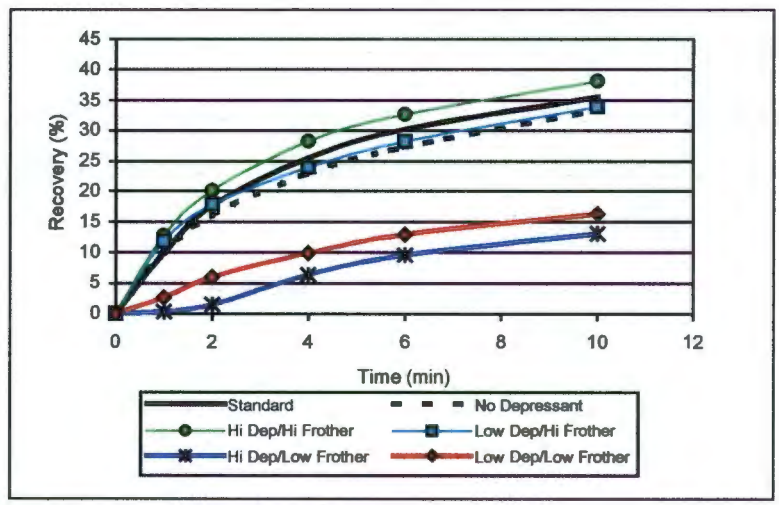

Figure 4.17: Water recovery versus time curves for the tests in which frother and depressant dosages were changed.

The water recovery versus time curves shown in Figure 4.17, shows groupings of the tests that are strongly aligned to the relative frother dosages applied. Furthermore, it would appear that when standard frother dosages or higher are applied, increasing the depressant leads to greater amounts of water being recovered, whereas the opposite seems apparent for frother dosages lower than the standard dosage.

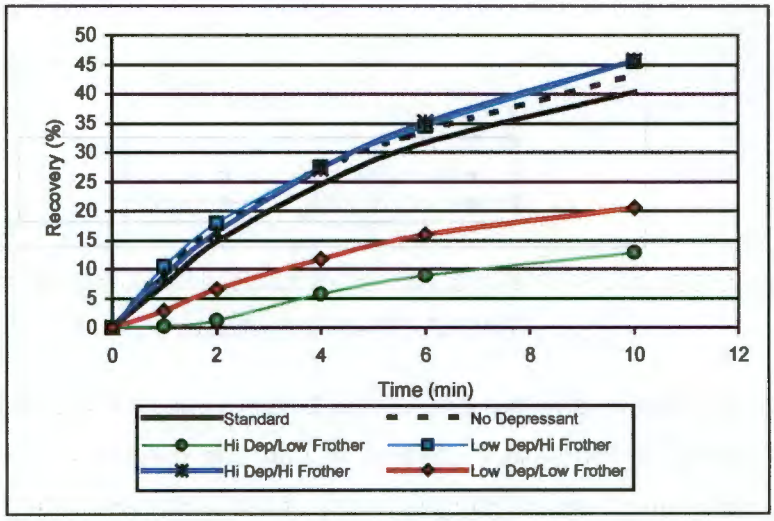

Figure 4.18: Dry solids recovery versus time curves for the tests in which frother and depressant dosages were changed.

Again there is a strong alignment of the curves in figure 4.18, with the relative frother dosage. In addition to this it would appear that decreasing the depressant dosage leads to higher solids recoveries.

4.2.6 Summary of the Metallurgical Results

To summarise the observations made to this point:

- The metallurgical results show that the tests in which the frother and the depressant were manipulated resulted operation representative of two regimes: a 'normal regime' and a 'sub – optimal regime'.
- The 'sub – optimal' regime is solely seen in tests with a low initial frother concentration, and is therefore thought to be indicative of froth limiting mechanisms. This is confirmed by the observed lag-times noticed for the 'low frother/high depressant' tests.
- In tests conducted in the 'normal regime', the copper bearing sulphide species respond to flotation in a consistent manner, regardless of an increase in the initial frother concentration or changes in the depressant dosage.

- The nickel recoveries were found to be low, primarily due to the fact that nickel in Merensky ore occurs partly in floatable species such as pentlandite and partly within gangue species with little or no response to flotation.
- Increased depressant dosages seem to be beneficial to the flotation of nickel bearing sulphides, when operation is in the 'normal regime'.
- All the points made above with respect to the nickel bearing species could equally well be made with respect to the sulphur bearing species.
- Water and solids recovery rates were found to be highly sensitive to the initial frother concentration.

4.3 Discussion of Key Findings of the Batch Flotation Programme

Of immense importance is the finding that changes in depressant dosage can be detected by means of the machine vision system. As the depressants' specific purpose is to prevent talcaceous gangue from floating, the depressant dependent changes in froth structure are therefore thought to be as a result of the presence or absence of talc in the froth. In addition to this, the depressant dosage was seen to play an important role in defining the metallurgical performance of the flotation system (particularly with respect to nickel and sulphur bearing species). Thus being able to detect when (and in what direction) the depressant changes, by virtue of its signature on the froth surface, holds promise for using a machine vision system for control purposes. This would however depend on being able to detect uniquely that the change in froth appearance is indeed due to the depressant dosage changing, while the other operating variables remain unchanged.

The two distinct regimes, which are dependent on the initial frother dosage, observed in metallurgical results alludes to the importance of ensuring that the frother dosage is kept above a "critical dosage". The results discussed above suggest that the only way of detecting whether or not the operation has moved into such a "frother starved" regime is for the rate of change in the froth surface appearance to be monitored. In the batch flotation system, this rate is with respect to time; however, in the context of a continuous system as found on an industrial operation, this would be with respect to position down the flotation bank. This alludes to the possible importance and benefit of placing more than one camera on a particular flotation bank.

In addition to the comments made above with respect to frother dosage, the increased instability brought about by increasing depressant dosage in the "frother starved" regime

further supports the concept that a froth's structure is to a large degree defined by the solids present in it. In this case in particular it is believed that in the absence of the stabilising effects of talc, the highly hydrophobic minerals present in the froth can cause destabilisation.

5 Plant Experimental Programme: Results and Discussion

5.1 Introduction and Description of Tests Conducted

During the plant-based experimental programme, three cells of the No. 1 Primary Rougher Bank of Amandelbult's Merensky Concentrator were identified for machine vision assessment in conjunction with metallurgical performance measurement. These were cells 2, 6 and 10, each being the second cell in the three four cell sub-banks that comprise the total Primary Rougher. Early in the analysis of the machine vision data it was found that the data gathered from cell 6 showed erratic behavior and was prone to "pluming" (an exaggerated upwelling of pulp which results pulp rather than a froth surface being visible). For this reason, it was decided to concentrate on cells 2 and 10 for both the image and the metallurgical performance data analysis.

In the sections that follow, the various salient aspects of the data collected during the plant campaign are presented. The results, as extracted from the machine vision database are described and presented. Following this, the errors associated with the various procedures and measurements carried out in the course of gathering the metallurgical performance data are briefly discussed (the complete results and analyses can be found in APPENDIX CI). The results of the metallurgical performance measurements are then presented in two parts: Firstly, a brief description of the mass and metallurgical balance around the Amandelbult Primary Roughers is given. This is then be followed by the presentation of the results pertinent to the tests conducted during the programme. Finally, relationships observed between the changes in the operating conditions imposed during the programme, their effects detected on the froth surface by means of the machine vision system; and their effect on the metallurgical performance of the system are presented.

The results from three of the five step tests conducted during the plant campaign will be analysed (the method employed during these tests is described in section 3.3.5). The tests that are to receive attention are those in which the frother dosage rate (1 test) and depressant dosage rate (2 tests) were manipulated. The data from the remaining two tests (a frother test and a cell level test) were discarded due to process fluctuations at the time of the tests rendering the data of limited value.

5.2 Machine Vision System Results

Description of image analysis results

The strategies and algorithms described in section 3.1 were employed to provide the machine vision analyses of the froth surface characteristics. Parameters measured and captured include colour, froth surface motion, bubble size and bubble shape information. This thesis concentrates on the importance and applicability of bubble size and motion information as a means of determining the timing and occurrence of changes in process performance. A comprehensive description of the other parameters monitored during the plant campaign can be found in the separate dissertation by Wright (1999).

An example of the appearance-based information gathered during the plant experimental programme is given in the following figure, which plots the changes in bubble size information at the time that incremental steps in depressant dosage are imposed on the system:

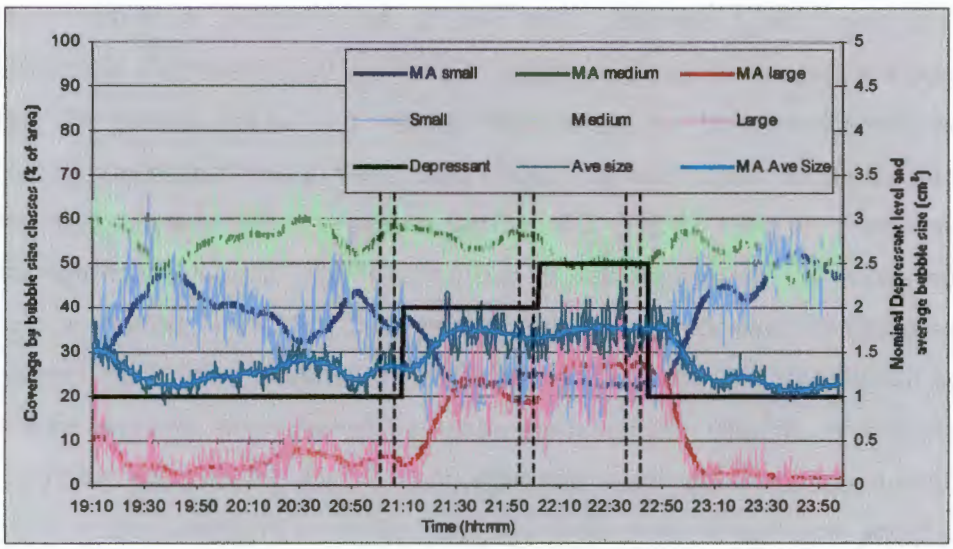

Figure 5.1: Plot of the bubble size, as well as the area coverage by three nominally chosen bubble size classes with respect to time and the 30 point moving average.

As discussed earlier, the work conducted on the batch flotation system highlighted the sensitivity of the bubble size distribution on the froth surface to the relative amount of depressant added to the flotation system. The plant experimental showed the similar trends. In order to highlight these trends, the bubble size distribution was again divided into three arbitrarily chosen bubble size classes; namely "small", "medium" and "large". The distribution was then described in terms of the degree of area coverage attributable

to each of these size classes, as shown in the figure above. The bounds of the three bubble size classes were as follows:

Bubble Size Class	Lower bound	Upper Bound
Small	Smallest bubble detected	2 cm^2
Medium	2.1 cm^2	9.9 cm^2
Large	10 cm^2	Largest bubble detected

Table 5.1: Bubble size classes, nominally chosen to allow the description of the bubble size distribution.

In order to minimise the influence of "noisy" data, a 30 period moving average was applied to all data. Each point in this moving average represented the mean value of all the points within the period, which spanned approximately ten minutes. Each average point was plotted in the middle of the period that it represents, and no weighting of the points was applied.

Once a change had been imposed on the flotation bank, the system was allowed between 45 and 60 minutes (2.5 to 3 residence times) to attain steady state. The required measurements were then made and samples were taken. Thereafter the following change in condition was imposed on the flotation system.

In terms of the image analysis data, the average of the "de-noised" data spanning a period of 10 minutes prior to the following change, was taken as the value of the parameters reached for that condition. Dashed lines in figure 5.1 indicate the periods over which the averages were taken. As an example, the following table shows the values of the variables shown in figure 5.1 that were taken as being representative of the conditions imposed on the system:

Condition	Average Bubble Size (cm^2)	Small Bubbles (% area coverage)	Medium Bubbles (% area coverage)	Large Bubbles (% area coverage)
Initial condition (initial depressant dosage)	1.33	36.51	57.34	6.16
First step in depressant (twice the initial depressant dosage)	1.66	22.61	58.13	19.26
Second step in depressant (2.5 times the initial depressant dosage)	1.76	21.81	50.19	28.00

Table 5.2: Typical bubble size data in a numerical form, as can be extracted from Figure 5.1.

In addition to the bubble size information depicted above, motion information was also extracted from the machine vision data. The following plot shows the original data as well as the moving average as applied to the bubble size data (as described above):

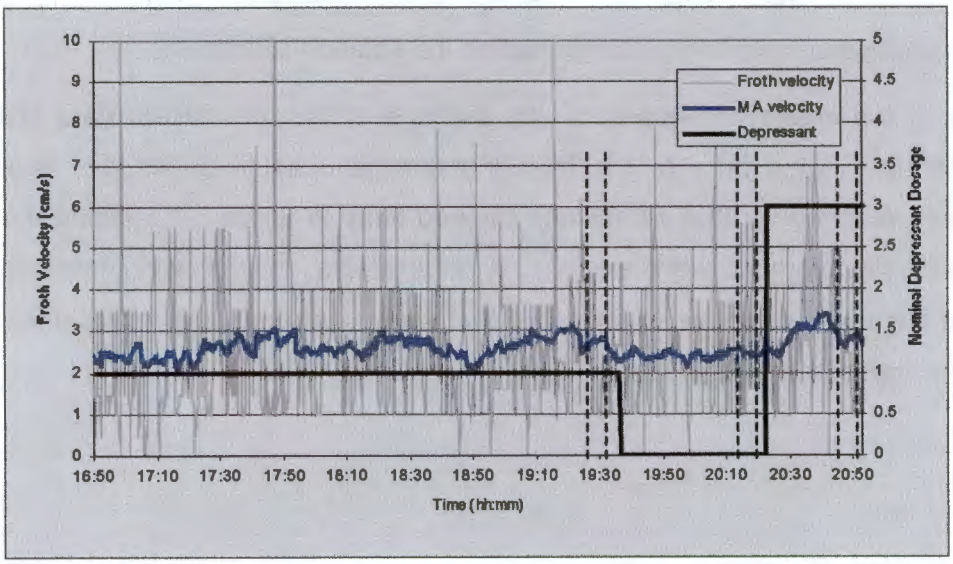

Figure 5.2: Typical Motion information gathered during the plant experimental programme.

It is clear that the above data is extremely noisy, and the average value of the velocity of the froth surface (for a particular condition) is questionable given the variance that is apparent. That said, it would appear from the above graph that the variable manipulated (in this case the depressant dosage) may have an influence on the velocity of the froth surface.

The reasons for this noise may be twofold: Firstly, the flotation equipment used at this site (comparatively large cells of the "Wemco" design) are known to have large and erratic surface movements. Secondly, the algorithm used to measure the surface motion (described in section 3.1) may indeed not be suitable for this application.

Therefore, in the absence of a more suitable method of measuring the velocity of the froth surface, the results (as shown above) will be used. The following results were extracted from figure 5.1.

Condition	Froth Surface Velocity (cm/s)
Initial condition (Initial depressant dosage)	2.70
Second condition (No depressant dosed)	2.43
Third condition (3 times the initial depressant dosage)	2.97

Table 5.3: Typical froth surface velocity values as extracted from the Figure 5.2.

Tabulated Image Analysis Results

The following tables contain the data furnished by the image analysis system at the time of the step tests, of which two were conducted on the depressant dosage rate and a further test on the frother dosage rate. As mentioned above, only the information gathered from cells 2 and 10 of the No. 1 Primary Rougher bank will be presented here.

Complete figures resembling figure 5.1, but also containing metallurgical performance information, are contained in APPENDIX CIII.

Depressant Test 1: Frother dosage set at 115 ml/min

Cell 2:

Depressant Flow rate (ml/s)	Froth Surface Velocity (cm/s)	Average Bubble Size (cm^2)	Small Bubbles (% of area)	Medium Bubbles (% of area)	Large Bubbles (% of area)
236.0	1.78	1.33	36.51	57.34	6.16
473.2	1.83	1.66	22.61	58.13	19.26
590.9	1.85	1.76	21.81	50.19	28.00

Cell 10:

Depressant Flow rate (ml/s)	Froth Surface Velocity (cm/s)	Average Bubble Size (cm^2)	Small Bubbles (% of area)	Medium Bubbles (% of area)	Large Bubbles (% of area)
236.0	2.08	2.44	15.84	39.50	44.66
473.2	2.93	2.20	19.24	42.68	38.08
590.9	2.49	2.08	21.31	42.66	36.03

Depressant Test 2: Frother dosage set at 0 ml/min

Cell 2:

Depressant Flow rate (ml/s)	Froth Surface Velocity (cm/s)	Average Bubble Size (cm^2)	Small Bubbles (% of area)	Medium Bubbles (% of area)	Large Bubbles (% of area)
102.2	2.74	1.82	21.66	42.93	35.42
0.00	2.43	1.56	25.32	57.46	17.21
312.7	2.97	1.67	32.35	31.91	35.74

Cell 10:

Depressant Flow rate (ml/s)	Froth Surface Velocity (cm/s)	Average Bubble Size (cm^2)	Small Bubbles (% of area)	Medium Bubbles (% of area)	Large Bubbles (% of area)
102.2	1.66	1.97	21.60	48.27	30.13
0.00	1.81	2.05	20.89	46.26	32.85
312.7	2.36	1.49	32.40	55.69	11.91

Frother Test: Depressant flow rate set at 174 ml/s.

Cell 2:

Frother Flow rate (ml/min)	Froth Surface Velocity (cm/s)	Average Bubble Size (cm^2)	Small Bubbles (% of area)	Medium Bubbles (% of area)	Large Bubbles (% of area)
0.0	2.28	1.89	21.11	37.96	40.93
300.0	2.68	1.94	20.05	40.61	39.34
590.0	3.19	1.79	21.93	45.76	32.31

Cell 10:

Frother Flow rate (ml/min)	Froth Surface Velocity (cm/s)	Average Bubble Size (cm^2)	Small Bubbles (% of area)	Medium Bubbles (% of area)	Large Bubbles (% of area)
0.0	2.66	2.10	20.46	42.73	36.81
300.0	2.15	1.83	24.38	50.23	25.39
560.0	2.47	1.74	25.61	53.15	21.24

5.2.1 Key Findings with respect to the Image Analysis Results

The following trends were drawn from the results of the three step tests carried out during the plant campaign:

5.2.1.1 Trends observed for changing frother dosages

It was found that increasing the frother dosage led to a decrease in bubble size both at the top of the flotation bank (cell 2) and at the bottom of the flotation bank (cell10). In the following figures, the percentage coverage for each bubble size class was normalised with respect to its initial value, so as to indicate the *relative movement* in the bubble size distribution as the frother dosage was increased.

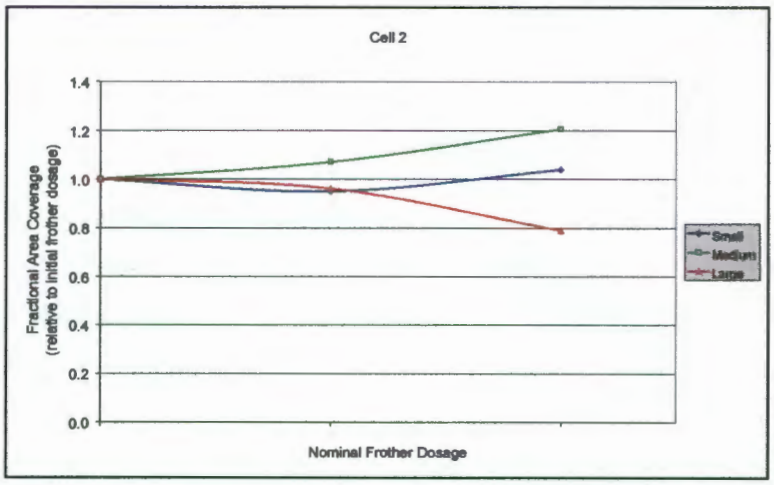

Figure: 5.3: The influence of increasing the frother dosage on the normalised bubble size distribution in Cell 2.

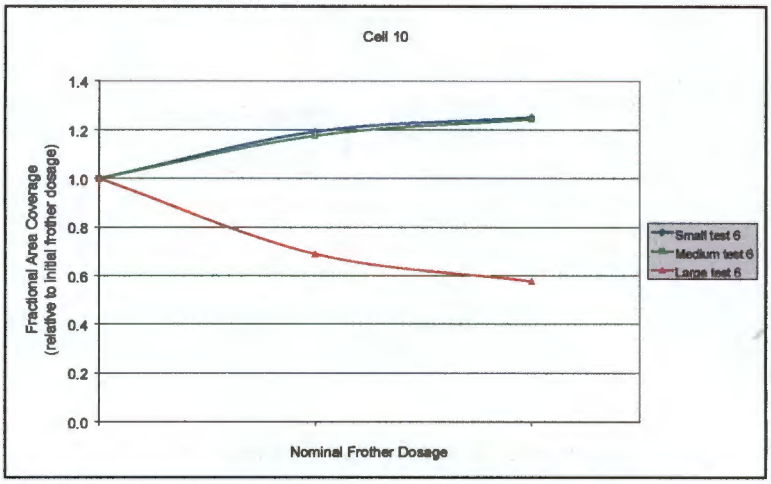

Figure: 5.4: The influence of increasing the frother dosage on the normalised bubble size distribution in Cell 10.

What is evident when comparing the above figures is that the decrease in bubble size, with respect to increasing frother dosage is far more dramatic in cell 10, than in cell 2.

5.2.1.2 Trends observed for changing depressant

The two tests in which depressant was manipulated were separated by more than a month. It is therefore not possible to compare (directly) the results from these two tests. The large differences in metallurgical results gathered for the two tests (presented in section 5.3.3) indicates that the plant may have been treating completely different ore types on the two days, which could very well have had completely different depressant requirement. This is further complicated by the differences in opinion that different operators have as to how the froth should look.

In order to draw a comparison between the two depressant tests, it was assumed that the flotation plant operators had set the depressant dosage rates based on their interpretation of the *depressant requirement* of the ore being treated on their respective shift. This allows the changes in the froth appearance brought about as a result of changes to the depressant dosage to be normalised with respect to the actual initial depressant dosage for each particular day. In addition to this, the data was normalised with respect to the initial bubble size distribution, as done for the previous two figures.

Based on the above the influences that changing the depressant dosage rate had on the froth structure at the top of the flotation bank (Cell 2) and at the bottom of the bank (Cell 10) are as follows:

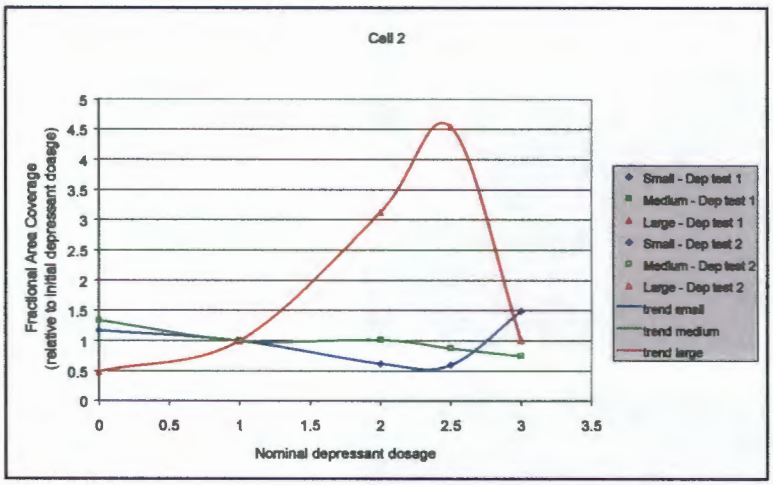

Figure: 5.5: The influence of increasing the depressant dosage on the normalised bubble size distributions in Cell 2.

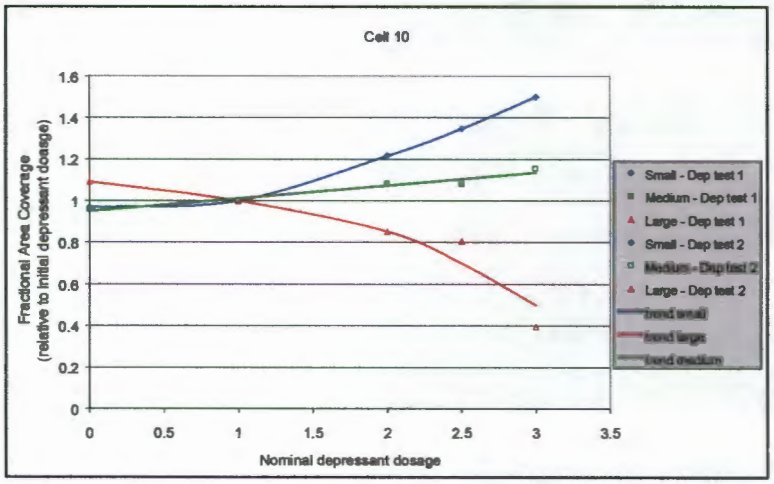

Figure: 5.6: The influence of increasing the depressant dosage on the normalised bubble size distributions in Cell 10.

From the above two figures it is clear that increasing the depressant dosage has markedly different influences at the opposite ends of the flotation bank. Consider first the trends seen in Cell 2: As the depressant dosage is increased, the bubble size distribution coarsens until a point is reached where the trend shifts sharply and the small bubbles dominate the surface coverage. In contrast to this, the increase in depressant dosage results in the bubbles getting smaller at the lower end of the bank (Cell10).

Comparing actual images gathered during the experiment can help to develop a clearer idea of the changes in froth surface structure on cell 2. The following four frames show the changes that occurred as the depressant dosage rate was increased:

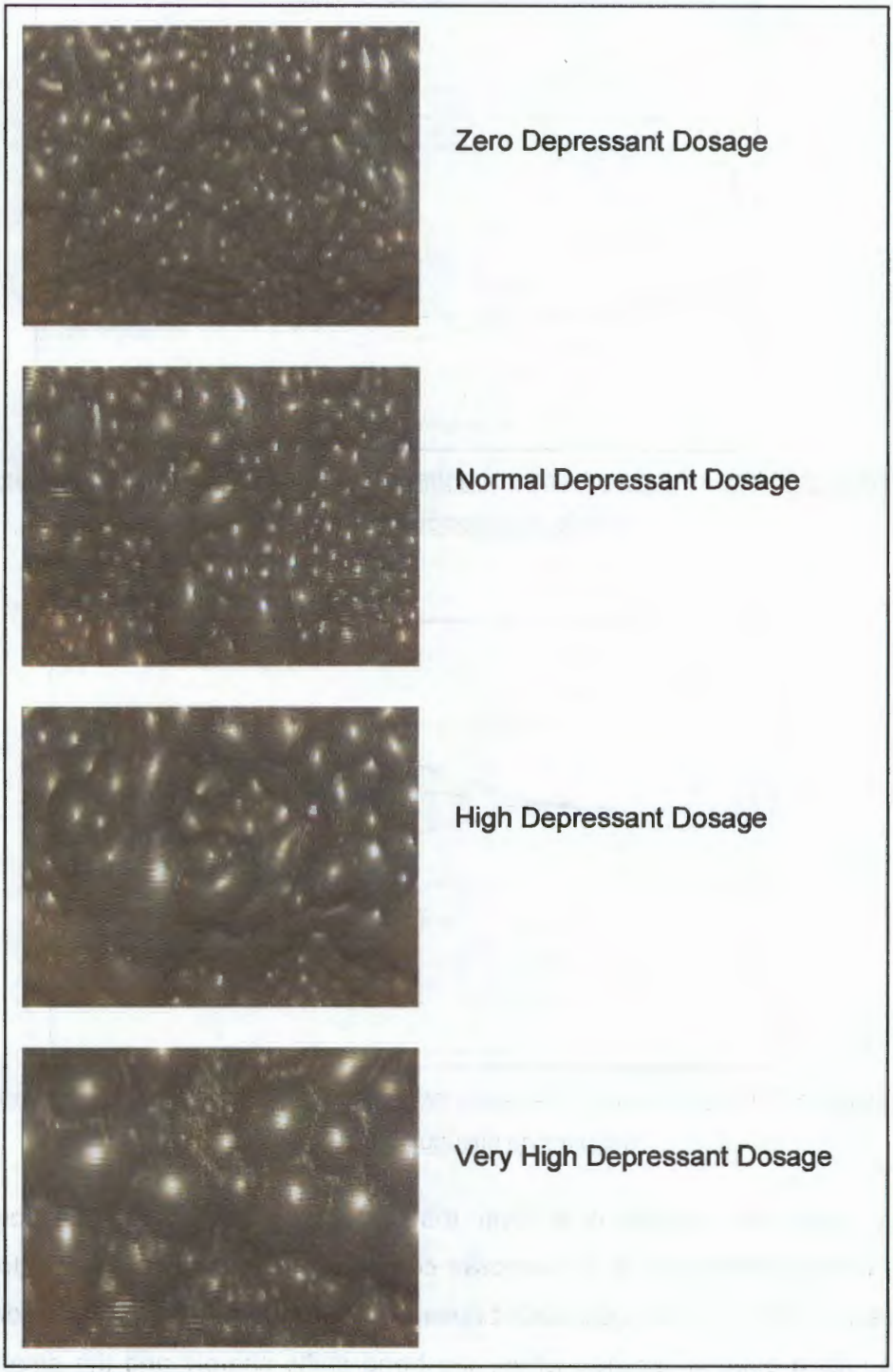

Figure: 5.7: The influence of increasing the depressant dosage on the froth surface structure on cell 2.

From figure 5.7 it is clear how the bubble size increases as the depressant dosage rate is increased. This continues to a point where a marked instability starts to influence the froth appearance and a "spitting" or "over-depressed" froth becomes evident.

Comparing figures 5.5 and 4.2, it can be seen that the influence of depressant on froth structure at the start of the flotation process on the plant is clearly opposite to that

observed in the batch flotation system. In the batch flotation system, increasing the depressant dosage lead to a *decrease* in average size at the start of the flotation test. A possible explanation for this would be that in the batch flotation system, the action of scraping the froth artificially inhibits the froth from attaining its equilibrium structure (i.e. prevents it from maturing). A more likely explanation however, is that the vastly different hydrodynamics of the batch flotation cell and the edge effects often clearly visible when observing batch flotation tests lead to a froth appearance which differs significantly from that seen on the industrial plant.

While it is difficult to explain the differences observed between the batch flotation tests and the plant-based tests, it must be borne in mind that the trend seen in figure 5.5 was observed for two separate tests in which depressant dosage was manipulated. For this reason confidence can be placed in this observation.

Figure 5.6, however confirms the influence of depressant dosage on froth structure seen towards the end of the batch flotation tests (figure 4.2).

By way of attempting to explain the phenomena observed on the plant as depressant dosage rate is increased, the most plausible explanation would be the influence that the depressant has on the talc in the flotation froth. One would expect that increasing depressant dosage to result a decrease in the amount of talc reporting to the froth phase. As discussed earlier with respect to the batch flotation results, talc would have a froth stabilising effect by Dippenaar's (1982a) arguments. If one looks at figure 5.5, it is quite plausible that as the talc is removed from the froth by increased depressant dosage, more coalescence would occur and the bubbles would increase in size. This would continue until a point is reached at which talc is completely excluded and the froth collapses (the far right hand side of figure 5.5). An compounding argument for the "over-depressed" froth seen at the far right hand side of figure 5.5 is that by removing the stabilising influences of the talc, the destabilising influences of the highly hydrophobic particles (Dippenaar, 1982a) such as chalcopyrite (see figure 3.9), would contribute to the collapse of the froth.

In terms of figure 5.6, however increasing depressant dosage would result in the little talc still present in froth (see figure 3.10) to be depressed and thereby remove its stabilising effect. The net result would be increased rates of bubble bursting and hence smaller bubbles would be visible on the froth surface.

A final point that needs to be made with respect to the trend seen in figure 5.5, is that it would be very easy to identify the "over-depressed" froth seen towards the right side of the figure, given that the method used to measure the bubble size (the *watershed*

transform) returns a complete bubble size distribution. The "bi-modal" distribution of bubble sizes seen in the last frame in figure 5.7 could simply be tested for in the rule base that would be used in a control strategy.

5.2.1.3 Other findings with respect to the froth surface appearance

The following is an additional observation made with respect to changes in froth appearance, attributable to changes in the frother and depressant dosage. It was found that increasing both the frother and the depressant dosage lead to an increase in the froth surface velocity, as can be seen in the following figure:

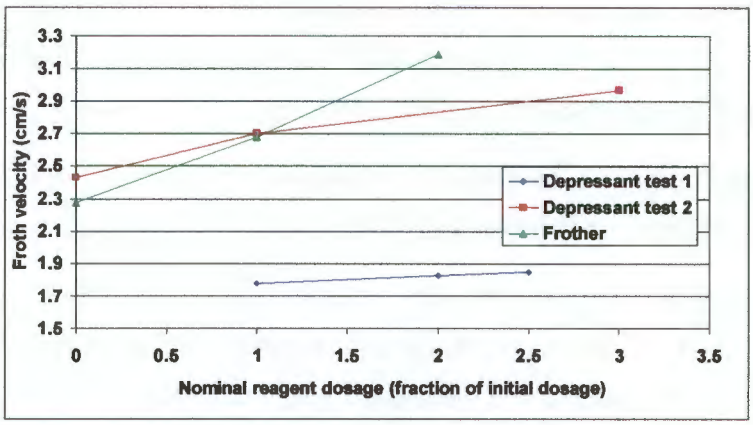

Figure 5.8: Changes in Froth Surface Velocity due to changes in the relative level of reagent dosage rates.

The reasons for the increase in froth velocity as both the frother and the depressant dosages are increased are difficult to explain. The influence of the depressant could be due to increased talc depression as depressant dosage rate is increased. The absence of talc would result in a froth that is less viscous and would therefore have greater mobility. Increasing the frother dosage, would on the other hand, retard coalescence in the froth phase. This could result in an increase in froth *volume* production rate and hence an increase in surface velocity.

5.3 Metallurgical Performance Data

5.3.1 Assessment of Errors in Collecting the Metallurgical Performance Information

Process fluctuations, as are typically experienced on an industrial flotation plant, confound the use of traditional reproducibility tests to quantify the errors encountered in the experimental programme. An exercise was thus conducted to assess what the influence of these errors and fluctuations on the metallurgical results would be. The test

was in the format of *a nested analysis of variance* experiment, and focused on assessing the influences of the following:

- The errors associated with the chemical analysis of concentrate samples, in conjunction with the errors associated with preparing the samples for such analysis.
- The errors associated with the physical sampling of the concentrate stream along with those associated with the initial sample preparation procedures of filtering, drying and coarse screening the sample.
- The variation imposed on the estimation of the stream grade over a short time period, as a result of time-based process fluctuations.

In terms of the analyses chosen for the purpose of the experiment, the 4E PGE, copper and nickel grades were chosen. The complete results of the experiment, as well as a breif statistical discussion of the analysis of the experimental results, are given in APPENDIX CI.

In brief, the results of the test showed the following:

- For the 4E PGE analysis results:
  - It was found that the variances associated with the analysis and sample preparation prevented a real difference being observed between the mean grades of duplicate samples taken at the same time. This implies that there was no significant error associated with the sampling and initial sample preparation (filtering etc.).
  - Further, it was found that no short term process variations could be detected over the combined variances associated with sampling, sample preparation and analysis.
- For the copper and nickel analysis results:
  - It was found that at one of the four sampling times a real difference (at the 90% confidence limit) attributable to sampling error could be detected over the lower order variances. As the same samples were analysed for copper and nickel as were analysed for 4E PGE, this implies that a greater degree of confidence can be placed on the analyses for copper and nickel. Furthermore it indicates that there is a real possibility of incurring sampling errors, but that this was only discernible in one out of four cases.

- As with the 4E PGE analysis data, the copper and nickel data showed that no short term process variations could be detected over the combined variances associated with sampling, sample preparation and analysis.

The implication of the above analysis was that if all the errors were combined, the analyses would have the greatest influence in any deviation between a measured grade of the stream and the true grade of that stream. In addition to this, it was found that errors associated with the sampling and initial sample preparation could indeed be a further source of discrepancy.

5.3.2 Mass Balances Around the Flotation bank

The reason for establishing a mass balance around the flotation bank was to place the performance of the observed cells into the context of the whole bank. Complete mass balance tables for the three surveys, providing measured as well as the smoothed values, are given in APPENDIX CII. For reasons of confidentiality, the 4E PGE grades for the flotation feed and tails have been omitted and the grades of the various concentrates have been divided by an arbitrarily chosen factor.

The following graph shows the average mass flows of the concentrates down the length of the flotation bank. The error bars indicate the upper and lower bounds of the measurements made:

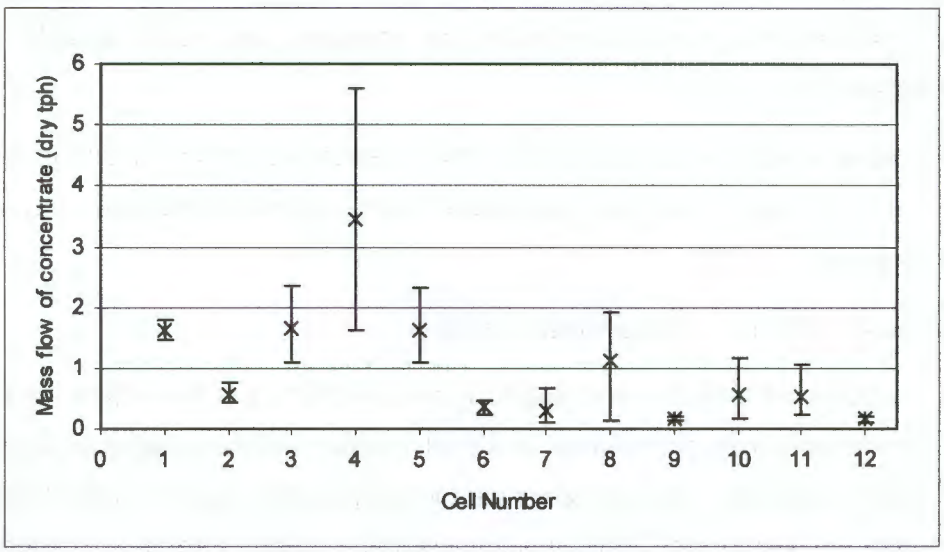

Figure 5.9: Plot of the average concentrate flow rates down the length of the flotation bank.

It is clear from the above graph that the flows of concentrates down the length of the flotation bank vary markedly and do not seem to follow any trend. Cells that have high average concentrate flow rates also show the greatest variation in flow rates. The cells to

be observed by the machine vision system proved to have low solids flow rates (especially so for cells 2 and 6).

The following graph shows the percentage solids measurements of the concentrates down the length of the flotation bank:

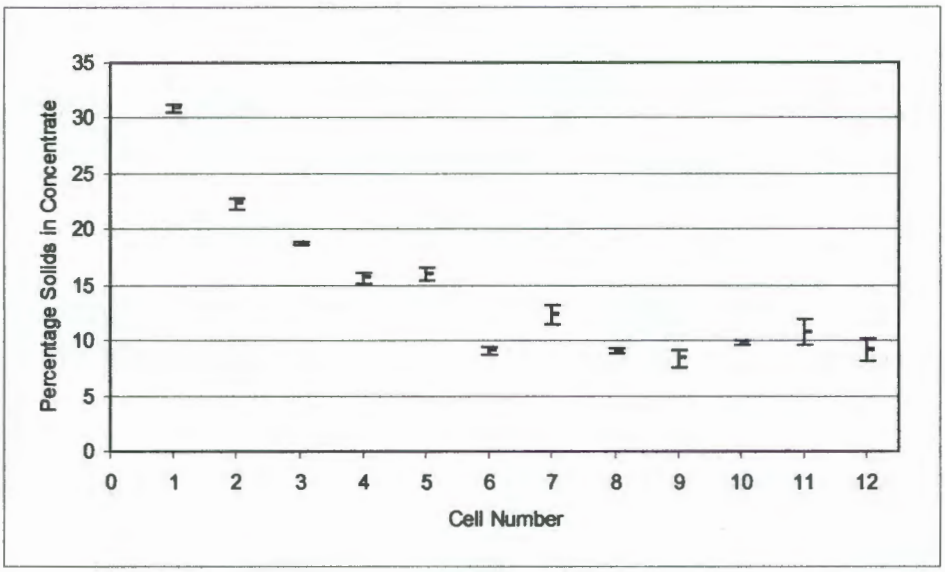

Figure 5.10: Plot of the percentage solids of the concentrates down the length of the flotation bank.

It is clear from the above graph that there is a marked decrease in the solids content of the concentrates as one progresses down the flotation bank. This is as expected as the amount of solids amenable to flotation decreases as the slurry passes from one cell to the next down the bank.

The grades of the concentrates also showed a large amount of variation. The following two figures give the 4E PGE (factored) grades; and the copper, nickel, iron and sulphur grades of the concentrates, respectively. Again the error bars indicate the upper and lower bounds of the measurements made:

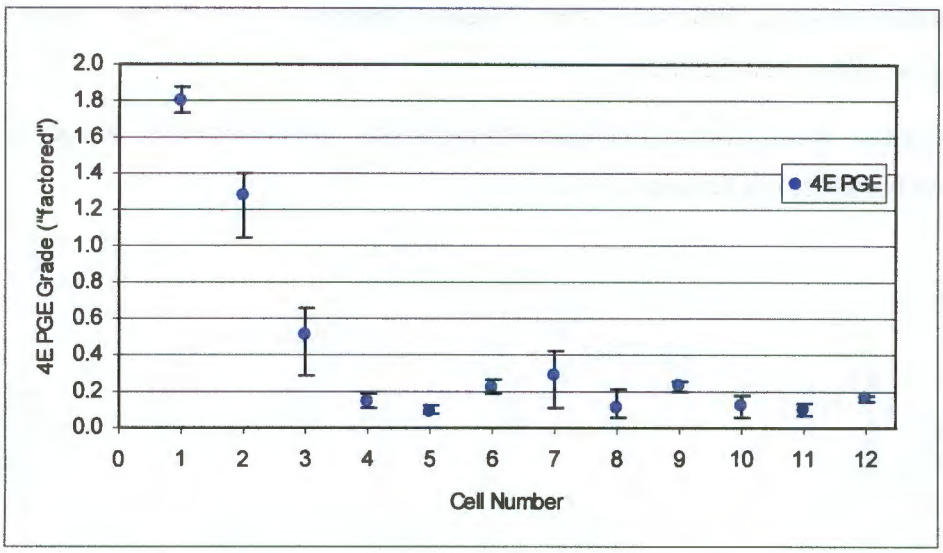

Figure 5.11: Plot of the 4E PGE grades of the concentrates down the length of the flotation bank. (The 4E PGE grades have been factored by dividing them by an arbitrary number.)

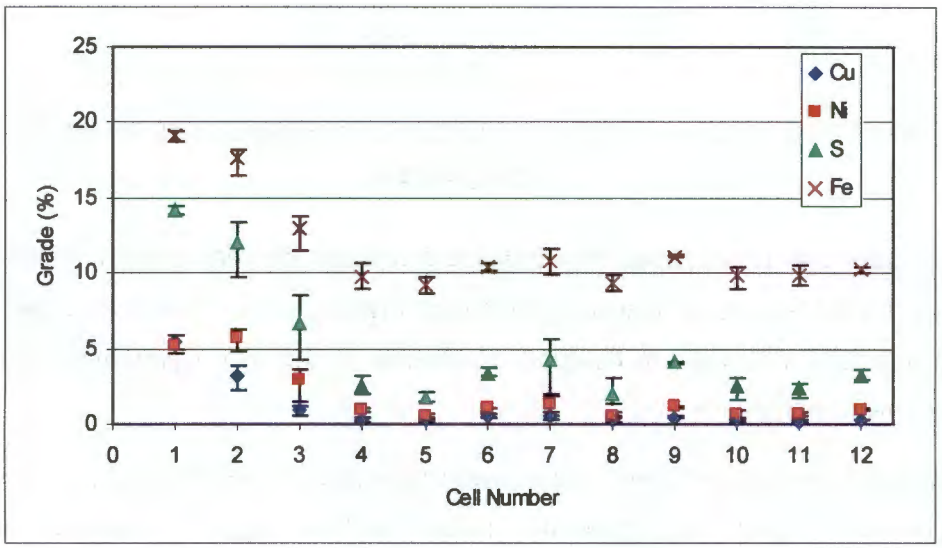

Figure 5.12: Plot of the Copper, Nickel, Iron and Sulphur grades of the concentrates down the length of the flotation bank.

From figures 5.11 and 5.12 it can be seen the grades of the concentrates are at their highest at the beginning of the flotation bank, which is as expected. In addition to the cells that have low concentrate flow rates (see figure 5.10), have higher grades. Examples of this are cells 6, 7 and 9.

The recovery profiles of the various species can be plotted by drawing on the information shown in figures 5.9, 5.11 and 5.12. The graph shown below expresses the recovery of each elemental species in terms of the total achieved in the flotation bank (in other words, a combined concentrate is used as the basis, instead of the more traditional feed basis).

This portrayal is used so that the recovery profile of 4E PGE species can be shown and compared with those of the base metal bearing species, without infringing on the operation's need for confidentiality.

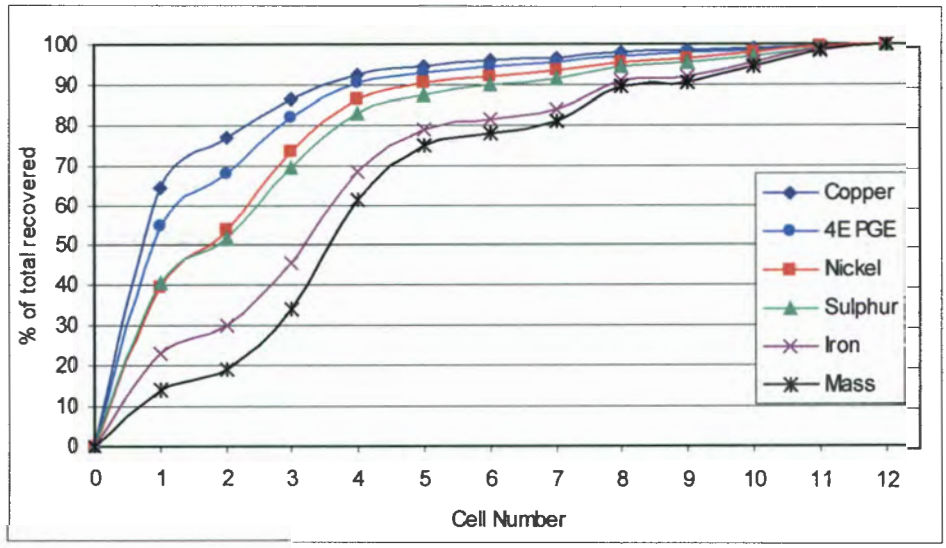

Figure 5.13: Recovery profiles of 4E PGE, base metals and sulphur down the length of the flotation bank.

The above figure indicates the "speed" with which the species bearing the various elements are recovered. Clearly the copper bearing species are recovered the fastest, followed by the 4E PGE bearing species. The nickel and sulphur profiles coincide well and the iron bearing species are the slowest to be recovered.

Important to note, is the fact that by cell 2, 78% of the copper bearing species and 70% of the 4E PGE bearing species that will be recovered in the flotation bank, have been recovered. At this point, only 20% of the total mass of dry solids that will be recovered has been recovered. After cell 4, these numbers have increased to over 90% for the copper and 4E PGE and copper bearing species, while only 35% of the total mass to be recovered has been recovered. At this point the nickel and sulphur bearing species have also exceeded 80% of the total amount that will be recovered. By the converse observation, the cells after cell 5 account for relatively little of the total recovery.

What the above observation points to is the importance of maintaining optimum conditions in the first four cells of the flotation bank, as these four cells account to a large degree for the performance of the flotation bank. An extension of this point is the concept that should conditions be such that the performance of the entire bank would be impaired, the detection of such sub-optimal conditions could be achieved early on in the bank. This is because small changes in flotation performance would have a far greater impact on the

part of the flotation bank that accounts for the bulk of the recovery than further down the bank.

5.3.3 Tabulated Metallurgical Results

The following tables contain metallurgical performance data gathered during the step tests, of which the image analysis data is tabulated in section 5.2. APPENDIX CIII contains figures which represent a combination of the image analysis and metallurgical data, as well as indicating the change in condition that each represents. The following figure is an example of the type of information contained in this appendix:

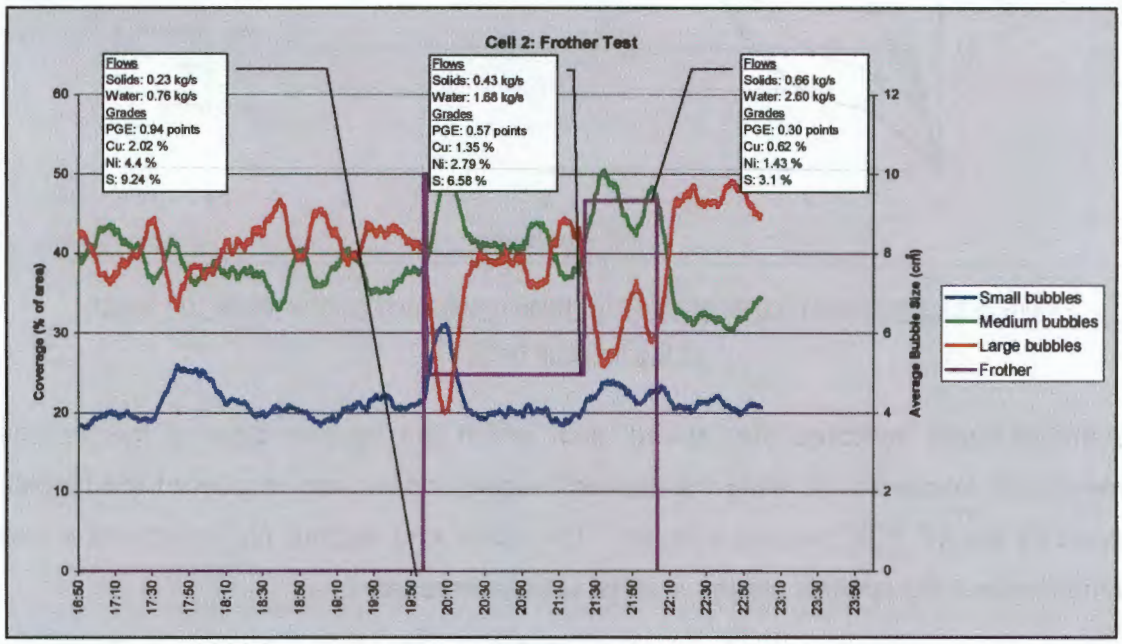

Figure 5.14: Combined metallurgical performance and image analysis information in a graphical form. (An example of the graphs that can be found in APPENDIX CIII).

As stated above, the erratic image analysis results gathered from cell 6 lead to no further analysis being carried out with respect to the appearance of its surface froth and (with reference to this section) its metallurgical performance. For this reason only the metallurgical responses of cells 2 and 10 will be given below.

In addition to purely metallurgical performance data, a further measurement was taken, namely the height of the froth bed travelling over the weir, and this will also be tabulated below:

Depressant test 1: Frother dosage set at 115 ml/min

Cell 2:

Depressant Flow rate (ml/s)	Solids Flow Rate (kg/s)	Water Flow Rate (kg/s)	4E PGE grade (factored)	Copper grade (%)	Nickel grade (%)	Sulphur grade (%)
236.0	0.11	0.26	1.55	4.42	6.09	13.7
473.2	0.08	0.19	2.51	5.01	9.07	17.9
590.9	0.06	0.15	2.33	5.69	9.19	19.2

Cell 10:

Depressant Flow rate (ml/s)	Solids Flow Rate (kg/s)	Water Flow Rate (kg/s)	4E PGE grade (factored)	Copper grade (%)	Nickel grade (%)	Sulphur grade (%)
236.0	0.04	0.42	0.26	0.41	1.30	4.15
473.2	0.05	0.34	0.25	0.38	1.24	4.21
590.9	0.06	0.39	0.22	0.38	1.18	3.97

Froth height over the weir

Depressant Flow rate (ml/s)	Cell 2 (cm)	Cell 10 (cm)
236.0	15	20
473.2	13	12
590.9	10	16

Increasing the depressant dosage rate lead to a decrease in the dry solids yield rate in cell 2. As expected, the grade of the concentrate was seen to climb at the same time (more noticeable for the Cu, Ni and S results than for the 4E PGE). In cell 10, quite the opposite was seen. The solids yield rate increased and the grade decreased as the depressant flow rate was increased.

The height of the froth over the weir tended to decrease in cell 2 as the depressant was increased, while no similar or opposite trend could be identified in cell 10.

Depressant test 2: Frother dosage set at 0 ml/min

Cell 2:

Depressant Flow rate (ml/s)	Solids Flow Rate (kg/s)	Water Flow Rate (kg/s)	4E PGE grade (factored)	Copper grade (%)	Nickel grade (%)	Sulphur grade (%)
102.2	0.24	0.64	0.92	2.14	4.14	8.64
0.00	0.28	0.90	0.73	1.61	3.77	7.91
312.7	0.17	0.37	1.07	2.23	4.64	11.0

Cell 10:

Depressant Flow rate (ml/s)	Solids Flow Rate (kg/s)	Water Flow Rate (kg/s)	4E PGE grade (factored)	Copper grade (%)	Nickel grade (%)	Sulphur grade (%)
102.2	0.03	0.22	0.12	0.34	0.71	2.18
0.00	0.08	0.57	0.11	0.22	0.68	2.19
312.7	0.19	1.25	0.04	0.10	0.27	0.84

Froth height over the weir

Depressant Flow rate (ml/s)	Cell 2 (cm)	Cell 10 (cm)
102.2	11	15
0.00	12	22
312.7	6	7

Similar trends to those identified in "Depressant 1" can be noted in the above data. However in addition to this, it would appear the increasing the depressant resulted in a drier froth being recovered.

It would also appear that increasing the depressant lead to the heights of froth over the weir decreasing in both cells 2 and 10.

Frother test: Depressant flow rate set at 174 ml/s.

Cell 2:

Frother Flow rate (ml/min)	Solids Flow Rate (kg/s)	Water Flow Rate (kg/s)	4E PGE grade (factored)	Copper grade (%)	Nickel grade (%)	Sulphur grade (%)
0.0	0.23	0.764	0.94	2.02	4.40	9.24
300.0	0.43	1.68	0.57	1.35	2.79	6.58
590.0	0.66	2.60	0.30	0.62	1.43	3.10

Cell 10:

Frother Flow rate (ml/min)	Solids Flow Rate (kg/s)	Water Flow Rate (kg/s)	4E PGE grade (factored)	Copper grade (%)	Nickel grade (%)	Sulphur grade (%)
0.0	0.05	0.18	0.12	0.30	0.77	2.66
300.0	0.05	0.28	0.09	0.21	0.55	1.91
590.0	Not measured.					

Froth height over the weir

Frother Flow rate (ml/min)	Cell 2 (cm)	Cell 10 (cm)
0.0	11	15
300.0	15	15
590.0	10	15

Increasing the frother rate led to an increase in dry solids and water yield rate, and a corresponding drop in concentrate grade in cell 2. While cell 10 did not show the same increase in solids yield rate, that of the water increased and comparing the only two samples in the test, the concentrate grade was observed to decrease.

5.3.4 Key findings with respect to Metallurgical Performance

5.3.4.1 Characterisation of the Flotation Bank

The mass balance surveys carried out on the Amandelbult Merensky Primary Rougher, showed that 78% of the copper bearing species and 70% of the 4E PGE bearing species that will be recovered in the flotation bank, had been recovered by cell 2. At this point, only 20% of the total mass of dry solids that are recovered has been recovered. By cell

4, these numbers have increased to over 90% for the copper and 4E PGE and copper bearing species, while only 35% of the total mass to be recovered has been recovered. At this point the nickel and sulphur bearing species have also exceeded 80% of the total recovery of the bank.

5.3.4.2 Information from the Step Tests

The following graphs, which represent the metallurgical performance data collected during the step test part of the plant programme, are drawn from the data represented in the tables above. The graphs represent the grade and mass yield (the combination of which define the "recovery" from a particular cell) of the concentrates gathered from Cell 2 in the rougher bank:

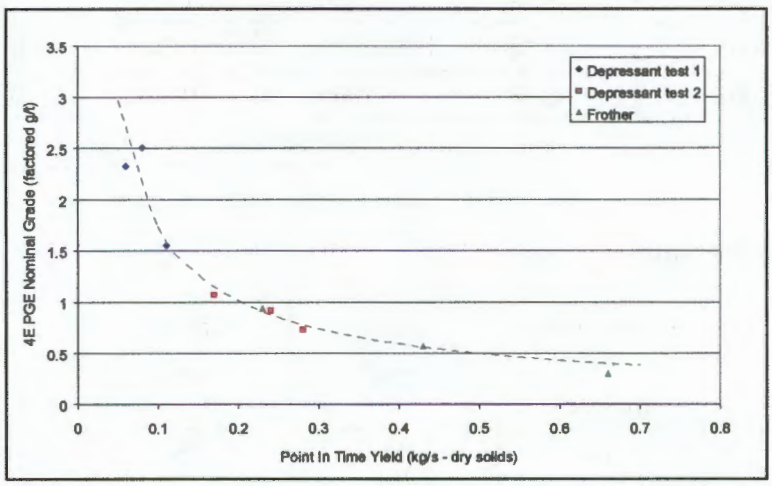

Figure 5.15: The relationship between the 4E PGE grade and mass yield from Cell 2.

The strong relationship observed above was found to hold for all the other elements analysed for, as can be seen in the following graph depicting the same relationship for sulphur. Included in this figure is an indication as to the direction of the changes in the depressant and frother dosages made, which resulted in the changes in flotation performance.

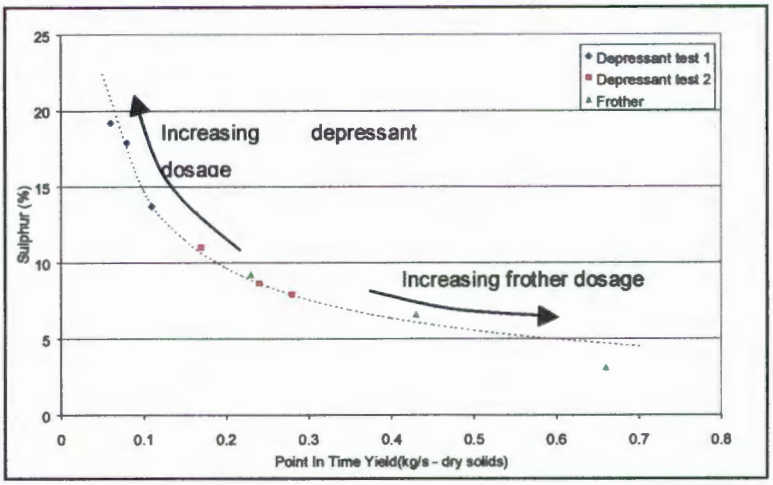

Figure 5.16: The relationship between the sulphur grade and mass yield from Cell 2.

The trends seen in the above figures appear to be remarkably strong. If it is assumed that they hold for a wider range of flotation conditions, the above trend implies that should one of the parameters (either the grade or the instantaneous mass yield) were to be measured, then the other could be inferred.

In addition to the above, it was found that increasing the depressant dosage rate lead to a decrease in dry mass (solids) recovery rate, while an increase in frother dosage rate led to an increase in the same parameter, as can be seen in the following figure:

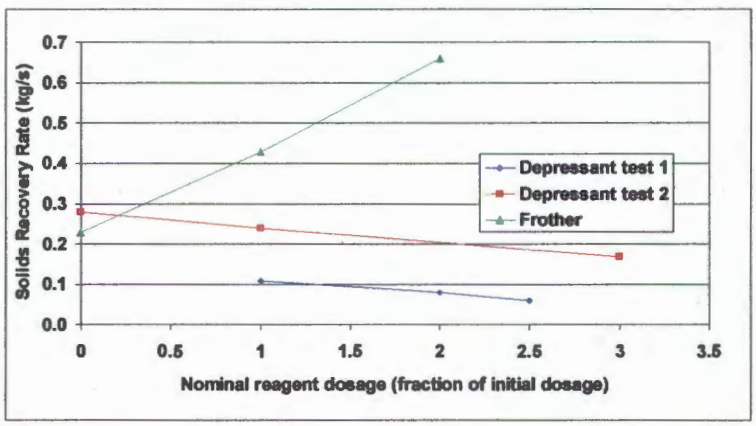

Figure 5.17: The influence of increasing the nominal reagent dosage rate on the solids recovery rate from Cell2.

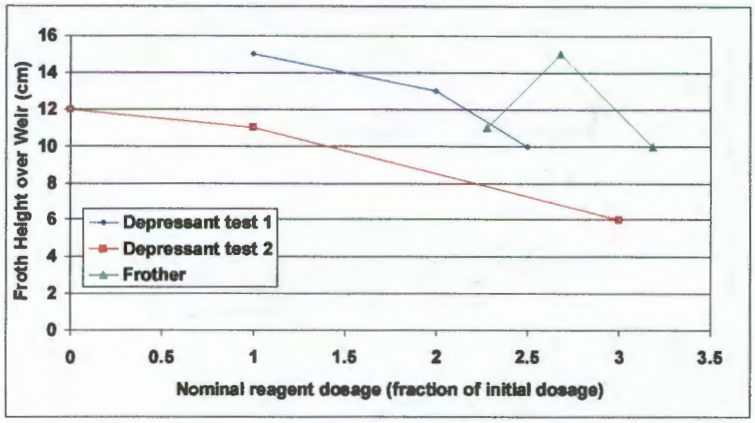

Figure 5.18: The influence of increasing the nominal reagent dosage rate on the height of froth overflowing the concentrate weir of Cell2.

As the depressant dosage is increased, the froth velocity increases (seen in figure 5.8), the height of froth travelling over the weir decreases (figure 5.18) and the mass recovery rate also decreases. A possible reason for this is that the increase in depressant dosage may be decreasing the "loading" of the froth, however, increasing the depressant dosage typically led to a drier froth (See APPENDIX CIII). An alternative and more plausible explanation is that increasing the depressant led to a change in the rate with which the froth would bear material across the weir. As the velocity increased as the depressant dosage increased, this decrease in mass recovery can only be explained by the fact that *less total volume of froth*, was reporting to the concentrate per unit time. In other words the decrease in froth height travelling over the weir had a greater influence on its mass transport characteristics than did the increase in velocity.

As the frother dosage is increased, the froth velocity increases (seen in figure 5.8), the height of froth travelling over the weir increases initially, but then returns to a value below its initial value (figure 5.18) and the mass recovery rate increases. The fact that there is no fixed trend visible in froth height overflowing the weir means that the argument followed above with respect to the depressant, can not be made with respect to the frother. Therefore, increasing the frother dosage rate may either increase solids recovery rate by rendering a more stable froth (which is capable of carrying larger quantities of material over the concentrate weir) or it may achieve the same by simply increasing the total amount of laden froth overflowing the weir. In this case the frother might be increasing both the velocity of the froth overflowing the weir as well as the height of the froth layer overflowing the weir.

If the argument made with respect to the decrease in solids yield rate with increasing depressant dosage, could be made with respect to the increase in solids yield rate with increasing frother dosage, it would imply that descriptors such as froth velocity and froth

height over the weir could provide the operator with an estimation of the solids yield rate. The following figure, which attempts to correlate the dry mass yield rate to the product of the froth height over the weir and froth velocity, indicates that this may be possible:

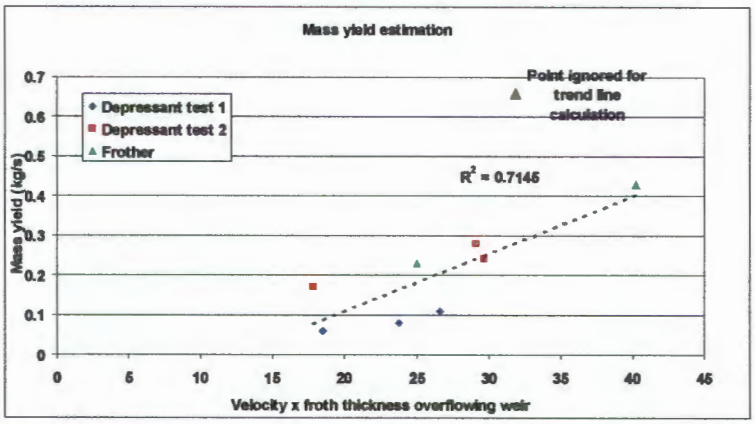

Figure 5.19: A possible relationship between the dry mass yield rate and the product of froth height over the weir and froth velocity on Cell2.

In the above figure, the only point that deviates from the trend is the one in which the froth height over the weir decreased as the frother dosage rate was increased.

5.4 Significance of the Findings of Plant Experimental Programme

From a metallurgical performance perspective, the finding that by far the largest contribution to the overall recoveries achieved in flotation bank are realized within the first few cells, is very important. This implies that if a machine vision system offers a means to detect changes in *flotation performance*, it would do so far more effectively at the beginning of the flotation bank where the greatest rates of change are found to occur. An extension to this is that should changes in conditions be such that a decline in flotation performance can be expected, the early detection made possible by positioning a machine vision system over the first part of the bank would allow control action to be taken before the decline in flotation performance has been effective across the entire bank. This would have considerable benefits, in that it would allow faster turnarounds in the control action, which would mean that the operation would be operating closer to the optimum for greater periods.

The finding that a change in the frother dosage had a far greater influence on the froth appearance of the later parts of the flotation bank, while a change in the depressant dosage influenced the appearance of the froth surface in the earlier stages, is of particular value. This indicates that before control strategies are proposed, based on

manipulating particular operating variables, cognizance must be taken of how these particular variables will influence parameters that dictate the froth structure at the proposed point of observation. This work has shown that changing the depressant dosage (which influences the nature of gangue particle surfaces) has its greatest influence at the beginning of the flotation bank where the solids loading of the froth is high. A control strategy aiming at optimising the depressant dosage would clearly be of limited success if the only point observed by the machine vision system is at the end of the flotation bank (where the froths are relatively depleted of solids).

Further to the above, the understanding as to how the frother and depressant dosages influence surface froth structure in the plant, provides a basis for a control strategy targeted at the optimisation of *froth structure*, should an optimum froth structure be identified. While the plant campaign did not identify an optimum froth structure (which would depend on the objectives of a particular flotation unit), the results of the tests in which the depressant dosage was varied indicated that the highest grade concentrates were achieved when the ratio of large bubble to small bubble area coverage was approximately one. This can be seen in figure 5.20 below:

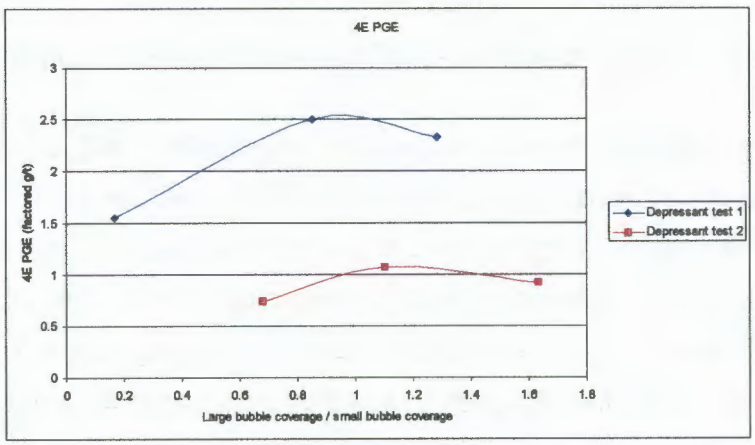

Figure 5.20: The Relationship between 4E PGE grade and the ration of large bubble to small bubble coverage, as an example of an optimum froth structure.

Figure 5.20 suggests that the depressant dosage could be manipulated so as to achieve a froth structure with roughly equal amounts of large and small bubble coverage, and that this would result in the highest grade of concentrate being recovered.

Undoubtedly, one of the most significant findings of this study is the idenitification of a method capable of detecting whether a change in either the frother or the depressant dosage of a plant, by comparing the *changes* in bubble size at the top and the bottom of

the flotation bank. The following section will briefly outline a strategy that could be employed to exploit this.

5.4.1 Proposed Control strategy

Based on figures 5.3 to 5.6, the following block diagram suggests a method of determining whether a change in frother or depressant dosage has occurred (or is occurring) on a flotation section such as the Amandelbult Primary Roughers. The output from the strategy is currently envisaged to occur in the form of prompts or suggestions to the human plant operator, but this information could just as easily be encapsulated in an expert control system.

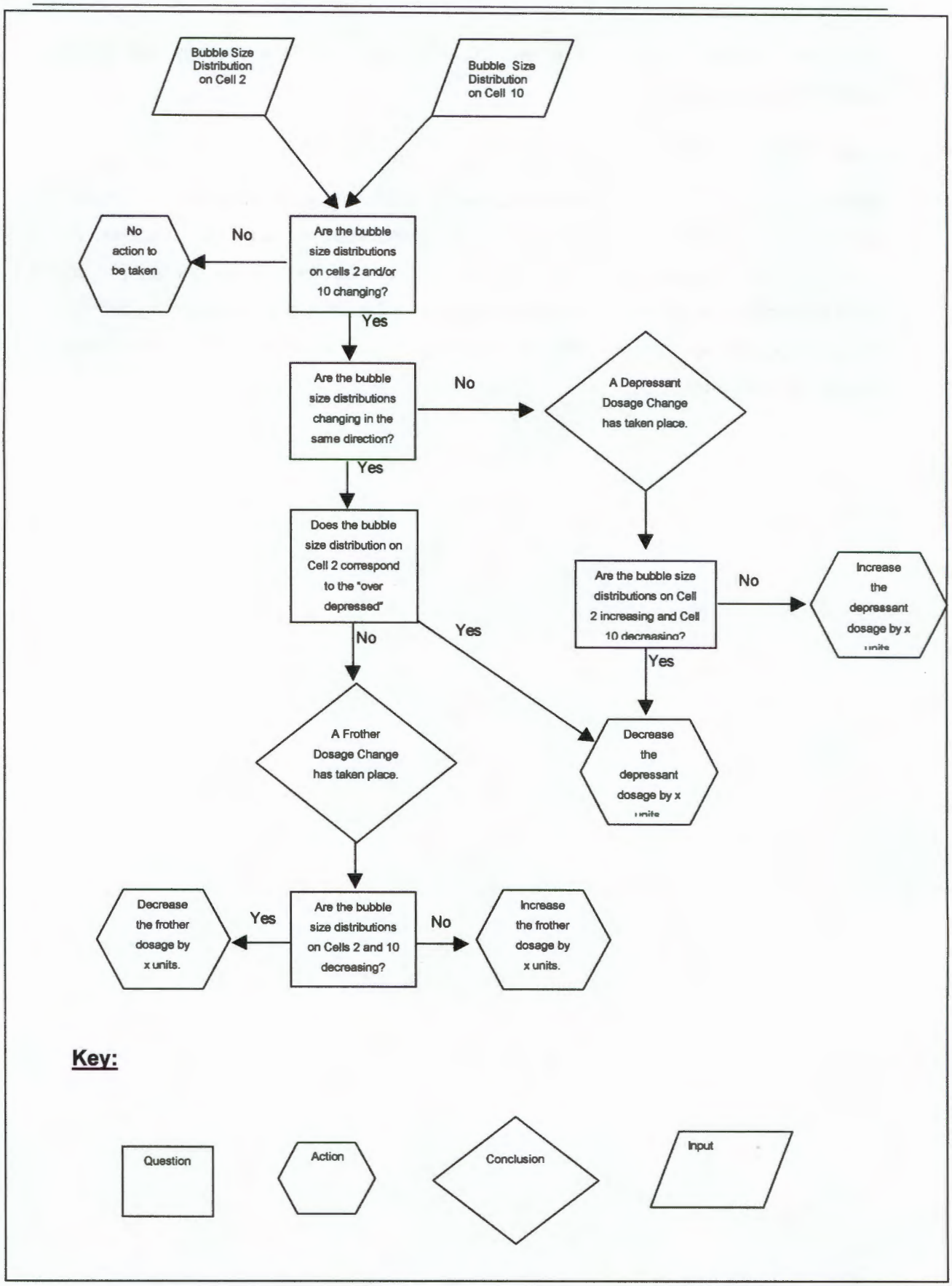

Figure 5.21: Suggested control strategy for determining whether a change in frother or depressant dosage is occurring on the Amandelbult Primary Roughers.

6 Conclusions

The following conclusions are drawn from the work presented and discussed in this thesis:

6.1 Batch Flotation Programme

Batch flotation experiments showed that the machine vision system which was under development was able to successfully detect and quantify changes in flotation froth surface structure in a PGM flotation system. These changes in surface froth structure were verified by simple, qualitative observation.

The *distribution of bubble sizes* on the flotation froth surface, as measured and presented by the machine vision system, was divided into three bubble size classes which resulted in a useful description of the froth structure and provided a simple means of quantifying changes to froth surface structure.

The froth surface appearance was found to be particularly sensitive to the depressant dosage. This is of particular value as the depressant dosage is a key factor in determining the flotation system's efficiency in concentrating the valuable minerals.

The machine vision system was also able to detect abnormal and inferior flotation performance caused by reducing the initial frother dosage. "Froth transport limiting" conditions, identified from a metallurgical performance perspective, could be identified by the rapid rate with which the froth appearance changed from its initial to its final structure under theses conditions.

6.2 Plant Experimental Programme

The machine vision system, despite operational "noise", was able to identify and track changes in the surface froth appearance, brought about by changes made to operating variables on an industrial PGM flotation plant. In addition to this, these changes in operating variables could be related to resultant changes in the metallurgical performance of the flotation system.

The change in froth appearance, brought about as a result of a change made to an operating variable, depended strongly on the location within the flotation circuit that was being observed. This implies that any control strategy, which aims to use machine vision

in the control of a particular operating variable, must first consider whether point to be observed will show sufficient sensitivity to the operating variable of interest.

Increasing the frother dosage led to a decrease in froth surface bubble size both at the start and at the end of the flotation bank. Increasing the depressant dosage, on the other hand, led to an increase in bubble size at the start of the flotation bank, but resulted in a decrease in bubble size at the end of the flotation bank. This means that it is possible to identify uniquely which of either the frother or the depressant dosage has moved to a sub-optimal level.

The changes in metallurgical performance brought about by changes to the frother and depressant dosages were measured, and were found to be consistent with expectation. By this it is meant that increasing the depressant dosage led to an increase in concentrate grade at a lower mass pull, while increasing the frother dosage led to an increase in mass recovery at a lower grade. In addition to this, it was found that the grade and mass pull from cell 2 showed a strong relationship which implies that should one of these parameters be either measured or estimated, it is possible to infer the value of other.

A strategy is proposed for the control of the depressant and frother dosages on a flotation operation based on the appearance of the flotation froth surface. This strategy compares the direction in which the bubble size distributions change both at the top and the bottom of the flotation bank, in order to determine which of either the frother dosage or the depressant dosage has deviated from the optimum. Appropriate action can then be suggested

It is shown in this thesis that the potential exists to use the machine vision system to estimate the mass recovery from a particular cell. If this could be achieved, the machine vision system could not only indicate when the performance of a particular flotation cell deviates from the optimum, but also indicate the reason for this deviation.

7 Critique, Recommendations and Further Work

A possible shortcoming of the work presented in this thesis, and in particular that discussed with respect to the plant campaign, is that the data set is indeed too small. Ideally, for the type of work discussed in this thesis, the data set should have been large enough to be divided into two sets: the first could be used to develop ideas and strategies, while the second would be used to test these ideas and strategies. This point is especially valid given that when the data from the plant campaign was interrogated, complete knowledge as to the type, time and magnitude of change imposed on the flotation system existed.

Based on the work presented and discussed in this thesis, the comments made above and conclusions drawn in this thesis, the following recommendations are made and future work suggested:

1. The results gathered during the plant-based experimental programme should be verified.
2. The influences of parameters, which are beyond the control of the operator, on the flotation froth surface need to be quantified so that the potential for incorrect diagnoses and incorrect subsequent control actions are minimised.
3. Future studies must address the issue of how the decision is taken as to whether a *significant* change in froth structure has taken place, or whether an observed change is simply as a result of noise.
4. A study should be carried out into the potential of the machine vision system to provide an estimation of the mass pull of concentrate from a particular cell, in real time.
5. There exists a need for an efficient and robust measure of flotation froth velocity.

8 Reference List

1. Aldrich C, Moolman DW, Bunkell S-J, Harris MC and Theron DA

   Relationship between Surface Froth Features and the Process Conditions in the Batch Flotation of a Sulphide Ore
   Miner. Eng., Vol. 110, No 11,pp 1207 – 1218, 1997.

2. Alexander DJ and Morrison RD

   Rapid Estimation of Floatability Components in Industrial Flotation Plants
   Miner. Eng., Vol. 11, No 2, pp 133 – 143,1998.

3. Arbiter N (Section Editor),Harison Cooper, Ferstenau MC, Harris CC, Kuhn MC, Miller JD and Yap RF

   Flotation
   SME Mineral Processing Handbook, ed. Weiss NL, AIME, 1985.

4. Asplin RA, Sadr-Kazemi N and Cilliers JJ

   The Effect of Surfactant Concentration on the Flotation Mineral Flux and Froth Structure
   Miner. Eng., Vol. 11, No 3, pp257 – 269, 1998.

5. Bascar OA and Herbst JA

   Dynamic Modeling of a Flotation Cell with a view toward Automatic Control
   XIV Int. Mineral. Proc. Congress, Canada, Vol. III, pp. 11.1 – 11.22, October 1982.

6. Banford AW, Aktas Z and Woodburn ET

   Interpretation of the Effect of Froth Structure on the performance of Froth Flotation using Image Analysis
   Powder Technology 98, pp. 61 – 73, 1998

7. Cipriano A, Guarini, M, Soto A, Briceno H and Mery D

   Expert Supervision of Flotation Cells using Digital Image Processing
   Proceedings of the XX IMPC – Aachen, pp. 281 – 292, September 1997.

8. Cipriano A, Guarini M, Vidal R, Soto A, Sepulveda C, Mery D and Briseno H

   A Real Time Visual Sensor for Supervision of Flotation Cells
   Miner. Eng., Vol. 11, No 6, pp. 489 - 499,1998.

9. Dippenaar A

   The Effect of Particles on the stability of Flotation Froths
   National Institute of Metallurgy, Report No. 1988, Randburg, South Africa, November 1978.

10. Dippenaar A

    The Destabilization of Froth by Solids I: The Mechanism of film rupture
    Int. J. Miner. Process., Vol 9, pp 1 – 14, 1982a

11. Dippenaar A

    The Destabilisation of Froth by Solids II: The Rate Determining Step
    International Journal of Mineral Processing, Vol 9, pp. 15 – 27, 1982b.

12. Francis JJ, Personal communications, 1999.

13. Flynn SA and Woodburn ET

Development of a Froth Model for the Fine-Particle beneficiation by Flotation
Trans. Instn. Min. Metall., Vol. 96, December 1987.

14. Gaudin AM,

Flotation, McGraw-Hill Book Company, New York, 2nd Edition, 1957.

15. Glembotskii VA, Klassen VI and Plaksin

Flotation
Primary Sources, New York, 1963.

16. Guarini M, Cipriano A, Soto A and Guesalaga A

Using Image Processing Techniques to Evaluate the Quality of Mineral Flotation Process
Proceedings of The International Conference on Signal Processing, Applications and Technology, pp 1227 – 1231, Boston, 1995.

17. Harris PJ, Personal Communications, 1998 and 1999.

18. Harris PJ,

"Frothing Phenomena and Frothers" a chapter in *Principles of Flotation (Edited by RP King)*
A Monograph of the South African Institute of Mining and Metallurgy, Johannesburg, 1982.

19. Hargrave JM, Miles NJ and Hall ST

The Use Grey Level Measurement in Predicting Coal Flotation Performance
Minerals Engineering, Vol. 9, No. 6, pp. 667 – 674, 1996

20. Hargrave JM and Hall ST

Diagnosis of Concentrate Grade and Mass Flowrate in Tin Flotation from Colour and Surface Texture Analysis
Minerals Engineering, Vol. 10, No. 6, pp. 613 – 621, 1997.

21. Hargrave JM, Brown GJ and Hall ST

Use of Fractal Dimensions in Describing Froth Structure
Proceedings of the XX IMPC – Aachen, pp. 281 – 292, September 1997.

22. Hey PM (Chief Mineralogist, AMPLATS), personal communications, 1998, 1999 and 2000.

23. Johansson G and Pugh RJ

The Influence of Particle Size and Hydrophobicity on the Stability of Mineralized Froths
Int J Miner. Process, Vol. 34, pp. 1 – 21, 1991.

24. Kinloch ED

Notes from "Geology and Applied Mineralogy for AMPLATS Metallurgists"
Presented at the AMPLATS Development Centre, Rustenburg, February 2000.

25. Klimpel RR

Considerations for Improving the Performance of Froth Flotation Systems.
Mining Engineering, pp. 1093 – 1100, December 1988.

26. Kordek J and Lenczokski S

The Evaluation of Flotation Froth Images by the Optical Method
XVI Int. Miner Proc. Congress, ed. Forssberg E, pp. 481 – 486, 1988

27. Kordek J and Kulig J

The Analysis of Diffraction Patterns of Flotation Froths as the Basis of Estimating the Content of the useful Component
Proceedings of the XX IMPC Congress – Aachen, pp. 457 – 464, September 1997.

28. Laskowski JS

Frothers and Frothing, Chapter 1 of *Frothing in Flotation II*
Eds Laskowski JS and Woodburn ET, Gordon and Breach Science Publishers, Amsterdam, pp. 1 - 52, 1998.

29. Lawyer JE and Barbarowics W

Mill Control. Part I: Automatic Control For Flotation Plants
Froth Flotation, Ed DW Fuerstenau, American Inst of Mining, Met and Petroleum Engrs, pp. 539 – 572, 1962.

30. Leja, J

Surface Chemistry of Froth Flotation
Plenum Press, New York, 1982

31. Lekki J and Laskowski J

A New Concept of Frothing in Flotation Systems and General Classification of Flotation Frothers
11th International Congress of Mineral Processing Proceedings, pp 429 – 448, Cagliari, 1975

32. Leonard RA and Lemlich R

A Study of Interstitial Liquid Flow in Foam. Part I: Theoretical Model and Application to Foam Fractionation.
AICHE Journal, pp. 18 – 25, January 1965.

33. Lotter NO

A Quality Control Model for the Development of High Confidence Flotation Test Data
MSc (Eng.)(Chem) Thesis, University of Cape Town, June 1995

34. Lynch AJ, Johnson NW, Manlapig EV and Thorne CG

Mineral and Coal Flotation Circuits – Their Simulation and Control
Elsevier Scientific Publishing Company, Amsterdam and New York, 1981.

35. Lynch AJ and McKee DJ

The Modelling and Control of Mineral Processing Plants
Plenary Lecture: Proceedings of MINTEK 50, International Conference on Mineral Science and Technology (ed. Haughton LF) Sandton, South Africa, 1984.

36. McKee DJ

Case Studies of Flotation Control
In "Innovations in Flotation Technology" Editors Mavros P and Matis KA, pp 235 – 262, Kluwer Academic Publishers, Netherlands, 1992.

37. Moolman DW, Aldrich C, van Deventer JSJ and Stange WW

Digital Image Processing as a Tool for on-line Monitoring of Froth in Flotation Plants
Minerals Engineering., Vol. 7, No. 9 , pp. 1149 - 1164, 1994.

38. Moolman DW, Aldrich C, van Deventer JSJ and Bradshaw DJ

The Interpretation of Flotation Froth Surfaces by using Image Analysis and Neural Networks
Chemical Engineering Science, Vol. 50, No. 22, pp. 3501 – 3513, 1995a.

39. Moolman DW, Aldrich C, van Deventer JSJ and Stange WW

The Classification of Froth Structures in a Copper Flotation Plant by means of a Neural Net
Int. J. Miner. Process., Vol. 43, pp. 193 – 208, 1995b.

40. Moolman DW, Aldrich C, and van Deventer JSJ

The Monitoring of Froth Surfaces on Industrial Flotation Plants using Connectionist Image Processing Techinques
Minerals Engineering, Vol. 8, No. 1/2, pp. 23 - 30, 1995c.

41. Moolman DW, Aldrich C, Schmitz GPJ and van Deventer JSJ

The Interrelationship between Surface Characteristics and Industrial Flotation Performance
Minerals Engineering, Vol. 9, No. 8, pp. 837 – 854, 1996a.

42. Moolman DW, Eksteen JJ, Aldrich C and van Deventer JSJ

The Significance of Flotation Froth Appearance for Machine Vision Control
Int. J. Miner. Process., Vol. 48, pp. 135 – 158, 1996b.

43. Napier-Munn TJ

An Introduction to Comparative Statistics and Experimental Design for Minerals Engineers
Course Notes, 2nd Edition, Version 2.2, The University of Queensland, 1996.

44. Nguyen KK and Thornton AJ

The Application of Texture Based Image Analysis Techniques in Froth Flotation
Conference Proceedings DICTA '95, Brisbane, 1995.

45. Nguyen KK and Holtham P

The Application of Pixel Tracing Techniques in the Flotation Process
Conference Proceedings DICTA/IVCNZ ' 97, 1997.

46. Nguyen KK, Personal communications, November 1999.

47. Rixom PM

Amandelbult Concentrator Survey: Report No1 [Mineralogical] Study of Amandelbult Merensky Rougher Circuit.
Unpublished Confidential Internal Report, Johannesburg Consolidated Investment Company Ltd., QEM*SEM Report No. 1/80, 14 July 1993.

48. Taggart AF

Handbook of Ore Dressing
John Wiley and Sons, New York, 1927.

49. Sadr-Kazemi N and Cilliers JJ

An Image Processing Algorithm for the Measurement of Flotation Froth Bubble Size and Shape Distributions
Minerals Engineering, Vol. 10, No. 10, pp. 1075 – 1083, 1997

50. Schubert JH, Henning RGD, Gebbie IR and Valenta M

Imporved Flotation Performance at Karee Platinum Mine through better Level Control
SAIMM, Vol. 99, No. 1, pp. 35 – 39, 1999.

51. Senior GD, Shannon LK and Trahar WJ

The Flotation of Pentlandite from Pyrrhotite with particular reference to the effects of particles size
Int. J. of Miner. Process., Vol 42, pp 169 – 190, 1994.

52. Smith PG and Warren LJ

Entrainment of Particles into Flotation Froths
Mineral Processing and Extractive Metallurgy Review, Vol. 5, pp. 123 – 145, 1989.

53. Subrahmanyam TV and Forssberg Eric

Froth Stability, Particle Entrainment and Drainage in Flotation – A Review
Int J. of Min Proc, Vol. 23, pp 33 - 35, 1988

54. Sutherland KL and Wark IW

Principles of Flotation
Australian Inst of Mining and Metallurgy, Melbourne, 1955.

55. Sweet C, van Hoogstraten J, Harris M and Laskowski J

The Effect of Frothers on Bubble Size and Frothability of Aqueous Solutions
Processing of Complex Ores – Proc. 2nd UBC – McGill Int. Symposium (Eds. JA Finch, SR Roa and I Holubec), CIM Metallurgical Society, Sudbury, 1997, pp 235 – 244 (+)

56. Symonds PJ and de Jager G

A Technique for Automatically Segmenting Images of the Surface Froth Structures that are Prevalent in Industrial Flotation Cells
Proceedings of the 1992 SA Symposium on Communications and Signal Processing, Rondebosch, pp 111 – 115, 1992

57. Taggart

Handbook of Ore Dressing
John Wiley and Sons, New York, 1927

58. Taylor JK

Statistical Techniques for Data Analysis
Lewis Publishers, Inc., Boca Raton, Florida, 1990

59. Trahar WJ

Rational Interpretation of the Role of Particle Size in Flotation
Int. J. of Miner. Process., Vol 8, pp 289 – 327, 1981.

60. van Deventer JSJ, Bezuidenhout M, and Moolman DW

On-line Visualisation of Flotation Performance using Neural Computer Vision of the Froth Texture

Proceedings of the XX IMPC – Aachen, September 1997.

61. Viljoen MJ, Theron, J, Underwood B, Walters BM, Weaver J and Peyerl W

The Amandelbult Section of Rustenburg Platinum Mines Limited, with reference to the Merensky Reef

Mineral Deposits of South Africa (Eds CR Anheausser and Maske S), Geol. Soc. S. Afr. , Johannesburg, pp 1041 – 1060, 1986.

62. Walters B, Chief Geologist RPM – Amandelbult Section, personal communications, 1998

63. Warren LJ

Ultrafine Particles in Flotation

Principles of Mineral Flotation, (Eds MH Jones and JT Woodcock). The Wark Symposium. Symp Series No. 40, Australian Institute of Mining and Metallurgy, pp. 185 - 213,1984.

64. Weiss NL (Editor-in-Chief),

SME Mineral Processing Handbook

Society of Mining Engineers, New York, 1985

65. Wills BA

Mineral Processing Technology

Pergamon Press, Oxford, 5th Edition, 1992

66. Woodburn ET, Stockton JB and Robbins DJ

Vision – Based Characterisation of 3 Phase Froths

International Colloquium, "Developments in Froth Flotation", Gordon's Bay Cape Town, Vol. 1, pp. 1 – 45, 1989.

67. Woodburn ET, Austin LG and Stockton JB

A Froth Based Flotation Kinetic Model

Trans IChemE, Vol. 72, Part A, pp. 211 – 226, 1994.

68. Wright BA

A Review of the Use of Image Processing Techniques in the Modelling and Control of Froth Flotation

(UCT document, unpublished), August 1998.

69. Wright BA, Personal Communications, 1998 and 1999

70. Wright BA

The Development of a Vision-Based Flotation Froth Analysis System

MSc Thesis, University of Cape Town, South Africa, 1999.

APPENDIX A:

Enterprise Overview

And

Geological Description of

Amandelbult Section

APPENDIX A: BACKGROUND

Enterprise Overview

Rustenburg Platinum Mines Ltd. (RPM), a wholey owned company in the Anglo American Platinum Corporation (or as it is known, AMPLATS) stable, mines and processes primarily two kinds of Platinum Group Mineral (PGM) bearing ores, namely the Merensky reef and the Upper Group 2 or UG2 reef. The two reef types are typically processed separately at the various sites' concentration facilities to produce separate UG2 and Merensky concentrates. A further reef type, known as "platreef" is mined and processed at the group's Potgietersrus Platinums Ltd business unit. These concentrates are transported by road to one of the AMPLATS group's smelting facilities, either Mortimer Smelter situated at the RPM -Union Section mine or the Waterval Smelter which is located in Rustenburg, for further processing. After the smelting process, the Platinum Group Element (PGE) and base metal rich sulphide matte receives further processing at Rustenburg Base Metal Refiners Ltd., which produces saleable nickel cathodes, copper cathodes and cobalt sulphate crystal. The PGE present in the matte are recovered via a magnetic separation and leachiat the Base Metal Refinery as a magnetic concentrate, which is of a very high grade. This magnetic concentrate is then further beneficiated at the Precious Metals Refinery, from where discrete, high purity, saleable precious metals are produced.

Amandelbult Section Overview and Geological Description

The ore used for the batch flotation programme of this study was collected at the Rustenburg Platinum Mine's Amandelbult Section. This was also the site chosen for the plant-based phase of the study. Amandelbult Section is approximately 100 km north of the Rustenburg, in the North Western Province of South Africa. This mine's lease area covers some 20 km of the Merensky reef's strike length on the western limb of the Bushveld Igneous Complex (Walters, 1998).

Amandelbult Section mines two kinds of Platinum Group Mineral (PGM) bearing ores, namely the Merensky reef mentioned above, and the Upper Group 2 or UG2 reef. The two reef types are processed separately at the mine's Concentrator facility, to produce separate UG2 and Merensky concentrates. These concentrates follow the processes described in the overview above, finally resulting in saleable base metal and precious metal products.

The Merensky reef at Amandelbult is described by Viljoen *et al.* (1986) as being a "pegmetoidal feldspathic pyroxenite". The reef is bounded on the top and bottom by chromitite layers, with an average width of 1 to 1.5m and dipping at an average of 20° to the South East. They state that Pentlandite and Chalcopyrite are the major base metal sulphides, while significant amounts of Pyrhotite and Troilite are present. Viljoen and co-authors further state that the Platinum Group Minerals present to be predominantly Pt-Fe alloys, Pt-Pd tellurides,

Pt-Pd sulphides and laurite ($Ru(Os,Ir)S_2$). Viljoen *et al.* (1986) state that the lower regions of the reef are olivine rich, and these areas contain significant amounts of base metals (nickel in particular). According to Hey (1998) a fairly large proportion of this base metal content is in a non-recoverable silicate form.

A point made by both Hey (1998) and Walters (1998) is that the characteristics of Merensky reef at Amandelbult change considerably both along the length of the strike and down the dip. Viljoen *et al.* (1986) mention a number of iron rich bodies found along the length of the Merensky strike, as well as features known as "potholes" at various positions within the lease area. These potholes are described as being areas where the Merensky reef "plunges down" and transgresses its footwall. Mineralogically, Viljoen *et al.* (1986) state that the pothole-type reef often has higher concentrations of valuable minerals than the normal reef, which warrants its exploitation.

The following figures are taken from the comprehensive paper by Viljoen *et al.* (1986) and show some of the variations in the Merensky reef mapped within the Amandelbult lease area:

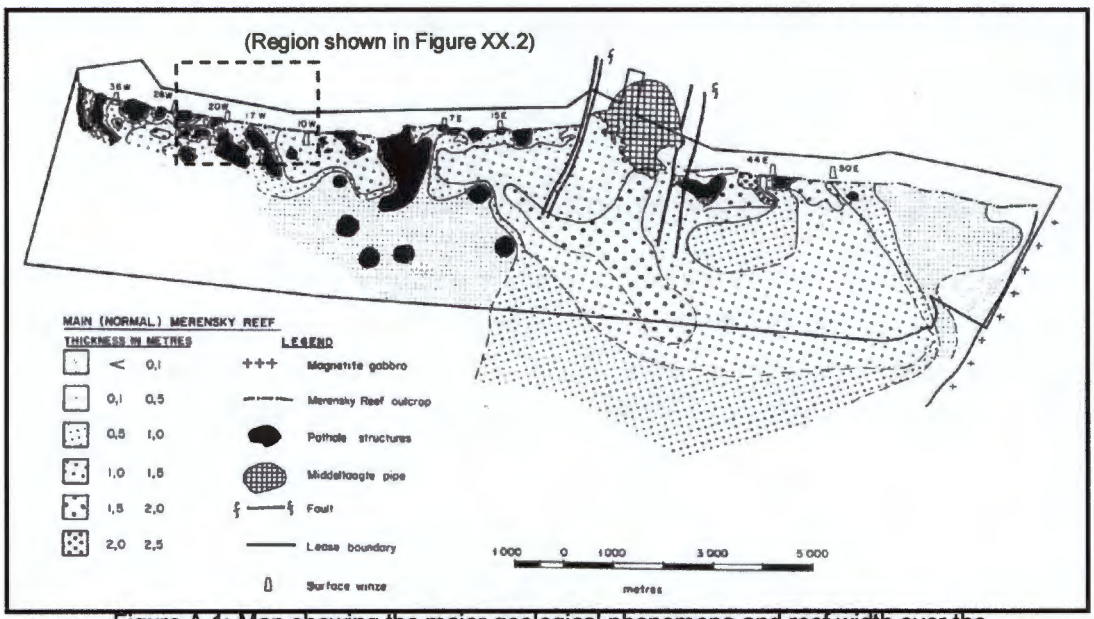

Figure A.1: Map showing the major geological phenomena and reef width over the Amandelbult lease area (taken from Viljoen *et al.*, 1986).

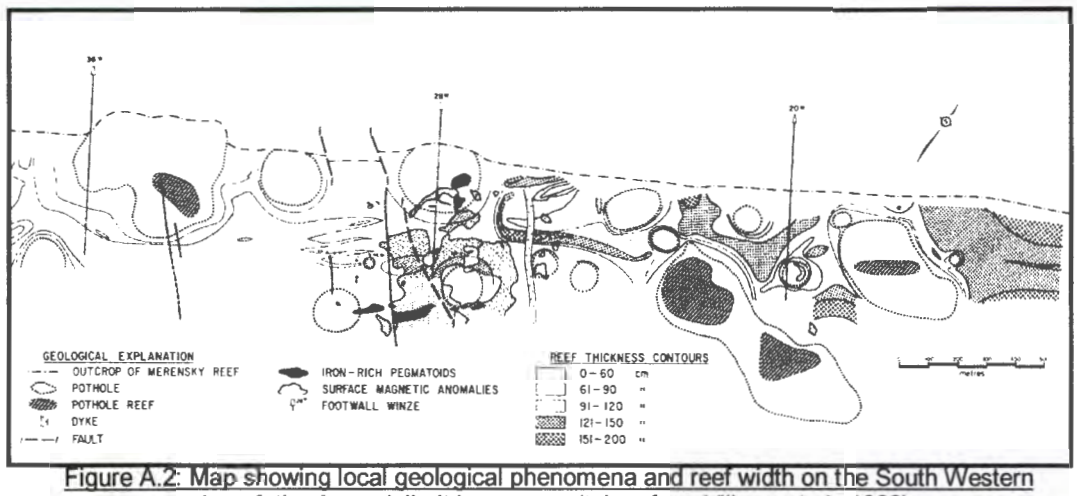

Figure A.2: Map showing local geological phenomena and reef width on the South Western edge of the Amandelbult lease area (taken from Viljoen *et al.*, 1986).

APPENDIX B:

Batch Flotation Results

APPENDIX BI: Reproducibility Tests Metallurgical Results

APPENDIX BII: Results from tests in which Depressant and Frother Dosages were manipulated

BIIa: Image Analysis Results

BIIb: Metallurgical Results

APPENDIX BIII: Results from tests in which a broader group of variables were manipulated

BIIIa: Brief Discussion of Results

BIIIb: Image Analysis results

BIIIc: Metallurgical Results

APPENDIX BI: Reproducibility Tests Metallurgical Results

Reproducibility Tests

A1.1 Standard (Test 3)

Quantities

	Mass (g)	Water (g)	Cu (%)	Ni (%)	S (%)
RC1	7.45	7.86	4.029	3.850	9.46
RC2	7.11	11.66	1.092	2.971	4.52
RC3	9.79	16.10	0.481	2.226	3.36
RC4	7.67	13.51	0.343	2.078	2.92
RC5	8.45	22.45	0.275	1.710	2.35
Tail	974.89		0.016	0.177	0.10
Total	1015.36	71.58			

Distribution

	Mass (%)	Water ---	Cu (%)	Ni (%)	S (%)
RC1	0.73		47.73	10.44	25.64
RC2	0.70		12.34	7.69	11.69
RC3	0.96		7.49	7.94	11.97
RC4	0.76		4.19	5.80	8.15
RC5	0.83		3.69	5.26	7.22
Tail	96.01		24.57	62.86	35.33

Cumulative Distribution (Recovery)

	Mass (%)	Water (g)	Cu (%)	Ni (%)	S (%)
RC1	0.73	7.86	47.73	10.44	25.64
RC1+2	1.43	19.52	60.07	18.14	37.33
RC1+2+3	2.40	35.62	67.56	26.07	49.30
RC1+2+3+4	3.15	49.13	71.74	31.88	57.45
RC1+2+3+4+5	3.99	71.58	75.43	37.14	64.67

Cumulative Grade

	Mass ---	Water ---	Cu (%)	Ni (%)	S (%)
RC1			4.029	3.850	9.46
RC1+2			2.595	3.421	7.05
RC1+2+3			1.745	2.941	5.57
RC1+2+3+4			1.409	2.734	4.93
RC1+2+3+4+5			1.172	2.520	4.39

Reconciliation

	Mass (g)	Water ---	Cu (%)	Ni (%)	S (%)
Built-up Head	1028.21		0.062	0.270	0.27
Assayed Head	1030.00		0.049	0.282	0.29
Call (%)	99.83		127.59	95.84	94.98

Reproducibility Tests

A1.2 Standard (Test 4)

Quantities					
	Mass (g)	Water (g)	Cu (%)	Ni (%)	S (%)
RC1	6.87	5.80	4.148	4.410	10.15
RC2	6.88	9.59	1.294	3.414	5.11
RC3	9.49	16.10	0.623	2.356	3.91
RC4	6.00	13.96	0.359	1.918	2.81
RC5	7.79	20.16	0.315	1.863	2.30
Tail	981.34		0.013	0.173	0.16
Total	1018.37	65.61			

Distribution					
	Mass (%)	Water —	Cu (%)	Ni (%)	S (%)
RC1	0.67		47.12	11.16	21.20
RC2	0.68		14.72	8.65	10.69
RC3	0.93		9.78	8.23	11.28
RC4	0.59		3.56	4.24	5.13
RC5	0.76		4.06	5.34	5.45
Tail	96.36		20.76	62.37	46.25

Cumulative Distribution (Recovery)					
	Mass (%)	Water (g)	Cu (%)	Ni (%)	S (%)
RC1	0.67	5.80	47.12	11.16	21.20
RC1+2	1.35	15.39	61.84	19.81	31.89
RC1+2+3	2.28	31.49	71.62	28.04	43.18
RC1+2+3+4	2.87	45.45	75.18	32.28	48.30
RC1+2+3+4+5	3.64	65.61	79.24	37.63	53.75

Cumulative Grade					
	Mass —	Water —	Cu (%)	Ni (%)	S (%)
RC1			4.148	4.410	10.15
RC1+2			2.720	3.912	7.63
RC1+2+3			1.864	3.276	6.11
RC1+2+3+4			1.555	2.998	5.43
RC1+2+3+4+5			1.294	2.759	4.77

Reconciliation					
	Mass (g)	Water —	Cu (%)	Ni (%)	S (%)
Built-up Head	1027.87		0.059	0.267	0.32
Assayed Head	1030.00		0.046	0.242	0.32
Call (%)	99.79		129.14	110.13	101.24

Reproducibility Tests

A1.4 Standard (Test 9)

Quantities

	Mass (g)	Water (g)	Cu (%)	Ni (%)	S (%)
RC1	7.23	7.09	3.512	3.087	8.27
RC2	7.82	11.19	1.182	2.584	4.27
RC3	10.20	16.68	0.461	2.329	3.36
RC4	7.10	11.07	0.263	1.710	2.62
RC5	8.56	14.28	0.242	1.583	2.21
Tail	972.35		0.015	0.199	0.21
Total	1013.26	60.31			

Distribution

	Mass (%)	Water —	Cu (%)	Ni (%)	S (%)
RC1	0.71		43.98	7.82	16.11
RC2	0.77		16.01	7.08	9.00
RC3	1.01		8.15	8.33	9.23
RC4	0.70		3.23	4.26	5.01
RC5	0.84		3.59	4.75	5.10
Tail	95.96		25.03	67.76	55.55

Cumulative Distribution (Recovery)

	Mass (%)	Water (g)	Cu (%)	Ni (%)	S (%)
RC1	0.71	7.09	43.98	7.82	16.11
RC1+2	1.49	18.28	59.99	14.91	25.11
RC1+2+3	2.49	34.96	68.15	23.24	34.34
RC1+2+3+4	3.19	46.03	71.38	27.49	39.36
RC1+2+3+4+5	4.04	60.31	74.97	32.24	44.45

Cumulative Grade

	Mass —	Water —	Cu (%)	Ni (%)	S (%)
RC1			3.512	3.087	8.27
RC1+2			2.301	2.826	6.19
RC1+2+3			1.558	2.625	5.05
RC1+2+3+4			1.274	2.424	4.51
RC1+2+3+4+5			1.058	2.248	4.03

Reconciliation

	Mass (g)	Water —	Cu (%)	Ni (%)	S (%)
Built-up Head	1028.00		0.057	0.282	0.37
Assayed Head	1030.00		0.042	0.246	0.29
Call (%)	99.81		136.87	114.63	128.51

Reproducibility Tests

A1.3 Standard (Test 13)

Quantities					
	Mass (g)	Water (g)	Cu (%)	Ni (%)	S (%)
RC1	7.85	7.62	3.742	3.154	9.11
RC2	7.52	11.34	0.840	2.504	3.85
RC3	9.78	16.08	0.303	1.595	3.10
RC4	7.76	13.31	0.184	1.516	2.66
RC5	9.84	20.75	0.164	1.326	2.26
Tail	975.47		0.013	0.161	0.14
Total	1018.22	69.10			

Distribution					
	Mass (%)	Water —	Cu (%)	Ni (%)	S (%)
RC1	0.77		54.29	10.28	22.98
RC2	0.74		11.67	7.82	9.30
RC3	0.96		5.47	6.48	9.74
RC4	0.76		2.64	4.89	6.63
RC5	0.97		2.98	5.42	7.15
Tail	95.80		22.94	65.11	44.20

Cumulative Distribution (Recovery)					
	Mass (%)	Water (g)	Cu (%)	Ni (%)	S (%)
RC1	0.77	7.62	54.29	10.28	22.98
RC1+2	1.51	18.96	65.96	18.10	32.28
RC1+2+3	2.47	35.04	71.44	24.58	42.02
RC1+2+3+4	3.23	48.35	74.08	29.47	48.66
RC1+2+3+4+5	4.20	69.10	77.06	34.89	55.80

Cumulative Grade					
	Mass —	Water —	Cu (%)	Ni (%)	S (%)
RC1			3.742	3.154	9.11
RC1+2			2.322	2.836	6.54
RC1+2+3			1.537	2.354	5.20
RC1+2+3+4			1.218	2.156	4.60
RC1+2+3+4+5			0.975	1.965	4.06

Reconciliation					
	Mass (g)	Water —	Cu (%)	Ni (%)	S (%)
Built-up Head	1031.28		0.053	0.236	0.31
Assayed Head	1030.00		0.055	0.260	0.33
Call (%)	100.12		97.26	91.12	92.34

APPENDIX BII: Results from tests in which Depressant and Frother Dosages were manipulated

BIIa: Image Analysis Results

BIIb: Metallurgical Results

Area Coverages By Small, Medium and Large Bubbles for the First Part of the Batch Flotation Programme

Test name and bubble size classes	Time (minutes)													
	0.25	0.5	0.75	1	1.5	2	3	4	5	6	7	8	9	10
Standard														
Small	26.3	28.9	26.9	24.5	26.3	26.9	29.3	30.2	34.5	42.0	45.3	48.7	48.8	48.7
Medium	20.5	25.7	29.6	30.3	35.9	36.3	28.8	29.0	34.5	30.0	29.1	32.3	36.2	36.6
Large	51.8	44.6	42.9	44.6	37.3	36.0	41.1	39.8	29.6	26.6	24.0	17.1	12.9	12.3
% of area accounted for	98.6	99.2	99.3	99.4	99.6	99.2	99.3	99.0	98.6	98.5	98.4	98.1	97.9	97.6
No Depressant														
Small	20.2	18.7	19.5	21.9	24.5	25.5	22.3	25.4	32.1	30.9	29.1	31.3	29.3	31.0
Medium	23.7	20.9	20.0	20.7	23.7	27.9	31.8	31.1	31.4	36.4	35.8	31.9	28.8	29.1
Large	54.9	59.5	60.0	56.8	51.4	46.1	45.0	42.0	34.7	30.7	32.8	33.9	38.0	35.7
% of area accounted for	98.8	99.1	99.5	99.4	99.6	99.5	99.1	98.5	98.2	98.0	97.7	97.1	96.1	95.8
High Frother High Depressant														
Small	28.4	28.4	28.9	28.3	28.4	31.5	37.1	46.6	44.3	41.6	47.0	54.2	64.6	63.1
Medium	18.8	19.6	21.7	27.1	26.1	24.8	27.9	28.0	29.8	31.0	31.5	27.8	27.3	32.7
Large	51.0	51.0	48.6	43.6	44.7	42.6	33.7	23.9	24.5	25.8	20.0	16.0	6.0	2.1
% of area accounted for	98.2	99.0	99.2	99.1	99.2	98.9	98.7	98.5	98.6	98.4	98.5	98.0	97.9	97.9
High Frother Low Depressant														
Small	17.6	17.2	22.0	22.2	17.2	21.4	26.3	26.3	27.9	28.6	32.2	31.7	28.9	36.3
Medium	25.2	22.1	19.4	21.4	21.8	23.4	26.1	25.6	29.0	28.6	28.5	36.6	38.6	34.8
Large	55.7	60.0	58.0	56.0	60.2	54.5	46.6	46.6	41.6	41.3	37.4	29.6	30.1	26.1
% of area accounted for	98.6	99.3	99.4	99.6	99.2	99.3	99.0	98.6	98.5	98.4	98.1	97.9	97.6	97.3
Low Frother High Depressant														
Small	52.6	40.0	35.4	41.2	41.7	51.6	57.3	56.6	56.1	50.5	51.9	61.0	64.7	61.1
Medium	20.2	20.9	23.8	24.3	24.6	27.4	32.3	30.7	23.0	24.6	28.8	26.8	28.4	35.1
Large	25.6	38.0	40.3	33.8	33.1	20.3	9.6	11.6	19.6	23.4	17.2	10.1	4.7	1.8
% of area accounted for	98.4	99.0	99.5	99.2	99.4	99.3	99.2	98.9	98.7	98.6	97.9	98.0	97.8	98.0
Low Frother Low Depressant														
Small	19.6	20.9	28.7	34.2	32.2	35.8	38.9	38.8	39.8	36.0	34.4	37.1	38.2	41.1
Medium	16.7	16.9	20.5	21.4	26.4	32.2	29.6	31.3	34.0	34.9	34.7	31.3	27.3	27.4
Large	62.7	61.2	50.2	44.0	40.8	31.4	30.7	29.2	25.5	28.1	29.6	30.2	32.9	29.5
% of area accounted for	99.0	99.0	99.4	99.6	99.4	99.3	99.2	99.2	99.3	99.0	98.7	98.6	98.4	98.0

Standard

Quantities					
	Mass (g)	Water (g)	Cu (%)	Ni (%)	S (%)
Conc1	7.35	6.84	3.858	3.625	9.25
Conc2	7.33	10.71	1.102	2.868	4.44
Conc3	9.82	16.29	0.467	2.127	3.43
Conc4	7.13	12.78	0.287	1.806	2.75
Conc5	8.66	18.40	0.249	1.620	2.28
Tail	976.01		0.014	0.177	0.15
Total	1016.30	65.01			

Distribution					
	Mass (%)	Water —	Cu (%)	Ni (%)	S (%)
Conc1	0.72		48.10	9.92	21.12
Conc2	0.72		13.71	7.83	10.11
Conc3	0.97		7.78	7.77	10.47
Conc4	0.70		3.48	4.80	6.10
Conc5	0.85		3.66	5.23	6.14
Tail	96.04		23.28	64.45	46.07

Cumulative Distribution (Recovery)					
	Mass (%)	Water (g)	Cu (%)	Ni (%)	S (%)
Conc1	0.72	6.84	48.10	9.92	21.12
Conc1+2	1.44	17.54	61.81	17.76	31.23
Conc1+2+3	2.41	33.83	69.59	25.53	41.70
Conc1+2+3+4	3.11	46.61	73.07	30.33	47.80
Conc1+2+3+4+5	3.96	65.01	76.72	35.55	53.93

Cumulative Grade					
	Mass —	Water —	Cu (%)	Ni (%)	S (%)
Conc1			3.858	3.625	9.25
Conc1+2			2.482	3.247	6.85
Conc1+2+3			1.674	2.798	5.48
Conc1+2+3+4			1.362	2.574	4.86
Conc1+2+3+4+5			1.123	2.369	4.31

Reconciliation					
	Mass (g)	Water —	Cu (%)	Ni (%)	S (%)
Built-up Head	1028.21		0.058	0.264	0.32
Assayed Head	1030.00		0.048	0.257	0.31
Call (%)	99.83		121.59	102.66	103.83

No Depressant

Quantities					
	Mass (g)	Water (g)	Cu (%)	Ni (%)	S (%)
Conc1	9.87	13.43	2.928	2.686	7.24
Conc2	7.47	14.41	0.714	2.147	3.24
Conc3	9.82	19.02	0.403	1.837	3.06
Conc4	6.46	12.53	0.308	1.752	2.65
Conc5	9.53	14.36	0.249	1.677	2.44
Tail	964.92		0.013	0.182	0.19
Total	1008.07	73.75			

Distribution					
	Mass (%)	Water —	Cu (%)	Ni (%)	S (%)
Conc1	0.98		52.12	10.05	20.59
Conc2	0.74		9.61	6.08	6.97
Conc3	0.97		7.14	6.84	8.65
Conc4	0.64		3.59	4.29	4.93
Conc5	0.95		4.29	6.06	6.70
Tail	95.72		23.25	66.67	52.16

Cumulative Distribution (Recovery)					
	Mass (%)	Water (g)	Cu (%)	Ni (%)	S (%)
Conc1	0.98	13.43	52.12	10.05	20.59
Conc1+2	1.72	27.84	61.73	16.13	27.56
Conc1+2+3	2.69	46.86	68.87	22.97	36.21
Conc1+2+3+4	3.33	59.39	72.46	27.27	41.14
Conc1+2+3+4+5	4.28	73.75	76.75	33.33	47.84

Cumulative Grade					
	Mass —	Water —	Cu (%)	Ni (%)	S (%)
Conc1			2.928	2.686	7.24
Conc1+2			1.974	2.454	5.51
Conc1+2+3			1.406	2.231	4.63
Conc1+2+3+4			1.195	2.139	4.24
Conc1+2+3+4+5			0.986	2.037	3.85

Reconciliation					
	Mass (g)	Water —	Cu (%)	Ni (%)	S (%)
Built-up Head	1015.13		0.055	0.262	0.34
Assayed Head	1030.00		0.048	0.275	0.30
Call (%)	98.56		114.13	95.26	113.00

High Frother/High Depressant

Quantities					
	Mass (g)	Water (g)	Cu (%)	Ni (%)	S (%)
Conc1	8.90	11.79	2.964	3.578	9.99
Conc2	7.50	16.70	0.593	2.506	4.24
Conc3	10.88	29.38	0.291	1.898	3.20
Conc4	7.85	22.42	0.187	1.406	2.26
Conc5	10.62	34.17	0.156	1.323	1.68
Tail	967.01		0.012	0.161	0.14
Total	1012.75	114.45			

Distribution					
	Mass (%)	Water ---	Cu (%)	Ni (%)	S (%)
Conc1	0.88		54.11	12.62	27.35
Conc2	0.74		9.12	7.45	9.78
Conc3	1.07		6.50	8.19	10.70
Conc4	0.78		3.01	4.38	5.46
Conc5	1.05		3.40	5.57	5.49
Tail	95.48		23.86	61.79	41.22

Cumulative Distribution (Recovery)					
	Mass (%)	Water (g)	Cu (%)	Ni (%)	S (%)
Conc1	0.88	11.79	54.11	12.62	27.35
Conc1+2	1.62	28.49	63.23	20.07	37.13
Conc1+2+3	2.69	57.87	69.73	28.26	47.83
Conc1+2+3+4	3.47	80.28	72.74	32.64	53.29
Conc1+2+3+4+5	4.52	114.45	76.14	38.21	58.78

Cumulative Grade					
	Mass ---	Water ---	Cu (%)	Ni (%)	S (%)
Conc1			2.964	3.578	9.99
Conc1+2			1.879	3.088	7.36
Conc1+2+3			1.246	2.613	5.70
Conc1+2+3+4			1.009	2.344	4.93
Conc1+2+3+4+5			0.811	2.107	4.17

Reconciliation					
	Mass (g)	Water ---	Cu (%)	Ni (%)	S (%)
Built-up Head	1026.62		0.048	0.249	0.32
Assayed Head	1030.00		0.047	0.260	0.31
Call (%)	99.67		102.92	95.89	102.99

High Frother/Low Depressant

Quantities					
	Mass (g)	Water (g)	Cu (%)	Ni (%)	S (%)
Conc1	10.46	18.98	3.172	3.466	7.88
Conc2	7.44	16.38	0.658	2.461	3.40
Conc3	9.60	25.49	0.371	1.935	2.94
Conc4	6.95	18.49	0.298	1.896	2.55
Conc5	11.02	24.21	0.217	1.599	2.21
Tail	969.65		0.013	0.211	0.21
Total	1015.10	103.54			

Distribution					
	Mass (%)	Water —	Cu (%)	Ni (%)	S (%)
Conc1	1.03		56.46	11.74	21.42
Conc2	0.73		8.33	5.93	6.57
Conc3	0.95		6.07	6.02	7.33
Conc4	0.68		3.53	4.27	4.61
Conc5	1.09		4.07	5.71	6.34
Tail	95.52		21.54	66.34	53.74

Cumulative Distribution (Recovery)					
	Mass (%)	Water (g)	Cu (%)	Ni (%)	S (%)
Conc1	1.03	18.98	56.46	11.74	21.42
Conc1+2	1.76	35.36	64.79	17.67	27.99
Conc1+2+3	2.71	60.85	70.86	23.69	35.32
Conc1+2+3+4	3.39	79.34	74.39	27.96	39.93
Conc1+2+3+4+5	4.48	103.54	78.46	33.66	46.26

Cumulative Grade					
	Mass —	Water —	Cu (%)	Ni (%)	S (%)
Conc1			3.172	3.466	7.88
Conc1+2			2.127	3.048	6.01
Conc1+2+3			1.514	2.660	4.94
Conc1+2+3+4			1.269	2.506	4.46
Conc1+2+3+4+5			1.014	2.286	3.91

Reconciliation					
	Mass (g)	Water —	Cu (%)	Ni (%)	S (%)
Built-up Head	1031.91		0.058	0.304	0.38
Assayed Head	1030.00		0.057	0.278	0.31
Call (%)	100.19		102.30	109.38	122.54

Low Frother/High Depressant

Quantities					
	Mass (g)	Water (g)	Cu (%)	Ni (%)	S (%)
Conc1	0.25	0.58	6.945	3.768	0.00
Conc2	0.96	2.64	4.288	3.240	8.99
Conc3	4.55	4.96	2.029	2.886	7.01
Conc4	3.14	0.91	1.620	2.890	6.16
Conc5	3.94	1.16	1.242	2.438	5.05
Tail	1002.09		0.024	0.242	0.24
Total	1014.92	10.25			

Distribution					
	Mass (%)	Water ---	Cu (%)	Ni (%)	S (%)
Conc1	0.02		3.49	0.33	0.00
Conc2	0.09		8.44	1.12	2.73
Conc3	0.45		18.91	4.71	10.09
Conc4	0.31		10.43	3.26	6.12
Conc5	0.39		10.04	3.45	6.30
Tail	98.74		48.70	87.13	74.76

Cumulative Distribution (Recovery)					
	Mass (%)	Water (g)	Cu (%)	Ni (%)	S (%)
Conc1	0.02	0.58	3.49	0.33	0.00
Conc1+2	0.12	3.21	11.93	1.45	2.73
Conc1+2+3	0.57	8.17	30.83	6.16	12.82
Conc1+2+3+4	0.88	9.08	41.27	9.42	18.94
Conc1+2+3+4+5	1.26	10.25	51.30	12.87	25.24

Cumulative Grade					
	Mass ---	Water ---	Cu (%)	Ni (%)	S (%)
Conc1			6.945	3.768	0.00
Conc1+2			4.828	3.347	7.16
Conc1+2+3			2.615	2.983	7.04
Conc1+2+3+4			2.264	2.950	6.73
Conc1+2+3+4+5			1.950	2.793	6.21

Reconciliation					
	Mass (g)	Water ---	Cu (%)	Ni (%)	S (%)
Built-up Head	1029.32		0.048	0.274	0.31
Assayed Head	1030.00		0.053	0.255	0.32
Call (%)	99.93		91.34	107.57	96.74

Low Frother/Low Depressant

Quantities					
	Mass (g)	Water (g)	Cu (%)	Ni (%)	S (%)
Conc1	2.81	1.04	3.447	2.297	10.73
Conc2	3.75	3.09	1.557	2.137	6.20
Conc3	5.16	6.08	0.868	1.860	5.11
Conc4	4.21	7.96	0.605	1.772	4.28
Conc5	4.61	4.72	0.486	1.754	3.55
Tail	996.39		0.026	0.205	0.22
Total	1016.92	22.90			

Distribution					
	Mass (%)	Water —	Cu (%)	Ni (%)	S (%)
Conc1	0.28		19.23	2.65	8.96
Conc2	0.37		11.58	3.29	6.90
Conc3	0.51		8.89	3.94	7.83
Conc4	0.41		5.06	3.06	5.35
Conc5	0.45		4.44	3.32	4.86
Tail	97.98		50.79	83.74	66.09

Cumulative Distribution (Recovery)					
	Mass (%)	Water (g)	Cu (%)	Ni (%)	S (%)
Conc1	0.28	1.04	19.23	2.65	8.96
Conc1+2	0.64	4.13	30.81	5.94	15.86
Conc1+2+3	1.15	10.21	39.70	9.88	23.70
Conc1+2+3+4	1.57	18.17	44.76	12.94	29.05
Conc1+2+3+4+5	2.02	22.90	49.21	16.26	33.91

Cumulative Grade					
	Mass —	Water —	Cu (%)	Ni (%)	S (%)
Conc1			3.447	2.297	10.73
Conc1+2			2.367	2.205	8.14
Conc1+2+3			1.707	2.053	6.80
Conc1+2+3+4			1.415	1.979	6.13
Conc1+2+3+4+5			1.207	1.928	5.55

Reconciliation					
	Mass (g)	Water —	Cu (%)	Ni (%)	S (%)
Built-up Head	1031.39		0.050	0.239	0.33
Assayed Head	1030.00		0.047	0.260	0.31
Call (%)	100.13		105.40	92.12	108.35

Standard Test Error Analysis

All figures quoted as percent 'relative standard deviation'

Quantities					
	Mass (%)	Water (%)	Cu (%)	Ni (%)	S (%)
Conc1	5.58	13.69	7.44	17.29	8.46
Conc2	5.72	9.06	17.56	14.53	11.87
Conc3	2.97	2.09	28.06	16.86	9.94
Conc4	11.35	11.86	28.08	13.57	5.03
Conc5	9.90	19.45	25.74	14.01	2.61
Tail	0.39		11.04	8.97	30.59
Total	0.24	6.81			

Distribution					
	Mass (%)	Water —	Cu (%)	Ni (%)	S (%)
Conc1	5.56		8.97	14.64	18.71
Conc2	5.87		14.82	8.25	12.32
Conc3	3.19		23.06	11.09	12.14
Conc4	11.40		18.95	15.35	23.70
Conc5	9.84		12.49	5.83	17.88
Tail	0.25		8.28	3.81	18.31

Cumulative Distribution (Recovery)					
	Mass (%)	Water (%)	Cu (%)	Ni (%)	S (%)
Conc1	5.56	13.69	8.97	14.64	18.71
Conc1+2	4.88	10.81	4.52	11.55	15.85
Conc1+2+3	3.92	5.99	3.07	8.09	14.55
Conc1+2+3+4	5.27	3.29	2.51	7.38	15.25
Conc1+2+3+4+5	5.97	6.81	2.52	6.94	15.18

Cumulative Grade					
	Mass —	Water —	Cu (%)	Ni (%)	S (%)
Conc1			7.44	17.29	8.46
Conc1+2			8.31	16.08	9.14
Conc1+2+3			9.33	14.24	8.62
Conc1+2+3+4			11.04	14.20	8.54
Conc1+2+3+4+5			12.34	14.45	8.03

Reconciliation					
	Mass (%)	Water —	Cu (%)	Ni (%)	S (%)
Built-up Head	0.16		6.47	7.30	12.55
Assayed Head	0.00		11.40	7.07	7.74
Call (%)	0.16		14.22	10.91	15.91

APPENDIX BIII: Results from tests in which a broader group of variables were manipulated

BIIIa: Brief Discussion of Results

BIIIb: Image Analysis results

BIIIc: Metallurgical Results

APPENDIX BIII:

Results of the batch flotation programme assessing the influence of a wider group of variables

The second part of the programme assessed the influences of variables other than those tested in the first part of the programme, which concentrated on the frother and depressant dosages. The following table shows the tests conducted and the level of each variable assessed:

Condition Name	Variable changed (and level assessed)
1. Standard Reference Test	(As for the initial experimental programme.)
2. Froth Depth (lower pulp level in cell)	Cell pulp level decreased (distance between pulp and lip increased from 3cm to 4cm.)
3. High Air Flow Rate	Air flow increased (from 6 //min to 8 //min)i
4. High Collector dosage	Combined SK5 and SIBX dosage increased (from 30 g/t to 45 g/t)
5. Std CMC	Changed depressant type (from IMP4 - guar type, to Dep267 – CMC type, at 28 g/t)
6. High CMC	Changed depressant type and increased dosage (from IMP4 - guar type, to Dep267 – CMC type, at 50 g/t)

Table BIII.1: Experimental conditions for the second part of the batch flotation programme.

The changes in the froth appearance caused by the changes in variables will be presented first, followed by the changes in metallurgical performance. Finally a summary table will be given which will highlight the key findings of this programme

B.III.1 The influence of various parameters on the froth appearance

In terms of the changes in froth appearance that occurred as a result of the changes in operating variables made in the second part of the batch flotation programme, the following figures draw the comparisons:

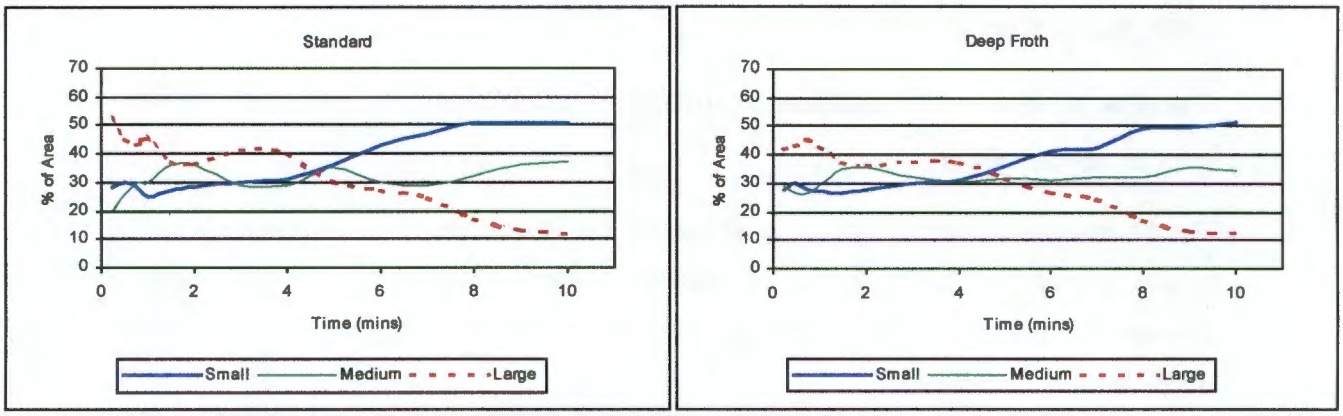

Figure BIII:1: Comparison of image analysis results between the standard condition and the "Deep froth" condition.

Not a great deal of difference can be detected between the standard condition and the test in which the pulp level was lowered (which resulted in a deeper froth layer) depicted above.

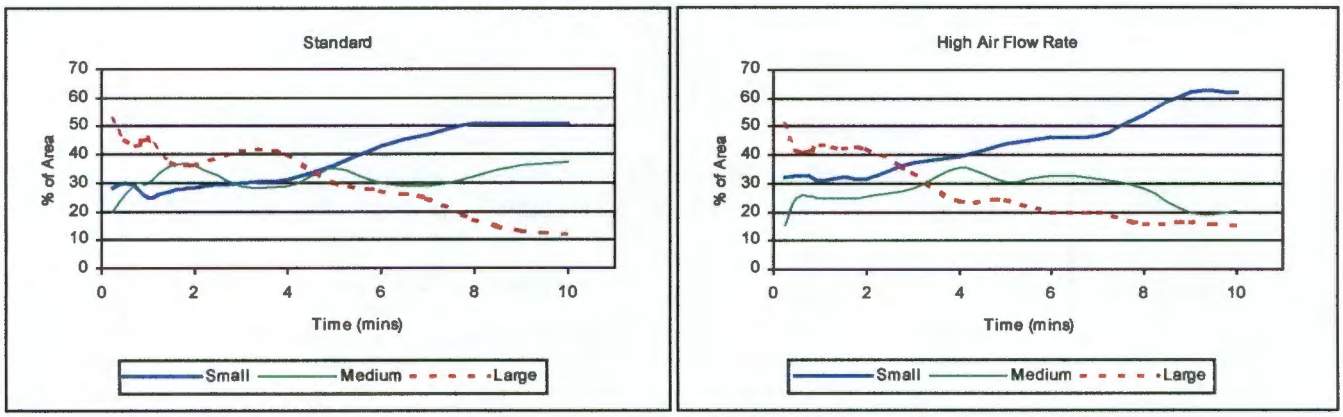

Figure BIII.2: Comparison of image analysis results between the standard condition and the "High Air" condition.

Increasing the air flow to the cell seemed to increase the degree with which the small bubbles covered the surface of the batch flotation cell.

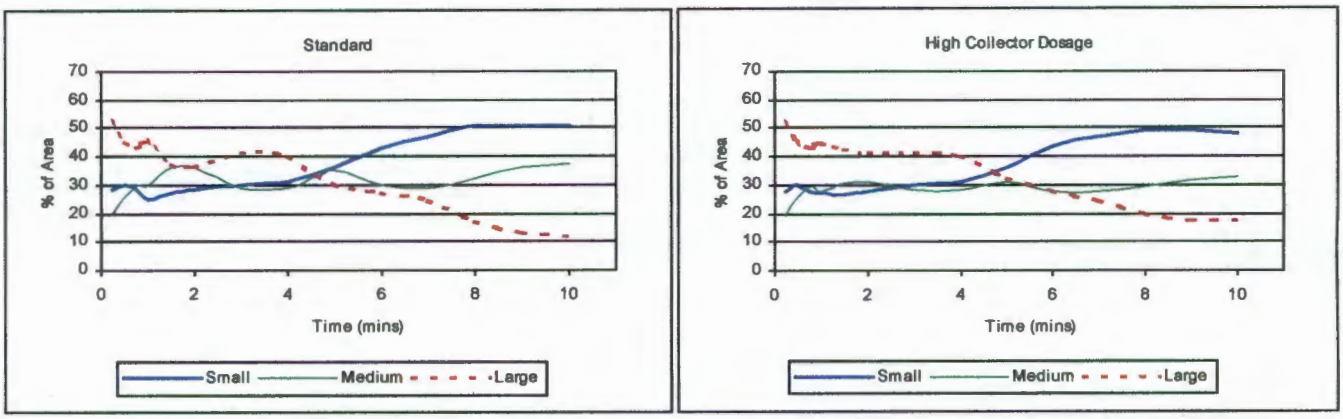

Figure BIII.3: Comparison of image analysis results between the standard condition and the "High Collector" condition.

The above figure shows that very little change in appearance can be detected, as a result of increasing the collector dosage.

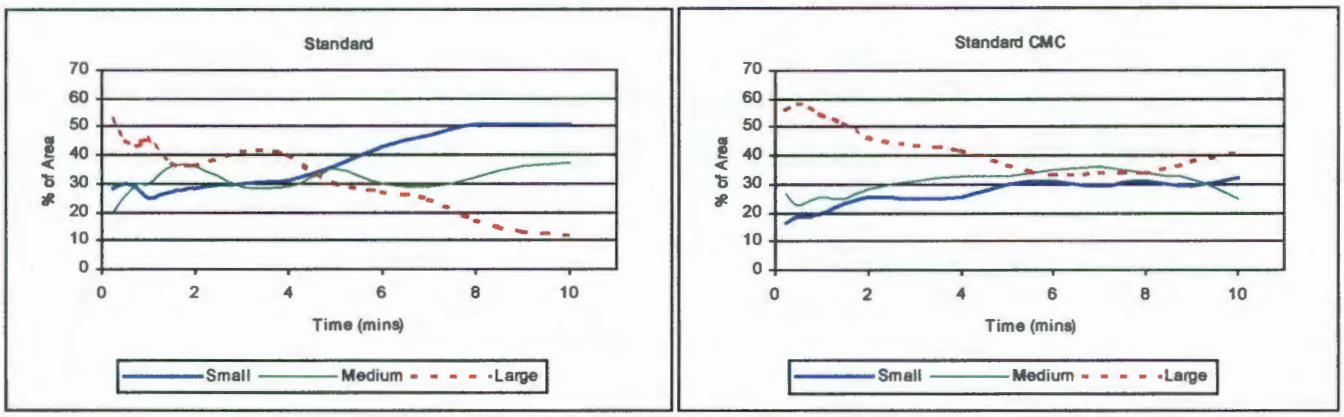

Figure BIII.4: Comparison of image analysis results between the standard condition and the "Standard CMC" condition, which represents a change in the depressant type from guar type (IMP4) to a CMC type (Dep267).

There is a marked similarity between the figures 4.2 and BIII.4, in that the surface appearance of the "standard CMC" test strongly resembles that of the "no depressant" test.

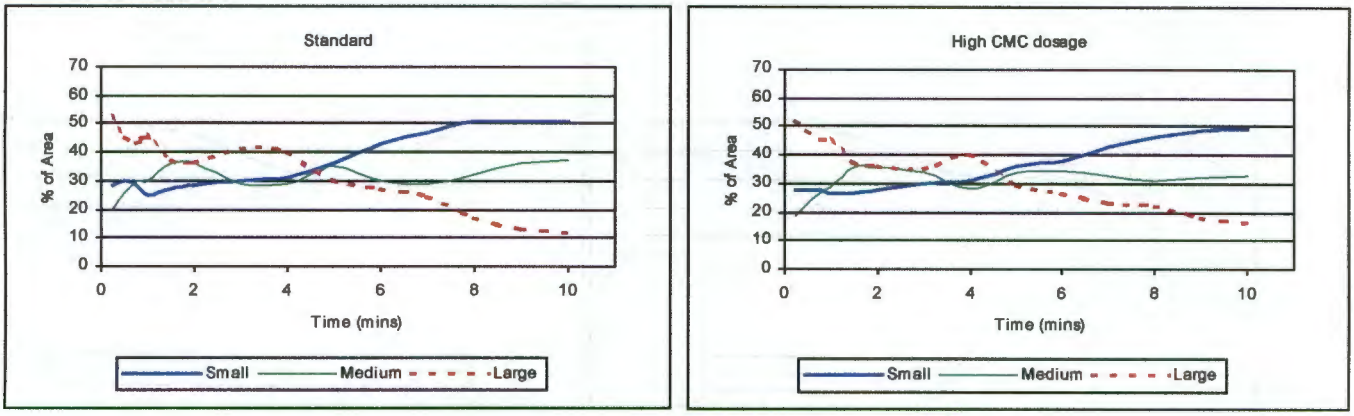

Figure BIII.5: Comparison of image analysis results between the standard condition and the "High CMC" condition, which represents a change in the depressant type from guar type (IMP4) to a CMC type (Dep267), and increasing the dosage from 28g/t to 50 g/t.

The high dosage of CMC-type depressant seems to result in a froth surface that strongly resembles that of the standard condition (of IMP4 at 28 g/t). This, together with figure BIII.4 indicates that the CMC type depressant used (DEP267) does not have the same degree of influence on the froth surface appearance as does the guar type depressant.

B.III.2 Metallurgical Performance Results

Detailed tables containing the metallurgical results gathered during the batch flotation programme can be found in Appendix BIIIc. The following tables summarise the metallurgical results with respect to the changes made to the flotation system, with respect to changes in frother and depressant dosage:

Test Name	Solids	Water	Copper		Nickel		Sulphur	
	Recovery (%)	Recovery (g)	Recovery (%)	Grade (%)	Recovery (%)	Grade (%)	Recovery (%)	Grade (%)
Standard	3.96	65.01	76.72	1.12	35.55	2.37	53.93	4.31
Deep Froth	3.88	47.65	79.01	1.35	32.35	2.15	52.15	4.21
High Air	5.41	105.45	79.81	0.95	35.45	1.73	59.61	2.84
High Collector	4.44	61.45	79.57	1.34	41.89	2.19	62.91	4.38
Standard CMC	3.68	48.56	79.65	1.54	35.18	2.13	48.28	3.81
High CMC	4.41	61.45	82.59	1.64	42.42	2.39	60.22	5.05

Table BIII.2: Final recovery data for the batch flotation programme.

In the section that follows, the presentation of the salient aspects of the results from Appendix BIIIc$_2$ which will be presented in a graphical form.

B.III.2.1 Copper

The flotation response of copper can be seen in Figures BIII.6 and BIII.7 below:

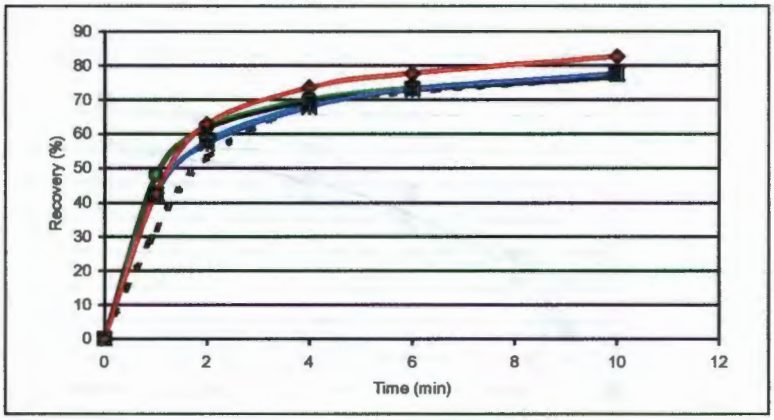

Figure BIII.6: Copper recovery versus time curves for the tests assessing the influences of variables other than frother and depressant dosage (legend in Fig BIII.7).

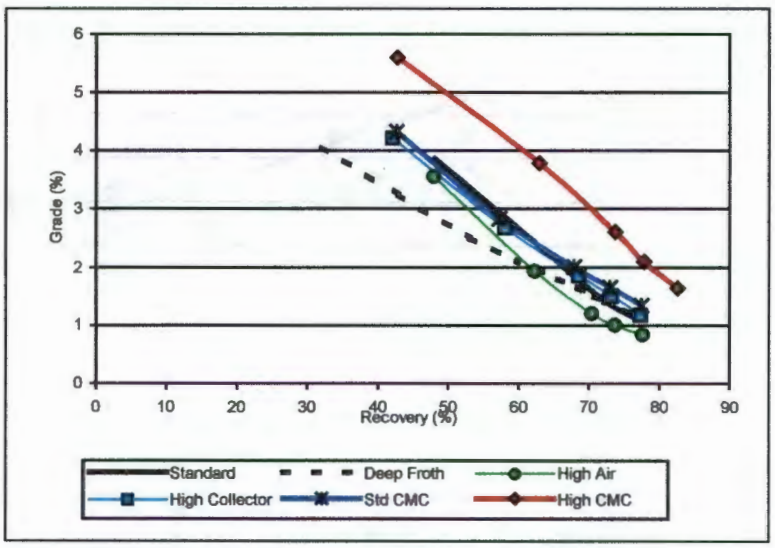

Figure BIII.7: Copper grade versus recovery curve for the tests assessing the influences of variables other than frother and depressant dosage.

In terms of the tests carried out in the second part of the test programme, there seems to be little difference in the kinetic response of the copper bearing minerals, which can be seen in Figure BIII.6. The grade-recovery relationships seen in figure BIII.7 show a different picture with the grade-recovery relationship for the "High CMC" test being significantly superior to all the other conditions.

B.III.2.2 Nickel

The following graphs show the nickel results for the tests assessing the influences of air flow rate, froth depth, collector dosage and alternative depressant:

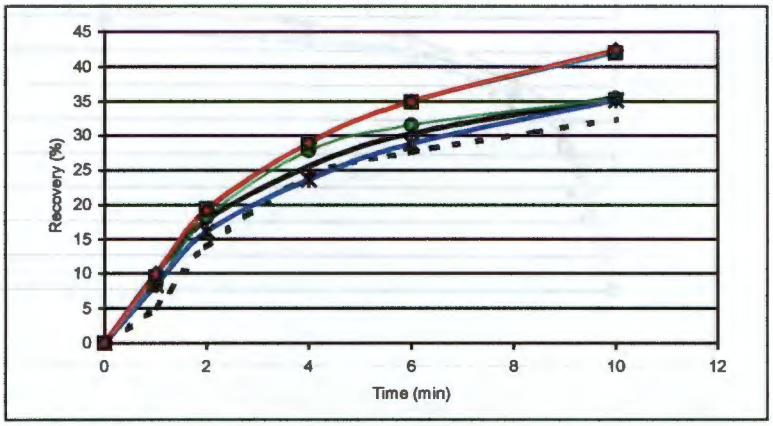

Figure BIII.8: Nickel recovery versus time curves for the tests assessing the influences of variables other than frother and depressant dosage (legend in Fig BIII.9).

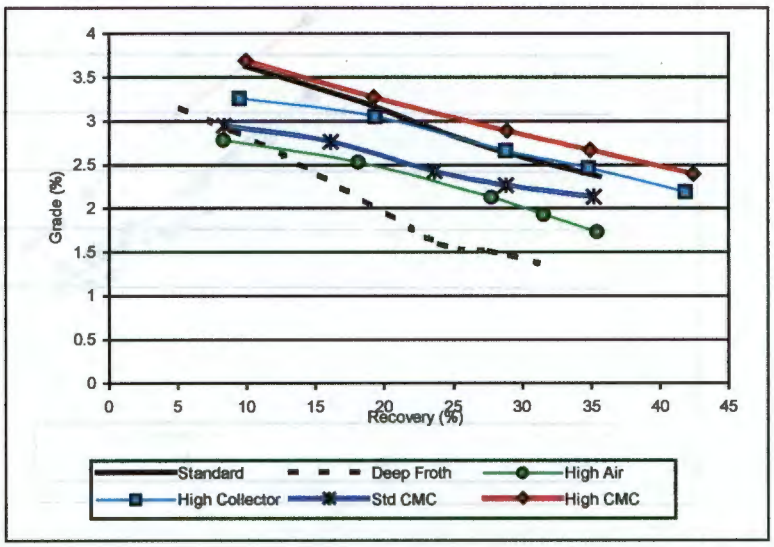

Figure BIII.9: Nickel grade versus recovery curves for the tests assessing the influences of variables other than frother and depressant dosage.

From the above figures, it can be seen that the nickel bearing species respond well to the CMC-type depressant at high dosages and high collector dosages, as both these tests enjoy higher than standard equilibrium recoveries. The deep froth test shows an inferior grade-recovery relationship.

B.III.2.3 Sulphur

The following graphs show the flotation response of the sulphur bearing species to the conditions tested:

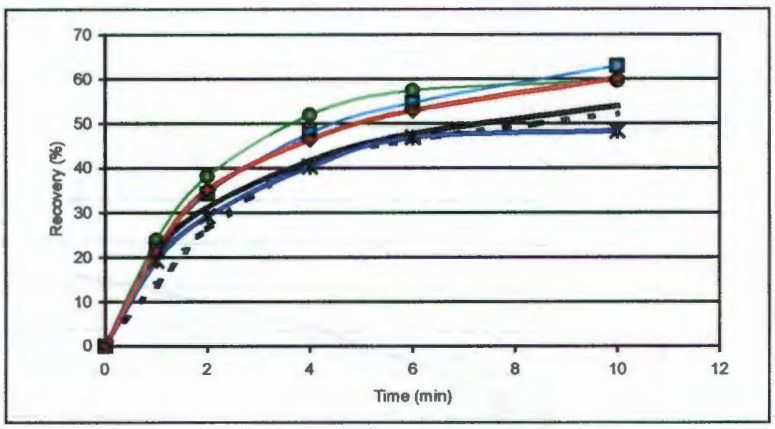

Figure BIII.10: Sulphur recovery versus time curves for the tests assessing the influences of variables other than frother and depressant dosage (legend in Fig BIII.11).

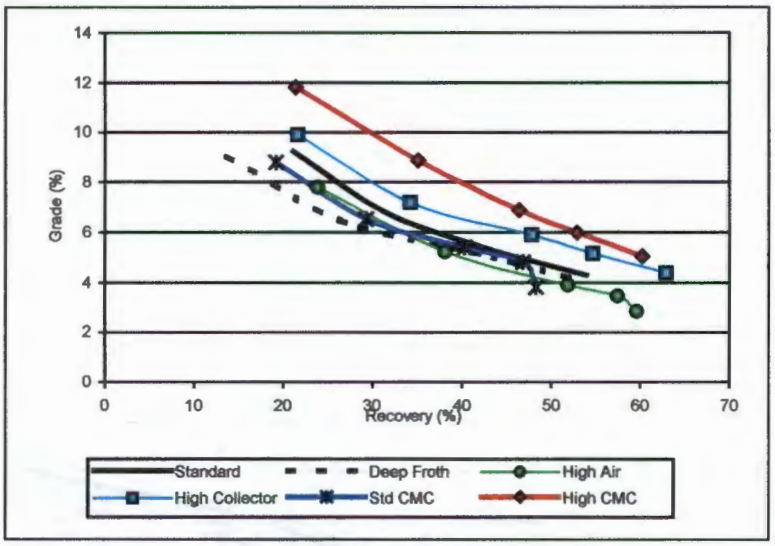

Figure BIII.11: Sulphur grade versus recovery curves for the tests assessing the influences of variables other than frother and depressant dosage.

Again the high dosage CMC-type depressant and the high collector dosage tests show improved grade-recovery relationships. The high air flow rate test showed faster initial kinetics for the sulphur bearing species, although the equilibrium recovery was lower than those for the "high CMC" and "high collector dosage tests.

B.III.2.4 Water and solids

The following graphs described the recovery of water and solids for the different conditions tested in the laboratory batch flotation programme:

The following graphs show the water and solids recoveries for the tests assessing the influences of air flow rate, froth depth, collector dosage and alternative depressant:

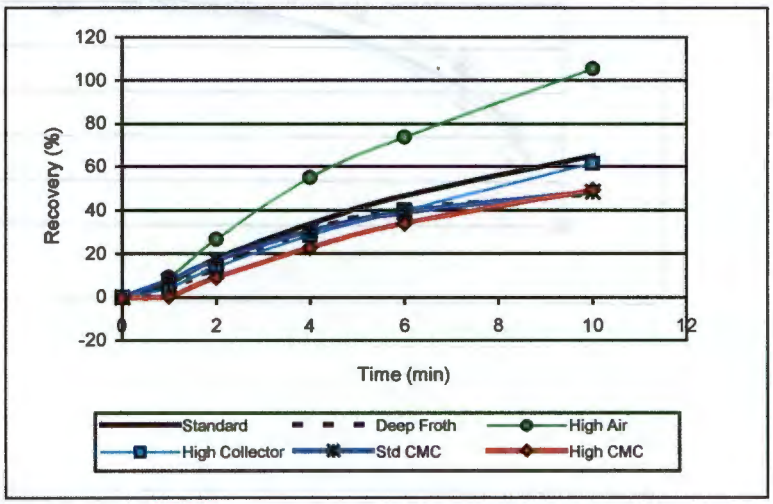

Figure BIII.12: Water recovery versus time curves for the tests assessing the influences of variables other than frother and depressant dosage.

Figure BIII.12 shows that increasing the air flow rate to the cell leads to drastically increased water recovery rates. In addition to this it would appear that high dosages of the CMC-type depressant restricts water recovery.

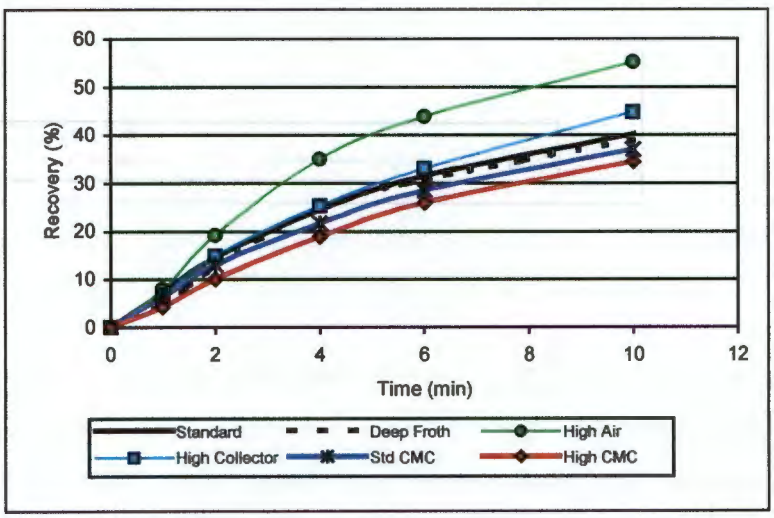

Figure BIII.13: Dry solids recovery versus time curves for the tests assessing the influences of variables other than frother and depressant dosage.

As in the previous figure, the high air flow test showed a noticeably higher solids recovery rate.

B.III.2.5 Summary of the metallurgical results

To summarise the observations made to this point:

- High CMC-type depressant dosage, as well as high collector dosages were seen to be beneficial for the recovery of the nickel bearing species.
- All the points made above with respect to the nickel bearing species could equally well be made with respect to the sulphur bearing species.
- Water and solids recovery rates were found to be sensitive to the air flow rate with which flotation is being conducted.

B.III.3 Summary of Key Findings

The following table represents the key findings, which are in comparison to the standard flotation test, drawn from the results presented in this section:

Parameter assessed	Detectable change in froth appearance	Change in metallurgical performance
Air Flow Rate	Slight changes detected, slightly finer bubble size distribution	Dramatic changes in the mass recovery and water recovery.
Froth Height	Little change observed	Little change detected
Collector Dosage	Little change observed	Appeared to be beneficial in the response of the nickel and sulphur bearing species.
Depressant type (changing from a guar based depressant to a CMC)	Froth appearance found to be less sensitive to the CMC when replacing the guar. At high CMC dosages froth has similar appearance to that at the standard guar type depressant dosage.	The CMC *at high dosages* seemed to be beneficial in all aspects

Table B.III.3 Summary of key findings for the wider group of operating variables.

Area Coverages By Small, Medium and Large Bubbles for the Second Part of the Batch Flotation Programme

Test name and bubble size classes	Time (minutes)													
	0.25	0.5	0.75	1	1.5	2	3	4	5	6	7	8	9	10
Deep Froth														
Small	27.7	29.7	27.6	27.0	26.7	27.7	30.0	31.2	35.9	41.0	42.5	49.2	49.8	51.1
Medium	28.9	26.5	26.8	29.5	35.1	35.6	32.0	30.7	31.6	31.1	32.1	32.4	35.8	34.4
Large	42.0	43.0	45.0	43.0	37.3	36.0	37.0	37.0	31.6	26.6	24.0	17.1	12.9	12.3
% of area accounted for	98.6	99.2	99.4	99.5	99.2	99.3	99.0	98.9	99.1	98.7	98.6	98.7	98.5	97.8
High Air Flow														
Small	32.2	32.5	33.0	31.2	32.3	31.5	37.1	39.6	44.3	46.3	47.0	54.2	62.2	62.1
Medium	15.5	25.1	25.4	24.6	25.1	25.4	28.4	35.8	30.4	32.6	31.7	28.2	19.8	20.6
Large	51.0	42.0	41.0	43.6	42.1	42.6	33.7	23.9	24.5	20.0	20.0	16.0	16.2	15.0
% of area accounted for	98.7	99.6	99.4	99.4	99.5	99.5	99.2	99.3	99.2	98.9	98.7	98.4	98.2	97.7
High Collector														
Small	27.7	29.7	27.6	27.0	26.7	27.7	30.0	31.2	35.9	43.5	46.9	49.2	49.1	48.0
Medium	19.3	25.3	29.1	27.8	30.3	30.8	28.1	28.0	30.8	27.8	27.9	29.4	31.8	32.7
Large	51.8	44.6	42.9	44.6	42.3	41.0	41.1	39.8	32.3	27.8	24.0	19.8	17.4	17.6
% of area accounted for	98.8	99.6	99.5	99.4	99.3	99.5	99.3	99.0	99.0	99.1	98.8	98.4	98.3	98.3
Standard CMC														
Small	16.3	18.7	18.5	20.0	23.0	25.5	25.0	25.4	29.9	30.9	29.1	31.3	29.3	32.0
Medium	26.7	22.3	24.1	25.5	25.0	28.0	31.2	32.5	32.8	34.9	35.9	33.6	31.4	25.0
Large	56.0	58.0	57.0	54.0	51.4	46.1	43.2	41.5	36.5	33.5	34.0	33.9	38.0	41.0
% of area accounted for	99.0	99.0	99.6	99.5	99.4	99.6	99.4	99.4	99.2	99.3	99.0	98.8	98.7	98.0
High CMC														
Small	27.7	27.5	27.6	26.3	26.7	27.7	30.0	31.2	35.9	38.0	43.0	46.1	48.7	48.9
Medium	18.7	22.3	26.5	28.6	35.5	35.7	34.0	28.3	33.6	34.6	33.0	31.3	32.2	32.7
Large	51.8	48.6	45.3	44.6	37.3	36.0	35.1	39.8	29.6	26.6	23.4	22.0	18.0	16.5
% of area accounted for	98.2	98.4	99.4	99.5	99.6	99.4	99.2	99.3	99.1	99.2	99.4	98.9	98.4	98.2

Standard

Quantities					
	Mass (g)	Water (g)	Cu (%)	Ni (%)	S (%)
Conc1	7.35	6.84	3.858	3.625	9.25
Conc2	7.33	10.71	1.102	2.868	4.44
Conc3	9.82	16.29	0.467	2.127	3.43
Conc4	7.13	12.78	0.287	1.806	2.75
Conc5	8.66	18.40	0.249	1.620	2.28
Tail	976.01		0.014	0.177	0.15
Total	1016.30	65.01			

Distribution					
	Mass (%)	Water —	Cu (%)	Ni (%)	S (%)
Conc1	0.72		48.10	9.92	21.12
Conc2	0.72		13.71	7.83	10.11
Conc3	0.97		7.78	7.77	10.47
Conc4	0.70		3.48	4.80	6.10
Conc5	0.85		3.66	5.23	6.14
Tail	96.04		23.28	64.45	46.07

Cumulative Distribution (Recovery)					
	Mass (%)	Water (g)	Cu (%)	Ni (%)	S (%)
Conc1	0.72	6.84	48.10	9.92	21.12
Conc1+2	1.44	17.54	61.81	17.76	31.23
Conc1+2+3	2.41	33.83	69.59	25.53	41.70
Conc1+2+3+4	3.11	46.61	73.07	30.33	47.80
Conc1+2+3+4+5	3.96	65.01	76.72	35.55	53.93

Cumulative Grade					
	Mass —	Water —	Cu (%)	Ni (%)	S (%)
Conc1			3.858	3.625	9.25
Conc1+2			2.482	3.247	6.85
Conc1+2+3			1.674	2.798	5.48
Conc1+2+3+4			1.362	2.574	4.86
Conc1+2+3+4+5			1.123	2.369	4.31

Reconciliation					
	Mass (g)	Water —	Cu (%)	Ni (%)	S (%)
Built-up Head	1025.48		0.058	0.264	0.32
Assayed Head	1030.00		0.048	0.257	0.31
Call (%)	99.56		121.59	102.66	103.83

High CMC

Quantities					
	Mass (g)	Water (g)	Cu (%)	Ni (%)	S (%)
Conc1	6.83	4.44	5.604	3.690	11.80
Conc2	8.05	9.50	2.236	2.915	6.39
Conc3	10.44	14.40	0.923	2.341	4.08
Conc4	7.80	11.59	0.474	1.958	3.13
Conc5	11.72	21.52	0.364	1.617	2.34
Tail	971.23		0.016	0.150	0.15
Total	1016.07	61.45			

Distribution					
	Mass (%)	Water —	Cu (%)	Ni (%)	S (%)
Conc1	0.67		42.79	9.95	21.42
Conc2	0.79		20.14	9.27	13.68
Conc3	1.03		10.78	9.66	11.33
Conc4	0.77		4.14	6.04	6.49
Conc5	1.15		4.77	7.49	7.29
Tail	95.59		17.39	57.58	39.78

Cumulative Distribution (Recovery)					
	Mass (%)	Water (g)	Cu (%)	Ni (%)	S (%)
Conc1	0.67	4.44	42.79	9.95	21.42
Conc1+2	1.46	13.94	62.93	19.23	35.10
Conc1+2+3	2.49	28.34	73.71	28.89	46.43
Conc1+2+3+4	3.26	39.93	77.84	34.93	52.92
Conc1+2+3+4+5	4.41	61.45	82.61	42.42	60.22

Cumulative Grade					
	Mass —	Water —	Cu (%)	Ni (%)	S (%)
Conc1			5.604	3.690	11.80
Conc1+2			3.781	3.270	8.87
Conc1+2+3			2.602	2.887	6.90
Conc1+2+3+4			2.101	2.668	6.01
Conc1+2+3+4+5			1.647	2.394	5.05

Reconciliation					
	Mass (g)	Water —	Cu (%)	Ni (%)	S (%)
Built-up Head	1023.47		0.088	0.249	0.37
Assayed Head	1030.00		0.047	0.331	0.33
Call (%)	99.37		185.52	75.23	111.79

Standard CMC

Quantities					
	Mass (g)	Water (g)	Cu (%)	Ni (%)	S (%)
Conc1	6.36	7.68	4.328	2.945	8.81
Conc2	6.71	9.48	1.411	2.590	4.38
Conc3	8.72	13.16	0.787	1.930	3.70
Conc4	6.72	8.61	0.489	1.724	2.85
Conc5	8.54	9.64	0.340	1.679	0.50
Tail	968.52		0.015	0.150	0.16
Total	1005.56	48.56			

Distribution					
	Mass (%)	Water —	Cu (%)	Ni (%)	S (%)
Conc1	0.63		42.63	8.36	19.18
Conc2	0.67		14.66	7.75	10.06
Conc3	0.87		10.63	7.51	11.04
Conc4	0.67		5.09	5.17	6.55
Conc5	0.85		4.49	6.40	1.45
Tail	96.32		22.50	64.82	51.72

Cumulative Distribution (Recovery)					
	Mass (%)	Water (g)	Cu (%)	Ni (%)	S (%)
Conc1	0.63	7.68	42.63	8.36	19.18
Conc1+2	1.30	17.16	57.29	16.11	29.24
Conc1+2+3	2.17	30.32	67.92	23.62	40.28
Conc1+2+3+4	2.83	38.92	73.01	28.79	46.83
Conc1+2+3+4+5	3.68	48.56	77.50	35.18	48.28

Cumulative Grade					
	Mass —	Water —	Cu (%)	Ni (%)	S (%)
Conc1			4.328	2.945	8.81
Conc1+2			2.830	2.763	6.54
Conc1+2+3			2.013	2.429	5.40
Conc1+2+3+4			1.654	2.263	4.80
Conc1+2+3+4+5			1.351	2.129	3.81

Reconciliation					
	Mass (g)	Water —	Cu (%)	Ni (%)	S (%)
Built-up Head	1022.95		0.064	0.223	0.29
Assayed Head	1030.00		0.056	0.331	0.33
Call (%)	99.32		114.66	67.34	87.78

High Collector

Quantities					
	Mass (g)	Water (g)	Cu (%)	Ni (%)	S (%)
Conc1	6.83	4.44	4.213	3.256	9.90
Conc2	8.05	9.50	1.361	2.876	4.88
Conc3	10.44	14.40	0.688	2.112	4.08
Conc4	7.80	11.59	0.403	1.805	2.73
Conc5	11.72	21.52	0.243	1.409	2.18
Tail	964.32		0.016	0.141	0.12
Total	1009.16	61.45			

Distribution					
	Mass (%)	Water —	Cu (%)	Ni (%)	S (%)
Conc1	0.68		42.09	9.50	21.66
Conc2	0.80		16.04	9.90	12.59
Conc3	1.03		10.51	9.42	13.65
Conc4	0.77		4.60	6.02	6.82
Conc5	1.16		4.18	7.06	8.19
Tail	95.56		22.59	58.11	37.09

Cumulative Distribution (Recovery)					
	Mass (%)	Water (g)	Cu (%)	Ni (%)	S (%)
Conc1	0.68	4.44	42.09	9.50	21.66
Conc1+2	1.47	13.94	58.13	19.39	34.25
Conc1+2+3	2.51	28.34	68.64	28.82	47.90
Conc1+2+3+4	3.28	39.93	73.24	34.83	54.72
Conc1+2+3+4+5	4.44	61.45	77.41	41.89	62.91

Cumulative Grade					
	Mass —	Water —	Cu (%)	Ni (%)	S (%)
Conc1			4.213	3.256	9.90
Conc1+2			2.670	3.051	7.18
Conc1+2+3			1.852	2.664	5.90
Conc1+2+3+4			1.511	2.461	5.16
Conc1+2+3+4+5			1.180	2.186	4.38

Reconciliation					
	Mass (g)	Water —	Cu (%)	Ni (%)	S (%)
Built-up Head	1023.47		0.068	0.232	0.31
Assayed Head	1030.00		0.047	0.331	0.33
Call (%)	99.37		142.77	70.05	93.41

High Air

Quantities					
	Mass (g)	Water (g)	Cu (%)	Ni (%)	S (%)
Conc1	8.04	8.99	3.55	2.781	7.80
Conc2	11.18	17.44	0.768	2.354	3.36
Conc3	15.88	28.53	0.305	1.631	2.28
Conc4	8.83	18.72	0.220	1.151	1.65
Conc5	11.25	31.77	0.209	0.933	0.50
Tail	964.98		0.014	0.180	0.11
Total	1020.15	105.45			

Distribution					
	Mass (%)	Water —	Cu (%)	Ni (%)	S (%)
Conc1	0.79		47.93	8.32	23.86
Conc2	1.10		14.41	9.79	14.29
Conc3	1.56		8.13	9.64	13.78
Conc4	0.87		3.26	3.78	5.54
Conc5	1.10		3.94	3.90	2.14
Tail	94.59		22.33	64.55	40.39

Cumulative Distribution (Recovery)					
	Mass (%)	Water (g)	Cu (%)	Ni (%)	S (%)
Conc1	0.79	8.99	47.93	8.32	23.86
Conc1+2	1.88	26.43	62.34	18.12	38.15
Conc1+2+3	3.44	54.96	70.47	27.76	51.93
Conc1+2+3+4	4.31	73.68	73.73	31.54	57.47
Conc1+2+3+4+5	5.41	105.45	77.67	35.45	59.61

Cumulative Grade					
	Mass —	Water —	Cu (%)	Ni (%)	S (%)
Conc1			3.554	2.781	7.80
Conc1+2			1.933	2.533	5.22
Conc1+2+3			1.197	2.125	3.89
Conc1+2+3+4			1.000	1.929	3.44
Conc1+2+3+4+5			0.839	1.726	2.84

Reconciliation					
	Mass (g)	Water —	Cu (%)	Ni (%)	S (%)
Built-up Head	1023.47		0.058	0.263	0.26
Assayed Head	1030.00		0.048	0.253	0.31
Call (%)	99.37		121.40	104.29	83.64

Deep Froth

Quantities					
	Mass (g)	Water (g)	Cu (%)	Ni (%)	S (%)
Conc1	4.76	4.41	4.059	2.855	9.07
Conc2	8.03	9.09	1.574	2.805	4.94
Conc3	12.33	17.00	0.750	2.143	3.85
Conc4	5.63	9.79	0.401	1.659	2.72
Conc5	8.29	7.36	0.331	1.474	2.25
Tail	965.54		0.014	0.182	0.16
Total	1004.56	47.65			

Distribution					
	Mass (%)	Water ---	Cu (%)	Ni (%)	S (%)
Conc1	0.47		32.11	5.22	13.70
Conc2	0.80		21.01	8.66	12.59
Conc3	1.23		15.37	10.17	15.08
Conc4	0.56		3.76	3.59	4.86
Conc5	0.82		4.57	4.70	5.92
Tail	96.12		23.19	67.65	47.85

Cumulative Distribution (Recovery)					
	Mass (%)	Water (g)	Cu (%)	Ni (%)	S (%)
Conc1	0.47	4.41	32.11	5.22	13.70
Conc1+2	1.27	13.50	53.12	13.89	26.29
Conc1+2+3	2.50	30.50	68.49	24.06	41.37
Conc1+2+3+4	3.06	40.29	72.25	27.65	46.23
Conc1+2+3+4+5	3.88	47.65	76.81	32.35	52.15

Cumulative Grade					
	Mass ---	Water ---	Cu (%)	Ni (%)	S (%)
Conc1			4.059	2.855	9.07
Conc1+2			2.499	2.824	6.48
Conc1+2+3			1.640	2.490	5.19
Conc1+2+3+4			1.413	2.338	4.74
Conc1+2+3+4+5			1.184	2.154	4.21

Reconciliation					
	Mass (g)	Water ---	Cu (%)	Ni (%)	S (%)
Built-up Head	1024.53		0.060	0.259	0.31
Assayed Head	1030.00		0.047	0.249	0.31
Call (%)	99.47		126.22	103.86	100.55

APPENDIX C:

Plant-based Programme Results

APPENDIX CI: ANOVA Discussion and Results

APPENDIX CII: Mass Balance Survey Results

APPENDIX CIII: Step Test Results

APPENDIX CI: ANOVA Discussion and Results

APPENDIX CI: Analysis of Variance

The data for the nested analysis of variance test for the 4E PGE analysis (or *four element - platinum group element*) are as follows:

Nominal Time	Duplicate Name	Level 3 Sub-sample Analyses	Level 2 Means of analyses	Level 1 Means of duplicates	Grand Mean stream grade
00:00	A	1.98	2.06	2.06	1.98
		2.08			
		2.05			
		2.12			
	B	2.09	2.06		
		2.09			
		1.99			
		2.06			
00:15	A	1.90	1.93	1.99	
		2.04			
		1.84			
		1.96			
	B	2.09	2.04		
		2.01			
		1.93			
		2.15			
00:30	A	2.00	2.01	1.96	
		1.98			
		2.12			
		1.92			
	B	1.82	1.92		
		1.93			
		1.90			
		2.01			
00:45	A	1.85	1.91	1.93	
		1.89			
		1.95			
		1.94			
	B	1.94	1.95		
		1.98			
		1.89			
		1.98			

Table CIa.1: Data for the nested analysis of variance test for the 4E PGE grades of the second rougher concentrate (Note: the above data have been "factored", by dividing the reported grades by an arbitrarily chosen factor, hence the figures quoted do not represent the analyses or stream grades as reported).

The variances detectable in the above data were analysed at two levels, notably:

- Interaction between Level 3 and Level 2: This investigates whether there exists a significant difference between the duplicate samples (taken at the same time), once the variances associated with sub-sampling and analysis have been accounted for, and;
- Interaction between Level 2 and Level 1: This, in turn, ascertains whether significant differences could be detected between the average grades of samples taken across the range of times over and above the variances imposed by sampling errors.

The variances associated with a mean grade of a stream, over a long period of time (i.e. Level 1 variances) were not assessed as this would be entirely dependant on how the term "long period of time" was defined. By looking at TABLE CIa.1 it would appear there is a decreasing trend in the grades quoted at Level 2 with respect to time. (This is also to a greater or lesser extent evident in the data for the copper and nickel analyses.) It therefore stands to reason that even if the analysis of the above data proved it not to be so, this trend could become significant if the time steps between the samples were great enough. It was however not the aim of the plant campaign to estimate an average grade (in the true sense of the word "average") of any of the process streams, but rather to provide information pertinent to the process at a particular point in time. It is for this reason that the analysis of the contributing variances will be carried out over the lower two levels only.

Complete data sets for the copper and nickel analyses showing information similar to that depicted above, as well as the complete statistical analyses (for all data sets) are given in APPENDIX CIb. For the purposes of comparison between the three analyses, the table below summarises some of the key aspects. As it turns out, the f statistic for the Level 3/Level 2 ANOVA needs to be analysed at 1 and 6 degrees of freedom. From statistical tables it is found that the f-statistic must be greater than 3.78 for there to be 90% confidence in a statement that there is indeed a difference between the two samples taken at any one time. This significant difference would be between the grades of duplicate samples (indicative of sampling error), over and above the error associated with the sample preparation and chemical analysis.

Time that duplicate samples were taken:	4E PGE f-statistic	Copper f-statistic	Nickel f-statistic
00:00	0.00	0.21	0.40
00:15	2.94	3.83	3.80
00:30	2.45	1.26	0.38
00:45	1.61	1.72	1.01

Table CIa.2: Comparison of the f-statistics of the ANOVA carried out on the interaction between Level 3 and Level2 of the "Nested Analysis of Variance" test. It compares the sampling error between the four sets of duplicate samples, once the error associated with the sample preparation and chemical analysis has been taken into account.

When looking at the above table, it is immediately apparent that there is a degree of consistency between the three analysis types assessed. For the samples taken at the first time, little or no difference in the duplicates can be determined above the errors associated with sample preparation and chemical analysis. Copper and nickel results for the second set of samples show that there is a significant difference (at a 90% confidence level) between the values of the duplicate samples, hence in this case the

sampling error exceeded the errors associated with sample preparation and analysis. The 4E PGE results also show their highest f-statistic in this test, but fail to reach the value that would indicate a 90% confidence in the result. This can be seen as an indication of the greater inherent error associated with the analysis method. Lotter's work (1995) confirms this, and he specifically indicates that high grade samples show an inherent bias when analysed by the fire assay method typically used in such applications.

What is encouraging, however, is that sampling error could only be detected above the inherent errors associated with sample preparation and analysis, in one out of the four sets of duplicate samples taken.

A similar comparison between the three sets of analyses can be made. This would show to what degree the mean grades of the samples taken across the time span in consideration showed detectable change, over the errors associated with the grades of the duplicate samples used to arrive at the mean grades. The following table shows this comparison:

Analysis	f-statistic
4E PGE	2.33
Copper	4.08
Nickel	4.10

Table CIa.3: Results from the Level 2/Level 1 analysis, which give an indication as to the validity of the hypothesis that there is a difference between samples taken across the time span of the test. Were this true, it would indicate that the short-term time-based variation of the process is detectable.

The f-statistics in the above table need to be analysed with 3, 4 degrees of freedom. From statistical tables it is found that the f-statistics must be greater than 4.19 for the conclusion at a 90% confidence level, that there is a significant difference between estimates of the stream grades taken at different times throughout the test. The results for nickel and copper are near to being significant, while those for the 4E PGE are substantially below the significance level. This may again be due to the degree of bias that is inherent in the analysis method. With reference to a point made above, it is entirely plausible that were the time frame (over which this exercise was conducted) longer, a significant time dependant difference could be detected.

What is evident is that any errors that are present shield the detection of short-term process variability. This in turn means that (given similar process conditions) a single increment sample taken of the stream would give a fair indication of a particular quantity within that stream in the short term, given the other typical errors associated with making such a measurement.

4E PGE Data for "Nested analysis of variance"
(4E PGE grades are factored and are therefore unitless)

Nominal Time	Duplicate Name	Level 3 Analyses	Level 2 Means of analyses	Level 1 Means of duplicates	Grand Mean stream grade
00:00	A	1.980 2.080 2.050 2.120	2.058	2.058	1.983
	B	2.090 2.090 1.990 2.060	2.058		
00:15	A	1.895 2.035 1.835 1.955	1.930	1.985	
	B	2.085 2.005 1.925 2.145	2.040		
00:30	A	2.000 1.980 2.120 1.920	2.005	1.960	
	B	1.820 1.930 1.900 2.010	1.915		
00:45	A	1.850 1.890 1.950 1.940	1.908	1.928	
	B	1.940 1.980 1.890 1.98	1.948		

4E PGE: Nested analysis of variance

Level 3/Level 2 ANOVA

This will show whether there is a significant difference between the duplicate samples, after accounting for the variance introduced due to sub-sampling and analysis.
If there is not, then it implies that the analysis and sub-sampling error is greater than the sampling error.

Data

Time	Sample	Analyses				Total
1	A	1.98	2.08	2.05	2.12	8.23
	B	2.09	2.09	1.99	2.06	8.23
	Total					16.46
2	A	1.895	2.035	1.835	1.955	7.72
	B	2.085	2.005	1.925	2.145	8.16
	Total					15.88
3	A	2	1.98	2.12	1.92	8.02
	B	1.82	1.93	1.9	2.01	7.66
	Total					15.68
4	A	1.85	1.89	1.95	1.94	7.63
	B	1.94	1.98	1.89	1.98	7.79
	Total					15.42

Analysis of variance results

Source of variation	SS	d.f..	MS	F
Between duplicate samples	0.000	1.0	0.000	0.00
Residual error (between analyses)	0.017	6.0	0.003	--
Total	0.017	7.0	--	--
Between duplicate samples	0.024	1.0	0.024	2.94
Residual error (between analyses)	0.049	6.0	0.008	--
Total	0.074	7.0	--	--
Between duplicate samples	0.016	1.0	0.016	2.45
Residual error (between analyses)	0.040	6.0	0.007	--
Total	0.056	7.0	--	--
Between duplicate samples	0.003	1.0	0.003	1.61
Residual error (between analyses)	0.012	6.0	0.002	--
Total	0.015	7.0	--	--

F to be analysed on the basis of 1, 6 degrees of freedom.
Therefore for the statement to be true that the samples are indeed different for the confidence limits of 90% and 95%, F needs to be larger than 3.78 or 5.99 respectively (from statistical tables).

		d.f..
Correction for mean	33.88645	
Total SS	0.01715	7
SS between duplicate samples	0	1
SS within samples	0.01715	6
		d.f..
Correction for mean	31.5218	
Total SS	0.0736	7
SS between duplicate samples	0.0242	1
SS within samples	0.0494	6
		d.f..
Correction for mean	30.7328	
Total SS	0.0558	7
SS between duplicate samples	0.0162	1
SS within samples	0.0396	6
		d.f..
Correction for mean	29.72205	
Total SS	0.01515	7
SS between duplicate samples	0.0032	1
SS within samples	0.01195	6

Level 2/Level 1 ANOVA

This will show how much of the variance in a sample is attributable to process fluctuations.
Should no significant time-based process fluctuations be found, it implies that a single increment sample of the process stream provides an adequate reflection of a particular quantity in that process stream.

Data

Time	Duplicate A	Duplicate B	Totals
1	2.1	2.1	4.1
2	1.9	2.0	4.0
3	2.0	1.9	3.9
4	1.9	1.9	3.9
Totals			15.9

Analysis of variance results

Source of variation	SS	d.f.	MS	F
Between Times	0.0	3.0	0.01	2.24
Residual error (between duplicates)	0.0	4.0	0.00	--
Total	0.0	7.0	--	--

F to be analysed on the basis of 3, 4 degrees of freedom.
Therefore for the statement to be true that there is are indeed time variation (detectable over all the other sources of variance) for the confidence limits of 90% and 95%, F needs to be larger than 4.19 or 6.59 respectively (from statistical tables).

		d.f..
Correction for mean	31.44245	
Total SS	0.029225	7
SS between times	0.018325	3
SS within duplicate samples	0.0109	4

Copper Data for "Nested analysis of variance"
(Cu grades in %)

Nominal Time	Duplicate Name	Level 3 Analyses	Level 2 Means of analyses	Level 1 Means of duplicates	Grand Mean stream grade
00:00	A	2.10 2.04 2.10 2.03	2.07	2.06	2.03
	B	2.00 2.09 2.06 2.07	2.06		
00:15	A	2.01 2.02 2.03 1.99	2.01	2.04	
	B	2.12 2.01 2.06 2.05	2.06		
00:30	A	1.99 1.92 1.99 2.01	1.98	1.99	
	B	2.02 2.02 1.99 1.98	2.00		
00:45	A	2.01 2.06 2.06 2.00	2.03	2.05	
	B	2.03 2.08 2.06 2.06	2.06		

Copper: Nested analysis of variance

Level 3/Level 2 ANOVA

This will show whether there is a significant difference between the duplicate samples, after accounting for the variance introduced due to sub-sampling and analysis.
If there is not, then it implies that the analysis and sub-sampling error is greater than the sampling error.

Data

Time	Sample	Analyses				Total
1	A	2.10	2.04	2.10	2.03	8.27
	B	2.00	2.09	2.06	2.07	8.22
	Total					16.49
2	A	2.01	2.02	2.03	1.99	8.05
	B	2.12	2.01	2.06	2.05	8.24
	Total					16.29
3	A	1.99	1.92	1.99	2.01	7.91
	B	2.02	2.02	1.99	1.98	8.01
	Total					15.92
4	A	2.01	2.06	2.06	2.00	8.13
	B	2.03	2.08	2.06	2.06	8.23
	Total					16.36

Analysis of variance results

Source of variation	SS	D.f.	MS	F
Between duplicate samples	0.0003	1.0	0.000	0.21
Residual error (between analyses)	0.0088	6.0	0.001	--
Total	0.0091	7.0	--	--
Between duplicate samples	0.0045	1.0	0.005	3.83
Residual error (between analyses)	0.0071	6.0	0.001	--
Total	0.0116	7.0	--	--
Between duplicate samples	0.0012	1.0	0.001	1.26
Residual error (between analyses)	0.0060	6.0	0.001	--
Total	0.0072	7.0	--	--
Between duplicate samples	0.0012	1.0	0.001	1.72
Residual error (between analyses)	0.0043	6.0	0.001	--
Total	0.0056	7.0	--	--

		d.f..
Correction for mean	33.99001	
Total SS	0.009087	7
SS between duplicate samples	0.000312	1
SS within samples	0.008775	6
Correction for mean	33.17051	
Total SS	0.011587	7
SS between duplicate samples	0.004513	1
SS within samples	0.007075	8
Correction for mean	31.6808	
Total SS	0.0072	7
SS between duplicate samples	0.00125	1
SS within samples	0.00595	6
Correction for mean	33.4562	
Total SS	0.0056	7
SS between duplicate samples	0.00125	1
SS within samples	0.00435	8

F to be analysed on the basis of 1, 6 degrees of freedom.
Therefore for the statement to be true that the samples are indeed different
for the confidence limits of 90% and 95%, F needs to be larger than
3.78 or 5.99 respectively (from statistical tables).

Level 2/Level 1 ANOVA

This will show how much of the variance in a sample is attributable to process fluctuations.
Should no significant time-based process fluctuations be found, it implies that a single increment sample of the
process stream provides an adequate reflection of a particular quantity in that process stream.

Data

Time	Duplicate A	Duplicate B	Totals
1	2.068	2.055	4.123
2	2.013	2.060	4.073
3	1.978	2.003	3.980
4	2.033	2.058	4.090
Totals			16.3

Analysis of varianca results

Source of variation	SS	D.f.	MS	F
Between Times	0.0056	3.0	0.0019	4.08
Residual error (between duplicates)	0.0018	4.0	0.0005	--
Total	0.0074	7.0	--	--

		d.f..
Correction for mean	33.06878	
Total SS	0.007434	7
SS between times	0.005603	3
SS within duplicate samples	0.001831	4

F to be analysed on the basis of 3, 4 degrees of freedom.
Therefore for the statement to be true that there is are indeed time variation
(detectable over all the other sources of variance) for the confidence limits of 90% and 95%,
F needs to be larger than 4.19 or 6.59 respectively (from statistical tables).

Nickel Data for "Nested analysis of variance"
(Ni grades in %)

Nominal Time	Duplicate Name	Level 3 Analyses	Level 2 Means of analyses	Level 1 Means of duplicates	Grand Mean stream grade
00:00	A	4.66 4.40 4.51 4.20	4.44	4.41	4.25
	B	4.24 4.39 4.44 4.43	4.37		
00:15	A	4.11 4.13 4.14 4.12	4.13	4.21	
	B	4.54 4.17 4.23 4.22	4.29		
00:30	A	4.31 4.01 4.11 4.40	4.21	4.18	
	B	4.19 4.21 4.04 4.15	4.15		
00:45	A	4.20 4.23 4.26 3.94	4.16	4.21	
	B	4.13 4.21 4.43 4.25	4.26		

Nickel: Nested analysis of variance

Level 3/Level 2 ANOVA

This will show whether there is a significant difference between the duplicate samples, after accounting for the variance introduced due to sub-sampling and analysis.
If there is not, then it implies that the analysis and sub-sampling error is greater than the sampling error.

Data

Time	Sample	Analyses				Total
1	A	4.66	4.40	4.51	4.20	17.764
	B	4.24	4.39	4.44	4.43	17.494
	Total					35.258
2	A	4.11	4.13	4.14	4.12	16.5
	B	4.54	4.17	4.23	4.22	17.16
	Total					33.66
3	A	4.31	4.01	4.11	4.40	16.83
	B	4.19	4.21	4.04	4.15	16.59
	Total					33.42
4	A	4.20	4.23	4.26	3.94	16.63
	B	4.13	4.21	4.43	4.25	17.02
	Total					33.65

Analysis of variance results

Source of variation	SS	D.f.	MS	F
Between duplicate samples	0.0091	1.0	0.009	0.40
Residual error (between analyses)	0.1382	6.0	0.023	--
Total	0.1473	7.0	--	--
Between duplicate samples	0.0545	1.0	0.054	3.80
Residual error (between analyses)	0.0859	6.0	0.014	--
Total	0.1404	7.0	--	--
Between duplicate samples	0.0072	1.0	0.007	0.38
Residual error (between analyses)	0.1133	6.0	0.019	--
Total	0.1206	7.0	--	--
Between duplicate samples	0.0190	1.0	0.019	1.01
Residual error (between analyses)	0.1132	6.0	0.019	--
Total	0.1322	7.0	--	--

		d.f..
Correction for mean	155.3908	
Total SS	0.147288	7
SS between duplicate samples	0.009113	1
SS within samples	0.138175	6
Correction for mean	141.6245	
Total SS	0.14035	7
SS between duplicate samples	0.05445	1
SS within samples	0.0859	6
Correction for mean	139.6121	
Total SS	0.12055	7
SS between duplicate samples	0.0072	1
SS within samples	0.11335	6
Correction for mean	141.5403	
Total SS	0.132187	7
SS between duplicate samples	0.019013	1
SS within samples	0.113175	6

F to be analysed on the basis of 1, 6 degrees of freedom.
Therefore for the statement to be true that the samples are indeed different
for the confidence limits of 90% and 95%, F needs to be larger than
3.78 or 5.99 respectively (from statistical tables).

Level 2/Level 1 ANOVA

This will show how much of the variance in a sample is attributable to process fluctuations.
Should no significant time-based process fluctuations be found, it implies that a single increment sample of the
process stream provides an adequate reflection of a particular quantity in that process stream.

Data

Time	Duplicate A	Duplicate B	Totals
1	4.441	4.374	8.815
2	4.125	4.290	8.415
3	4.208	4.148	8.355
4	4.158	4.255	6.413
Totals			34.0

Analysis of variance results

Source of variation	SS	D.f.	MS	F
Between Times	0.067	3.0	0.022	4.00
Residual arror (between duplicates)	0.022	4.0	0.006	--
Total	0.090	7.0	--	--

		d.f..
Correction for mean	144.4745	
Total SS	0.089851	7
SS between times	0.067407	3
SS within duplicate samples	0.022444	4

F to be analysed on the basis of 3, 4 degrees of freedom.
Therefore for the statement to be true that there is are indeed time variation
(detectable over all the other sources of variance) for the confidence limits of 90% and 95%,
F needs to be larger than 4.19 or 6.59 respectively (from statistical tables).

APPENDIX CII: Mass Balance Survey Results

Mass Balance Survey 1: 17/2/99 16h30 to 20h00

Stream		Mass Flow Dry (tph)	4E PGE "factored"	Cu %	Ni %	Fe %	MgO %	SiO2 %	Al2O3 %	S %
	Measured	292.05		0.062	0.190	8.55	16.60	47.10	10.40	0.43
Survey 1 Feed	Mass Balance	292.01		0.063	0.192	8.44	16.34	46.91	10.50	0.39
	% Difference	0.01		-1.64	-1.02	1.27	1.57	0.40	-0.95	10.36
	Measured			0.0151	0.1172	8.21	16.1	47	10.8	0.17
Survey 1 Tail	Mass Balance	276.46		0.015	0.116	8.30	16.33	47.16	10.70	0.18
	% Difference			0.38	0.61	-1.14	-1.43	-0.35	0.94	-3.86
	Measured	1.47	1.80	5.83	4.70	18.70	13.20	29.40	2.07	14.00
Survey 1 Cell 1	Mass Balance	1.47	1.73	5.84	4.68	18.66	13.36	29.90	2.11	13.88
	% Difference	0.13	3.98	-0.22	0.42	0.20	-1.18	-1.70	-1.86	0.87
	Measured	0.47	1.42	3.87	6.17	18.20	13.80	30.80	2.00	13.40
Survey 1 Cell 2	Mass Balance	0.47	1.40	3.87	6.16	18.19	13.85	30.97	2.01	13.36
	% Difference	-0.18	0.90	-0.06	0.18	0.07	-0.39	-0.57	-0.58	0.27
	Measured		1.58	5.38	5.01	18.50	13.70	30.90	2.14	13.60
Survey 1 Comb Conc 1+2	Mass Balance	1.94	1.65	5.36	5.04	18.55	13.48	30.16	2.09	13.75
	% Difference		-4.71	0.29	-0.58	-0.24	1.62	2.40	2.55	-1.11
	Measured	1.76	0.64	1.09	3.82	13.80	16.50	38.60	3.92	8.67
Survey 1 Cell 3	Mass Balance	1.56	0.59	1.06	3.67	13.81	16.55	38.67	3.93	8.54
	% Difference	11.16	7.96	2.62	3.81	-0.10	-0.33	-0.18	-0.22	1.46
	Measured	4.03	0.12	0.19	0.79	8.99	16.10	44.20	8.85	2.00
Survey 1 Cell 4	Mass Balance	5.60	0.11	0.18	0.77	9.01	16.29	44.68	9.00	1.98
	% Difference	-39.19	5.11	1.60	2.84	-0.27	-1.16	-1.09	-1.71	1.21
	Measured		0.19	0.36	1.32	10.10	16.60	44.00	8.06	3.32
Survey 1 Comb Conc 3+4	Mass Balance	7.16	0.21	0.37	1.40	10.06	16.35	43.35	7.90	3.41
	% Difference		-10.95	-3.99	-6.06	0.40	1.53	1.48	2.01	-2.57
	Measured	1.62	0.18	0.41	1.11	10.20	17.40	44.10	7.01	3.30
Survey 1 Cell 5	Mass Balance	1.40	0.12	0.27	0.72	9.77	17.25	43.98	7.23	2.14
	% Difference	13.47	34.00	34.15	34.74	4.24	0.88	0.27	-3.15	35.00
	Measured	0.56	0.22	0.49	1.23	10.40	18.30	44.30	5.49	3.63
Survey 1 Cell 6	Mass Balance	0.41	0.19	0.43	1.10	10.25	18.26	44.40	5.52	3.20
	% Difference	26.87	11.39	13.25	10.34	1.46	0.19	-0.23	-0.62	11.71
	Measured	0.19	0.37	0.81	1.81	11.10	19.00	43.10	3.35	5.37
Survey 1 Cell 7	Mass Balance	0.15	0.34	0.75	1.71	11.08	18.92	43.00	3.35	5.06
	% Difference	23.10	9.84	7.93	5.55	0.19	0.44	0.22	-0.11	5.75
	Measured	1.42	0.07	0.18	0.52	9.57	17.60	44.80	7.98	1.71
Survey 1 Cell 8	Mass Balance	1.91	0.06	0.14	0.41	9.20	17.09	44.98	8.29	1.28
	% Difference	-34.64	17.82	22.14	20.71	3.89	2.88	-0.40	-3.88	24.99
	Measured		0.10	0.22	0.60	8.88	16.70	44.60	8.17	1.79
Survey 1 Comb Conc 5 - 8	Mass Balance	3.87	0.10	0.24	0.65	9.58	17.35	44.45	7.43	1.94
	% Difference		-7.95	-8.69	-7.89	-7.91	-3.92	0.34	9.08	-8.45
	Measured	0.19	0.21	0.37	1.22	11.10	19.50	45.30	4.04	4.08
Survey 1 Cell 9	Mass Balance	0.17	0.20	0.36	1.17	11.08	19.47	45.27	4.05	4.01
	% Difference	7.42	3.05	2.24	3.92	0.21	0.17	0.08	-0.24	1.67
	Measured	1.08	0.06	0.11	0.49	9.12	17.50	46.10	7.96	1.70
Survey 1 Cell 10	Mass Balance	1.15	0.06	0.11	0.44	8.97	17.32	45.58	8.10	1.62
	% Difference	-5.96	4.71	4.32	10.70	1.67	1.02	1.13	-1.78	4.46
	Measured	1.03	0.07	0.11	0.53	9.40	18.00	46.40	7.59	1.87
Survey 1 Cell 11	Mass Balance	1.06	0.06	0.10	0.47	9.25	17.85	45.97	7.71	1.78
	% Difference	-3.50	5.37	3.93	10.69	1.62	0.83	0.92	-1.57	4.59
	Measured	0.21	0.17	0.30	1.17	10.40	19.30	45.50	4.63	3.67
Survey 1 Cell 12	Mass Balance	0.20	0.17	0.29	1.12	10.38	19.27	45.43	4.64	3.62
	% Difference	6.67	3.11	2.03	4.25	0.15	0.13	0.15	-0.16	1.46
	Measured		0.07	0.13	0.53	9.09	17.50	45.40	7.73	1.81
Survey 1 Comb Conc 9 - 12	Mass Balance	2.58	0.08	0.14	0.55	9.32	17.81	45.64	7.40	2.00
	% Difference		-12.55	-1.96	-4.18	-2.50	-1.77	-0.54	4.28	-10.37
Overall Recovery (%):	(Mass Balance)	5.32		77.55	42.43	6.86	5.37	4.81	3.54	56.63
Combined Concentrate Grade				0.92	1.53	10.88	16.48	42.36	6.97	4.10

Mass Balance Survey 2: 25/2/99 19h30 to 21h00

Stream		Mass Flow Dry (tph)	4E PGE "factored"	Cu %	Ni %	Fe %	MgO %	SiO2 %	Al2O3 %	S %
Survey 2 Feed	Measured	283.50		0.059	0.178	8.24	16.30	46.10	10.60	0.41
	Mass Balance	283.90		0.066	0.188	8.32	16.25	45.91	10.64	0.37
	% Difference	-0.14		-10.99	-5.82	-0.95	0.29	0.40	-0.41	9.49
Survey 2 Tail	Measured			0.0151	0.1193	8.26	16.2	46	10.9	0.17
	Mass Balance	272.22		0.015	0.115	8.18	16.24	46.16	10.85	0.18
	% Difference			2.69	3.74	0.92	-0.27	-0.35	0.41	-3.75
Survey 2 Cell 1	Measured	2.09	1.83	5.67	5.26	19.30	12.90	26.20	1.96	14.60
	Mass Balance	1.78	1.87	5.65	5.31	19.30	13.00	27.20	1.98	14.48
	% Difference	14.52	-2.70	0.34	-0.88	-0.02	-0.80	-3.83	-1.17	0.80
Survey 2 Cell 2	Measured	0.43	1.37	3.61	6.33	18.20	13.80	30.10	1.91	13.20
	Mass Balance	0.42	1.38	3.61	6.35	18.20	13.83	30.41	1.92	13.18
	% Difference	2.99	-0.44	0.05	-0.24	0.01	-0.20	-1.01	-0.27	0.18
Survey 2 Comb Conc 1+2	Measured		1.84	5.24	5.57	19.10	13.30	29.40	2.00	14.10
	Mass Balance	2.20	1.78	5.26	5.51	19.09	13.16	27.84	1.97	14.23
	% Difference		3.25	-0.39	1.16	0.03	1.03	5.30	1.48	-0.95
Survey 2 Cell 3	Measured	1.08	0.65	1.15	3.69	13.80	17.30	38.90	3.06	6.90
	Mass Balance	1.08	0.66	1.14	3.55	13.81	17.32	38.91	3.06	7.14
	% Difference	0.36	-0.97	1.10	3.75	-0.09	-0.11	-0.03	-0.08	-3.54
Survey 2 Cell 4	Measured	3.09	0.14	0.24	0.96	9.44	17.00	44.10	7.90	2.39
	Mass Balance	3.15	0.14	0.24	0.93	9.46	17.06	44.16	7.95	2.48
	% Difference	-1.85	-0.62	0.67	2.84	-0.18	-0.32	-0.13	-0.62	-3.57
Survey 2 Comb Conc 3+4	Measured		0.28	0.46	1.51	10.60	17.20	42.90	6.75	3.99
	Mass Balance	4.23	0.27	0.47	1.60	10.57	17.12	42.82	6.70	3.67
	% Difference		1.65	-1.72	-6.00	0.28	0.45	0.18	0.72	8.01
Survey 2 Cell 5	Measured	2.08	0.08	0.17	0.49	8.70	16.90	44.20	8.39	1.50
	Mass Balance	2.33	0.08	0.14	0.46	8.67	16.53	43.76	8.61	1.40
	% Difference	-11.95	4.19	16.80	6.89	0.34	2.21	1.01	-2.65	6.41
Survey 2 Cell 6	Measured	0.51	0.21	0.47	1.06	10.20	19.20	44.70	4.84	3.38
	Mass Balance	0.46	0.20	0.43	1.03	10.20	19.09	44.68	4.86	3.28
	% Difference	10.56	2.48	9.25	2.89	-0.04	0.58	0.04	-0.35	2.97
Survey 2 Cell 7	Measured	0.12	0.42	0.84	1.84	11.70	19.30	43.50	3.45	5.66
	Mass Balance	0.11	0.42	0.81	1.82	11.69	19.30	43.45	3.45	5.61
	% Difference	6.21	0.58	3.98	1.24	0.09	-0.02	0.12	-0.03	0.92
Survey 2 Cell 8	Measured	1.33	0.09	0.23	0.54	8.87	17.90	43.80	6.94	1.78
	Mass Balance	1.33	0.08	0.20	0.52	8.85	17.70	43.67	7.03	1.70
	% Difference	-0.46	2.77	13.13	4.29	0.28	1.11	0.29	-1.26	4.56
Survey 2 Comb Conc 5 - 8	Measured		0.10	0.20	0.56	8.93	17.00	44.30	7.96	1.77
	Mass Balance	4.23	0.10	0.21	0.57	8.97	17.25	43.82	7.57	1.81
	% Difference		-1.56	-5.68	-2.25	0.46	-1.45	1.08	4.87	-2.19
Survey 2 Cell 9	Measured	0.19	0.22	0.38	1.21	11.10	20.00	45.40	3.38	4.16
	Mass Balance	0.19	0.22	0.36	1.20	11.09	19.91	45.25	3.42	4.16
	% Difference	2.89	-1.62	5.16	0.83	0.11	0.43	0.34	-1.15	0.06
Survey 2 Cell 10	Measured	0.33	0.13	0.26	0.87	10.40	20.40	46.60	4.02	2.98
	Mass Balance	0.33	0.14	0.24	0.86	10.39	20.20	46.39	4.12	2.97
	% Difference	0.37	-1.81	6.35	1.05	0.14	0.97	0.44	-2.38	0.20
Survey 2 Cell 11	Measured	0.32	0.11	0.21	0.81	9.86	19.90	46.40	4.39	2.57
	Mass Balance	0.32	0.12	0.20	0.80	9.84	19.77	46.06	4.51	2.57
	% Difference	-2.15	-1.57	5.01	0.96	0.21	0.67	0.74	-2.65	-0.01
Survey 2 Cell 12	Measured	0.18	0.14	0.23	0.93	10.30	19.80	46.00	4.37	3.07
	Mass Balance	0.18	0.14	0.22	0.92	10.29	19.68	46.00	4.43	3.07
	% Difference	-0.84	-1.09	3.11	0.63	0.10	0.60	0.00	-1.41	0.08
Survey 2 Comb Conc 9 - 12	Measured		0.16	0.24	0.91	10.30	19.50	45.40	4.56	3.07
	Mass Balance	1.02	0.15	0.25	0.91	10.32	19.92	46.01	4.17	3.08
	% Difference		7.01	-2.88	-0.54	-0.23	-2.17	-1.35	8.48	-0.22
Overall Recovery (%):	(Mass Balance)	4.12		78.61	41.59	5.72	4.22	3.64	2.28	54.57
Combined Concentrate Grade				1.26	1.90	11.58	16.67	40.64	5.90	4.94

Mass Balance Survey 3: 4/3/99 19h15 to 20h45

Stream		Mass Flow Dry (tph)	4E PGE "factored"	Cu %	Ni %	Fe %	MgO %	SiO2 %	Al2O3 %	S %
Survey 3 Feed	Measured	282.03		0.054	0.181	9.29	16.40	43.40	9.99	0.36
	Mass Balance	281.62		0.056	0.177	9.23	16.26	43.80	10.20	0.34
	% Difference	0.15		-4.81	2.27	0.68	0.85	-0.92	-2.09	4.53
Survey 3 Tail	Measured			0.0131	0.1072	9.05	16.1	44.3	10.6	0.16
	Mass Balance	272.52		0.013	0.109	9.11	16.23	43.89	10.37	0.16
	% Difference			1.15	-1.30	-0.63	-0.79	0.92	2.16	-1.95
Survey 3 Cell 1	Measured	1.31	1.82	4.81	5.88	19.40	12.90	28.10	2.00	14.30
	Mass Balance	1.63	1.79	4.92	5.83	19.43	12.94	28.33	2.01	14.27
	% Difference	-23.91	1.56	-2.28	0.90	-0.14	-0.27	-0.81	-0.53	0.20
Survey 3 Cell 2	Measured	0.66	1.05	2.31	4.81	16.40	16.10	34.70	2.23	9.75
	Mass Balance	0.76	1.05	2.32	4.79	16.40	16.12	34.86	2.24	9.75
	% Difference	-15.83	0.41	-0.51	0.37	-0.03	-0.10	-0.47	-0.28	0.05
Survey 3 Comb Conc 1+2	Measured		1.52	4.22	5.43	18.50	14.00	30.80	2.10	12.80
	Mass Balance	2.39	1.55	4.09	5.50	18.46	13.95	30.39	2.08	12.83
	% Difference		-2.22	2.98	-1.23	0.19	0.38	1.32	0.83	-0.24
Survey 3 Cell 3	Measured	2.18	0.27	0.48	1.47	11.30	17.70	42.00	5.53	4.15
	Mass Balance	2.34	0.29	0.49	1.49	11.45	17.79	42.21	5.56	4.25
	% Difference	-7.49	-4.17	-2.23	-1.52	-1.32	-0.50	-0.49	-0.51	-2.52
Survey 3 Cell 4	Measured	1.78	0.18	0.37	1.08	10.60	18.10	43.10	5.76	3.14
	Mass Balance	1.62	0.19	0.37	1.09	10.69	18.16	43.23	5.78	3.18
	% Difference	8.83	-1.96	-1.19	-0.77	-0.85	-0.34	-0.31	-0.35	-1.31
Survey 3 Comb Conc 3+4	Measured		0.26	0.46	1.36	11.40	18.10	43.00	5.70	3.98
	Mass Balance	3.96	0.25	0.44	1.33	11.14	17.94	42.64	5.65	3.82
	% Difference		6.82	3.62	2.38	2.26	0.86	0.83	0.88	4.08
Survey 3 Cell 5	Measured	1.05	0.09	0.22	0.49	9.46	17.10	43.60	8.00	1.63
	Mass Balance	1.09	0.09	0.21	0.47	9.34	16.79	42.91	8.01	1.60
	% Difference	-3.70	0.47	4.43	4.03	1.24	1.84	1.59	-0.14	1.87
Survey 3 Cell 6	Measured	0.25	0.27	0.62	1.03	10.70	19.40	43.80	3.94	3.75
	Mass Balance	0.24	0.27	0.60	1.01	10.67	19.33	43.67	3.94	3.71
	% Difference	3.17	-0.09	2.80	1.90	0.32	0.36	0.29	-0.01	0.95
Survey 3 Cell 7	Measured	0.67	0.11	0.22	0.53	10.00	18.90	44.90	6.01	2.00
	Mass Balance	0.67	0.11	0.21	0.51	9.92	18.70	44.45	6.01	1.97
	% Difference	-0.44	-0.11	2.73	2.85	0.85	1.05	0.99	-0.07	1.42
Survey 3 Cell 8	Measured	0.13	0.21	0.54	0.87	9.92	19.30	45.10	4.12	3.13
	Mass Balance	0.13	0.21	0.53	0.86	9.91	19.25	45.00	4.12	3.12
	% Difference	1.21	0.27	1.22	0.87	0.10	0.28	0.22	-0.02	0.41
Survey 3 Comb Conc 5 - 8	Measured		0.12	0.27	0.56	9.50	17.30	42.80	6.71	2.03
	Mass Balance	2.13	0.12	0.27	0.57	9.70	17.82	43.60	6.69	2.04
	% Difference		-0.08	-1.70	-1.47	-2.15	-3.01	-1.86	0.27	-0.71
Survey 3 Cell 9	Measured	0.12	0.26	0.51	1.14	11.20	19.40	45.20	4.22	4.14
	Mass Balance	0.12	0.26	0.51	1.13	11.17	19.38	45.13	4.22	4.16
	% Difference	0.58	0.08	0.90	1.04	0.28	0.11	0.16	-0.02	-0.49
Survey 3 Cell 10	Measured	0.16	0.17	0.33	0.89	10.40	19.70	45.90	4.61	3.12
	Mass Balance	0.16	0.17	0.33	0.88	10.36	19.65	45.83	4.61	3.13
	% Difference	0.03	0.19	0.71	1.14	0.36	0.23	0.15	-0.01	-0.33
Survey 3 Cell 11	Measured	0.23	0.13	0.23	0.75	10.60	19.70	45.60	4.67	2.72
	Mass Balance	0.23	0.13	0.23	0.74	10.54	19.65	45.46	4.67	2.73
	% Difference	-0.55	0.25	0.77	1.32	0.55	0.23	0.32	-0.03	-0.54
Survey 3 Cell 12	Measured	0.10	0.18	0.31	0.89	10.10	19.20	45.70	5.20	2.99
	Mass Balance	0.10	0.18	0.31	0.88	10.08	19.17	45.66	5.20	3.00
	% Difference	-0.02	0.13	0.44	0.72	0.24	0.14	0.09	-0.01	-0.28
Survey 3 Comb Conc 9 - 12	Measured		0.17	0.32	0.87	10.40	19.40	45.20	4.66	3.21
	Mass Balance	0.62	0.17	0.32	0.88	10.53	19.51	45.51	4.65	3.16
	% Difference		-0.64	-0.44	-0.65	-1.28	-0.59	-0.68	0.11	1.63
Overall Recovery (%):	(Mass Balance)	3.23		77.74	40.50	4.45	3.37	2.94	1.55	53.96
Combined Concentrate Grade				1.35	2.21	12.69	16.97	39.84	4.89	5.72

APPENDIX CIII: Step Test Results

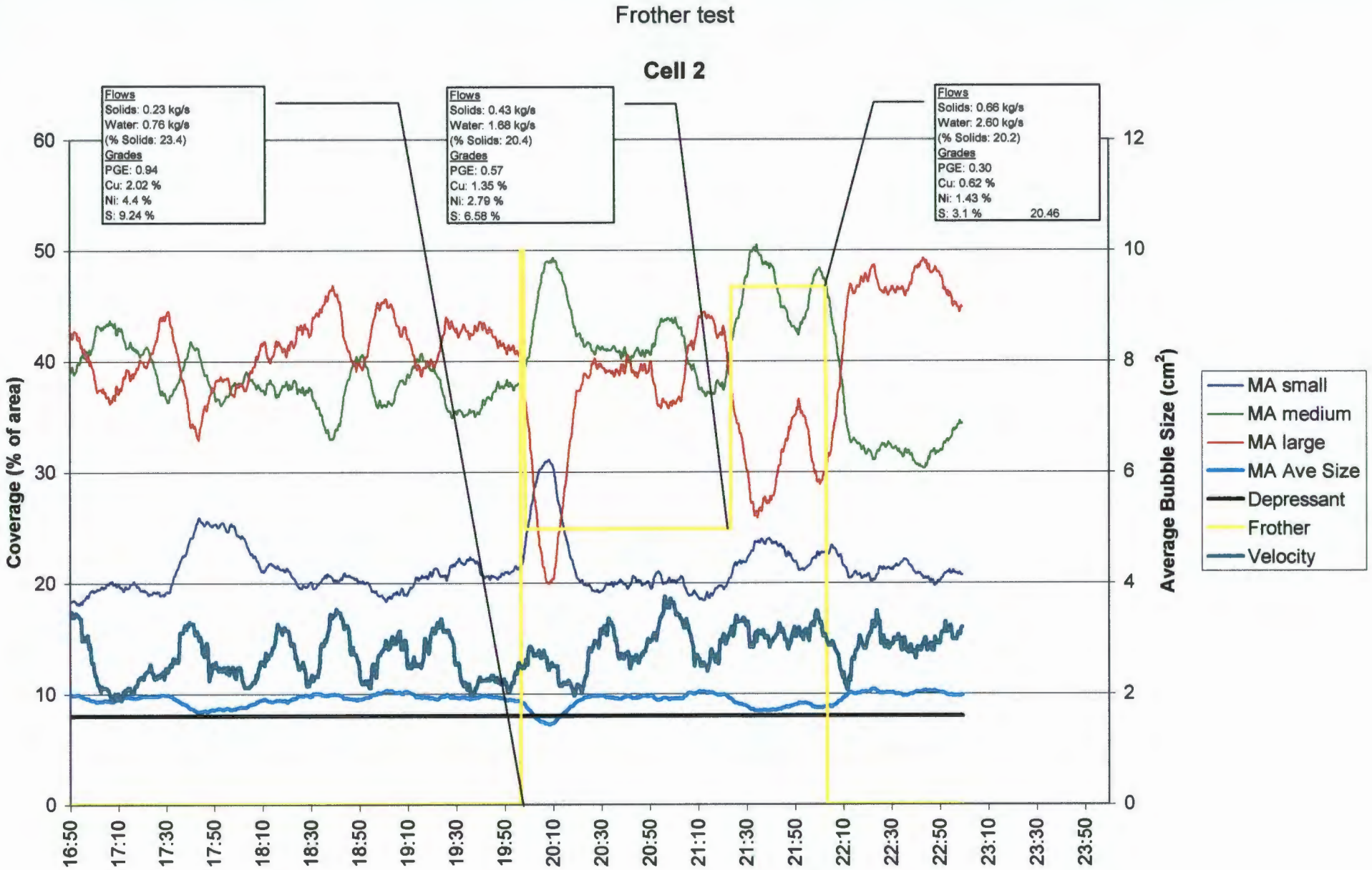
Frother test
Cell 2
Flows
Solids: 0.23 kg/s
Water: 0.76 kg/s
(% Solids: 23.4)
Grades
PGE: 0.94
Cu: 2.02 %
Ni: 4.4 %
S: 9.24 %
Flows
Solids: 0.43 kg/s
Water: 1.68 kg/s
(% Solids: 20.4)
Grades
PGE: 0.57
Cu: 1.35 %
Ni: 2.79 %
S: 6.58 %
Flows
Solids: 0.66 kg/s
Water: 2.60 kg/s
(% Solids: 20.2)
Grades
PGE: 0.30
Cu: 0.62 %
Ni: 1.43 %
S: 3.1 %
20.46
Coverage (% of area)
Average Bubble Size (cm²)
0
10
20
30
40
50
60
0
2
4
6
8
10
12
16:50
17:10
17:30
17:50
18:10
18:30
18:50
19:10
19:30
19:50
20:10
20:30
20:50
21:10
21:30
21:50
22:10
22:30
22:50
23:10
23:30
23:50
MA small
MA medium
MA large
MA Ave Size
Depressant
Frother
Velocity

Frother test

Cell 10

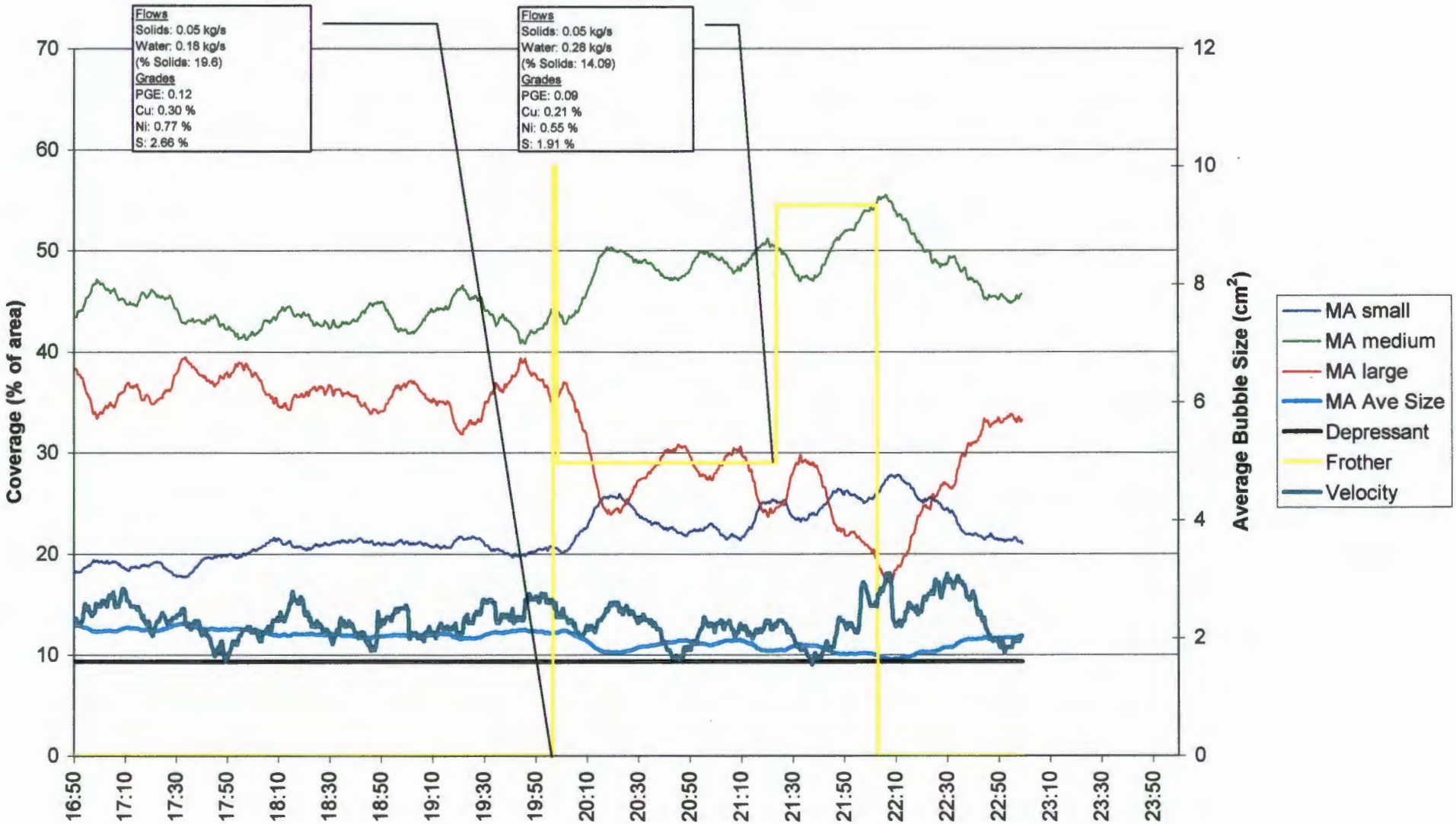

Depressant test 1

Cell 2

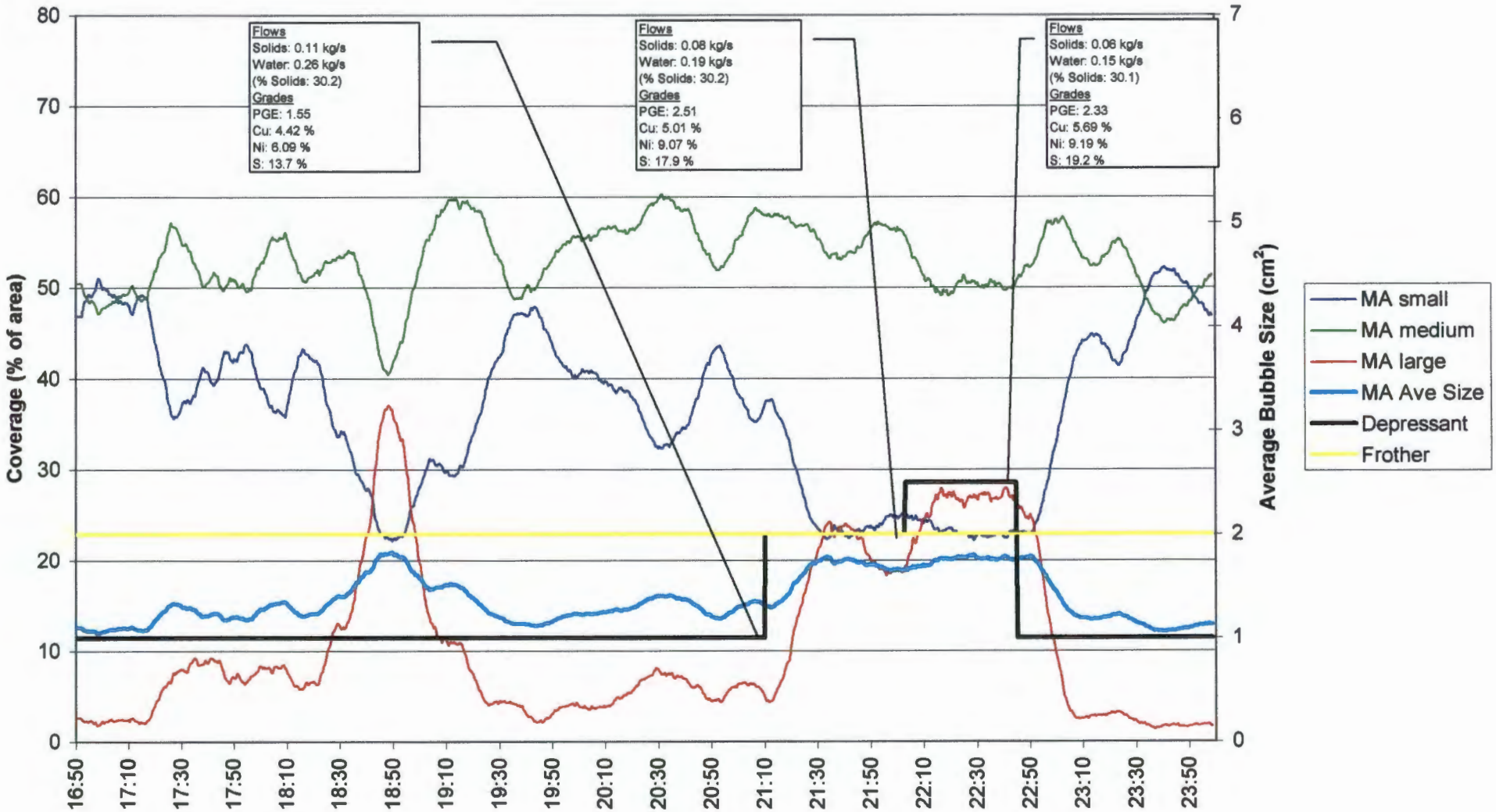

Depressant test 1

Cell 10

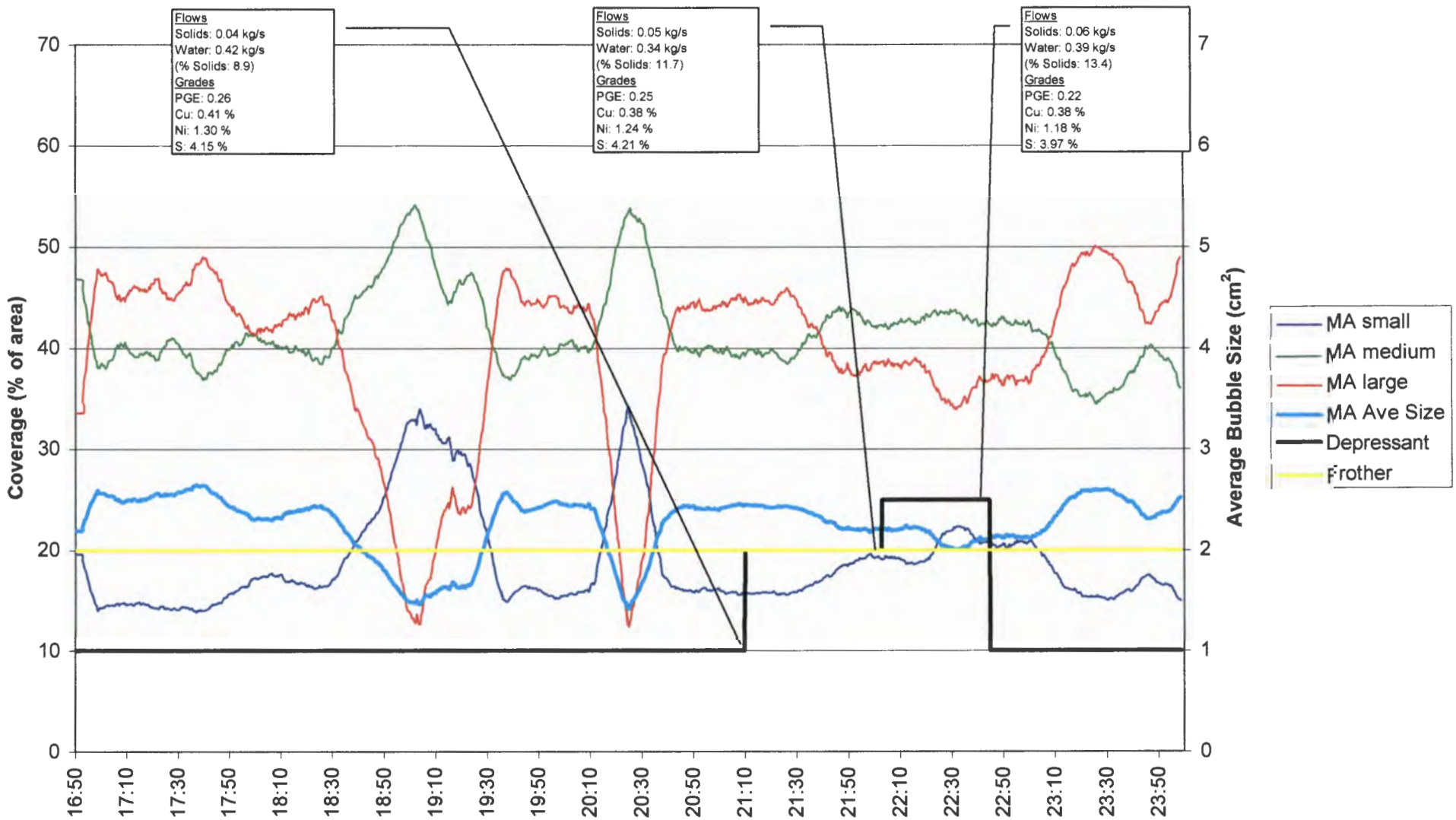

Depressant test 2

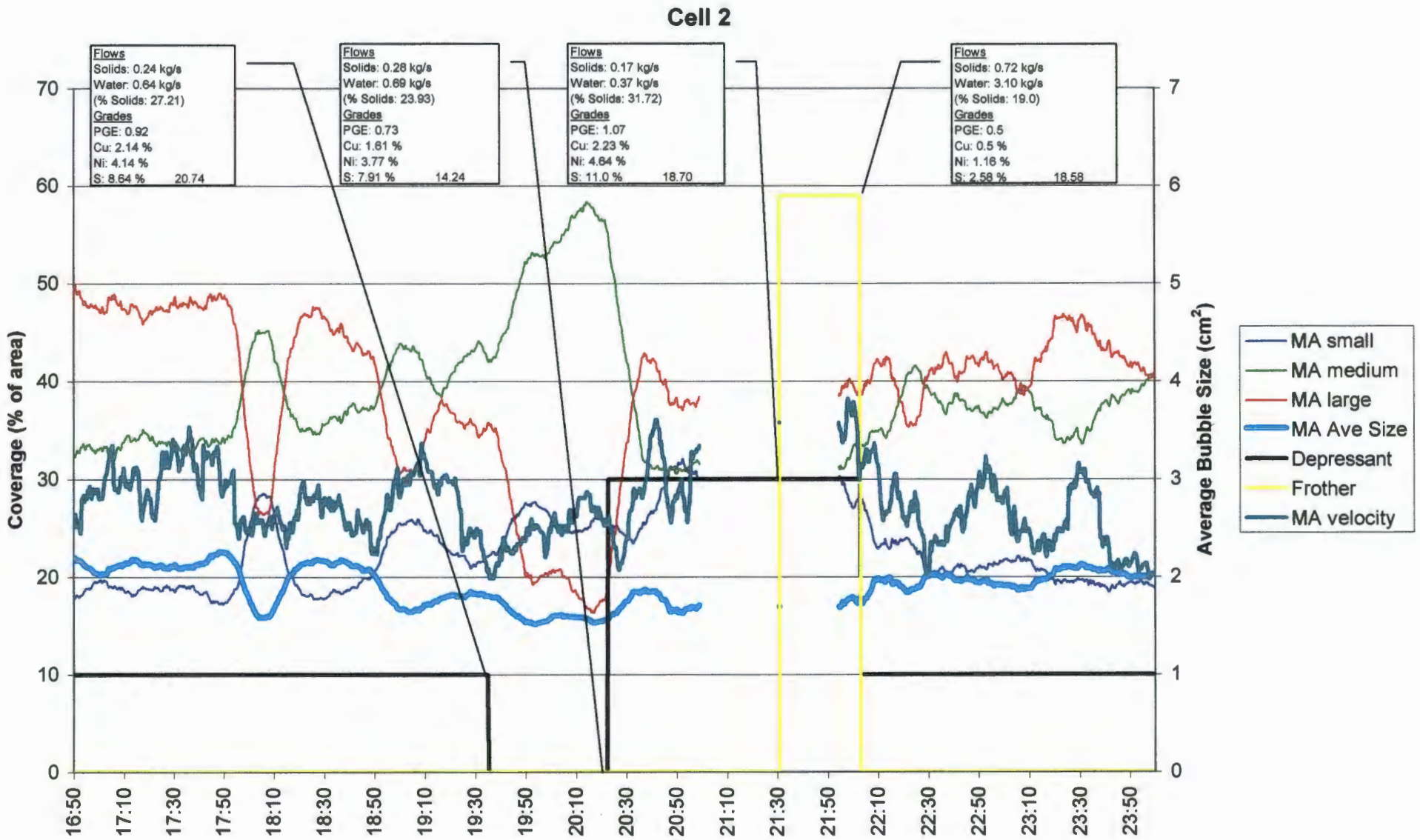

Depressant test 2